



Beachmed-e Mesure 3.3. Le cycle sédimentaire :
Gestion des stocks interceptés par les infrastructures côtières et
récupération du transport solide dans les lits des fleuves

Sous projet GESA :
**Gestion des stocks Sableux interceptés par les
ouvrages côtiers et fluviaux. Récupération du
transport solide**

**Rapport Technique de Phase B
2007**



Sous projet GESA :

GEstion des stocks SAbleux interceptés par les ouvrages côtiers et fluviaux. Récupération du transport solide

Belén Alonso (CdF)¹, Ruth Durán¹, Gemma Ercilla¹, David Casas¹, Ana Bernabeu¹, Farran Estrada¹, Marcel.li Ferran¹, Marta Nuez¹, Jordi Serra², Xenia Valois², Alberto Lamberti³, Luca Martinelli³, Davide Merli³, Michele Piemontese³, Pier Luigi Aminti⁴, Gianluca Barbieri^{4a}, Andrea Battistini^{4a}, Lorenzo Cappietti⁴, Claudia D'Eliso⁴, Enrica Mori⁴, Maria Grazia Tecchi⁴, Alberto Petaccia⁵, Alessandro Greco⁵, Alberto Maistri⁵, Paolo Sammarco⁵, Sergio Camilletti⁵, Raphael Certain⁶, Nikolas Kotsovinos⁷, Christoforos Koutitas⁷, Vlassios Hrissanthou⁷, Panagiotis Angelidis⁷, Manolia Andredaki⁷, Anastasios Georgoulas⁷, Achilleas Samaras⁷, Antonis Valsamidis⁷, Koutandos Evangelos⁸, Karambas Theofanis⁸ and Kampanis Nikolaos⁸

Chef de File

1.- Institut of Marine Sciences (Catalunya)

Responsable : Belén Alonso

2.- University of Barcelona (Catalunya)

Responsable : Jordi Serra

3.- University of Bologna/DISTART (Emilia-Romagna)

Responsable: Alberto Lamberti

4.- University of Florence/ Dip. Civil Engineering (Toscana)

Responsable: Pier Luigi Aminti

5.- Registro Italiano Dighe (Lazio)

Responsable: Alberto Petaccia

6.- Laboratory of Marine Géo-Environmental Study, LEGEM (Languedoc-Roussillon)

Responsable : Raphael Certain

7.- Democritus University of Thrace-School of Engineering (East Macedonia-Thrace)

Responsable: Nikolas Kotsovinos

8.- Foundation of Research and Technology-Hellas, Inst. of Applied Mathematics (Crete)

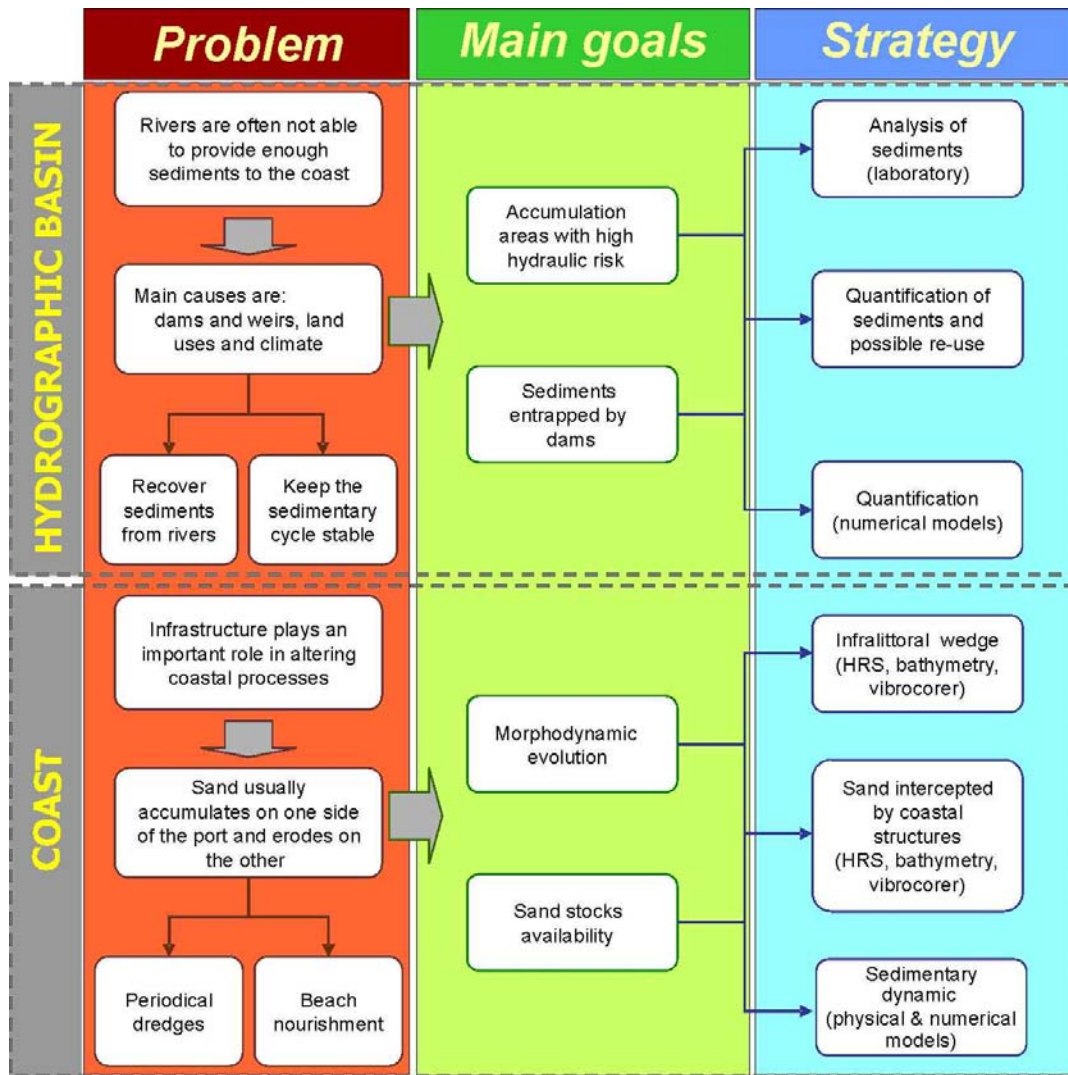
Responsable: Evangelos Kountandos



INTRODUCCIÓN	4
1. Rapport of Phase B: Institut of Marine Sciences (Catalunya)	6
2. Rapport of Phase B: University of Barcelona (Catalunya)	19
3. Rapport of Phase B: University of Bologna/DISTART (Emilia-Romagna)	29
4. Rapport of Phase B: University of Florence/ Dip. Civil Engineering (Toscana)	45
5. Rapport of Phase B: Registro Italiano Dighe (Lazio)	62
6. Rapport of Phase B: Laboratory of Marine Géo-Environmental Study, LEGEM (Languedoc-Roussillon)	83
7. Rapport of Phase B: Democritus University of Thrace-School of Engineering (East Macedonia-Thrace)	103
8. Rapport of Phase B: Foundation of Research and Technology-Hellas, Inst. of Applied Mathematics_(Crete)	119

INTRODUCTION

During the Phase B of GESA subproject has defined the research methodologies and strategies for the management of sand deposits collected by coastal and fluvial infrastructures and the recovery of fluvial sediment. It has been designed from a multidisciplinary approach which includes research methodologies on hydrologic basin and coastal areas (fig. 1). The research methodology and strategies proposed for the hydrologic basin are focused to understand the impact of fluvial inputs reduction into coastal areas (fig. 1). Regarding to the coastal areas, the research has to be focused on the improvement of knowledge relative to sand stocks available and the evolution of morphodynamic and shoreface nourishment (fig. 1).



Sous-projet GESA- Phase B

Figure .1. Scheme showing the problems, main goals and research strategies in the framework of GESA sub-project, in relation to the hydrologic basin and the coastal area.

In this report of the Phase B, each partner exposes its research strategies, methodologies and field measures to carry out the study of management of the sandy deposits intercepted by infrastructures in the six Mediterranean regions evolved into GESA subproject. To summarize the contributions of the eight partners are addressed to the following the topics



- **Research strategies to the hydrographic basin: applied to budget-stock sands management:** In the following sections the partners give specific information on calculate or/and estimation of contributions and losses for sand budget:
 - (1) Reduction of fluvial inputs by accumulation in the hydrographic basins,
 - (2) Reduction of fluvial inputs by anthropogenic factors (dams),
 - (3) Reduction of fluvial inputs by turbidity currents,
 - (3) Recovery of sediments in reservoirs (dams), and
 - (4) River contribution from deltaic systems.

- **Research strategies to the study coastal area: applied to stock sands management:** In the following sections the partners give specific information about:
 - (1) Evaluation the sand availability,
 - (2) Understand the morphodynamic and shoreface nourishment evolution.

Eight partners belonging to four European countries (Spain, Italy, France, and Greece) with different disciplines contribute with a common effort on the above issues. The selection of case-studies should aim to present a compressive view of the Mediterranean coastal area. It has added advantage of validating the research strategy and producing a better understanding of complex spatial and dynamic coastal processes.

**1. RAPPORT OF PHASE B:
INSTITUT OF MARINE SCIENCES-CSIC – P1
MEASURE 3.3
GESA**

INTRODUCTION

During the Phase B has been designed the methodological approach that allows to achieve the objectives and resolve the problems which had been previously identified during the phase A. The main problem of the Maresme coast (Catalunya) is the presence of coastal infrastructures that alters the coastal processes. In order to re-establish the sedimentary budget in the Maresme coast, it has been developed different anthropogenic activities. They include dredge of sand in front of the infrastructures and beach nourishment in the beaches located at the southern of the ports. In this context, it has been defined two main goals (fig.1):

- **Sand stocks availability.** The location and characterization of candidate littoral borrow areas for beach nourishment allows understanding of the sedimentary budget of the Maresme coast. It is developed from the characterization of sand volume intercepted by the coastal structures and the infralittoral wedge.
- **Morphodynamic evolution.** The morphodynamic evolution of the dredged and nourished areas. It is described by means of numerical models and real data.

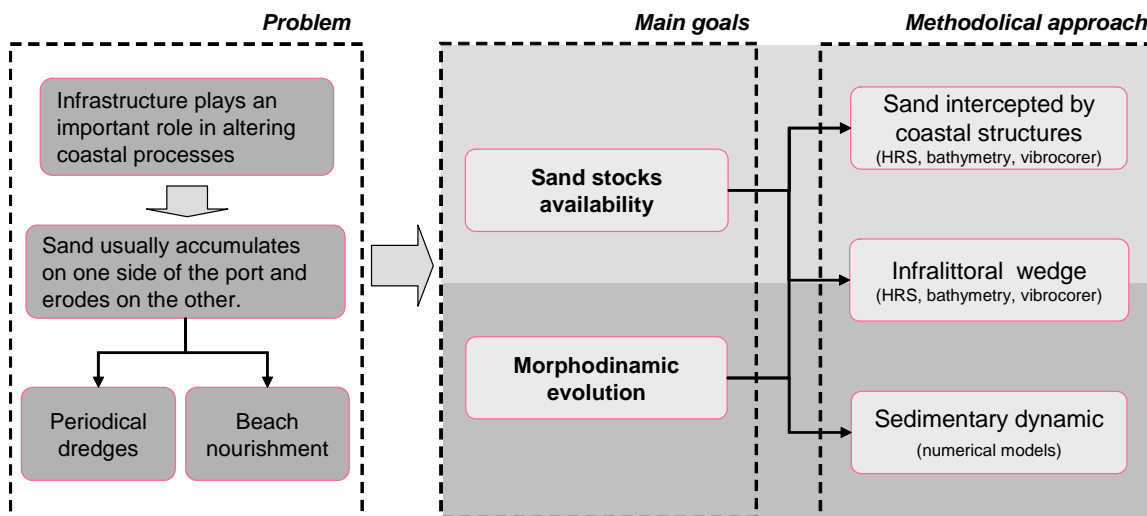


Figure.1. Schematic representation of the main problems and goals, and the methodological approach designed in the Phase B of Gesa subproject.

RESEARCH STRATEGIES TO THE COASTAL STUDY: APPLIED TO STOCK SANDS MANAGEMENT

The methodological approach has been designed during the Phase B of Gesa subproject. It takes into account the two main goals previously described:

- (i) the morphodynamic evolution of the dredged and nourished areas; and
- (ii) the characterization of sand stocks availability, mainly the infralittoral wedge and the sand intercepted by coastal structures (fig. 2).

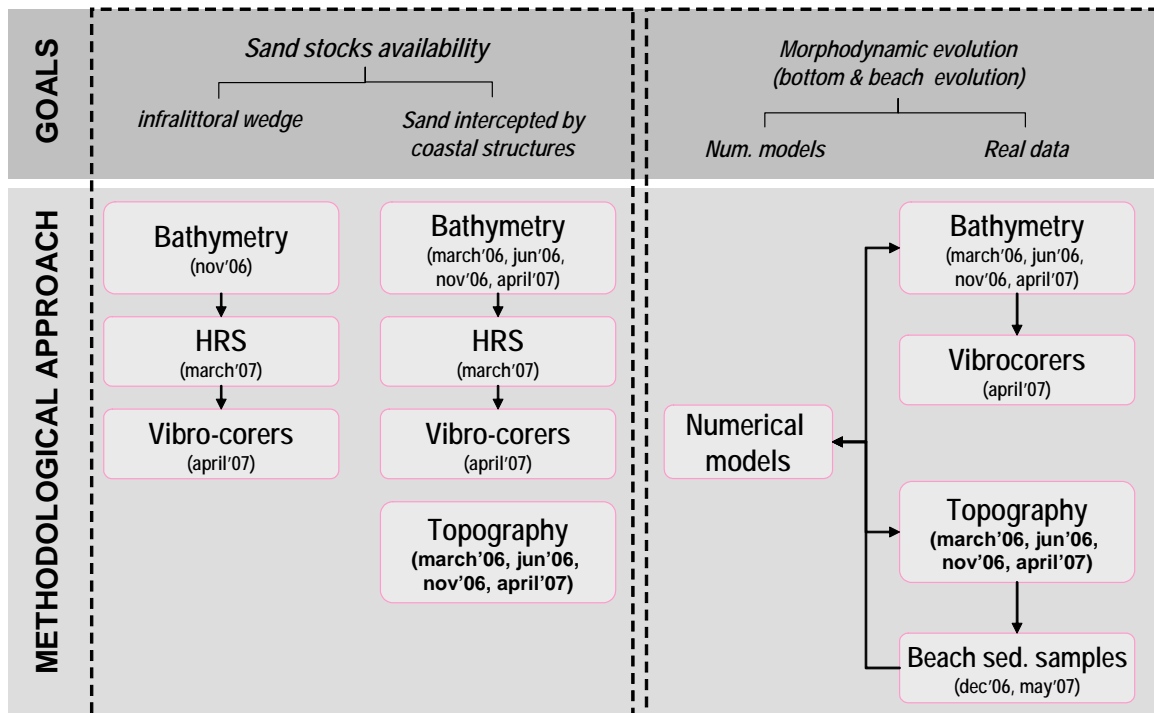


Figure 2. Schematic representation of the methodological approach.

1. Sand stocks availability

The coastal sand stock includes the sand intercepted by coastal structures and the infralittoral wedge (fig. 2). In relation to the evaluation and characterization of the sand stock availability, the multibeam bathymetry of the area from Premiá to Masnou constitutes the first stage. A high resolution seismic survey is planned based on this seafloor bathymetry. In this way, two different scales are defined, a large scale for the study of the infra-littoral wedge and a small scale on the area of dredge area (sand accumulation). After this geophysical cruise the location of vibrocorers is defined according to the preliminary interpretation of seismic records.

The analysis of the bathymetric, geophysical, and sedimentological data collected in these different cruises allows evaluating the morphology, volume and characteristics of the sand stocks in the Maresme coast. The volume of sand that is annually accumulated by the presence of coastal structures can be defined by means of these data and periodical topo-bathymetries and sediment samples.

2. Morphodynamic evolution

The methodological approach for defining the morphodynamic evolution of coastal areas is mainly based on the application of numerical models (fig. 2). The ICM (P1) partner uses the SMC (Coastal Modelling System) in order to define the numerical simulation of wave propagations from indefinite depths towards the coast line of Masnou area. With these data, the induced current in the break zone can be obtained. Therefore the morphodynamic evolution of a beach can be simulated.

It includes the following models:

- (i) Mild slope parabolic model for wave propagation (both monochromatic and spectral wave);
- (ii) Model for beach currents induced by the spectral wave breaking; and
- (iii) Erosion model-sedimentation and bathymetric evolution of the beaches.

The data acquired during the last year (from april'06 to may'07) constitute the input data of the model. They include periodical topographies and bathymetries, and sediment samples (from beach and nearshore). The results of the numerical hydrodynamic model show the preferential areas of erosion and accumulation of sand, which can be confirmed by the real data. The morphodynamic model shows the predicted changes in coastal morphology.

METHODOLOGIES AND FIELD MEASURE

The topographic, bathymetric, geophysical and sedimentological data have been collected during different cruises according to the previously described methodological approach. The work developed during the phase B includes the cruise planning, the data acquisition and the first steps of the work in desk and laboratory.

The accuracy and resolution of methods proposed to carry out the sand stock availability and morphodynamic of coastal areas (fig. 3) have been described in the OPTIMAL and ReSaMMé subprojects (measures 2.1. and 2.3 respectively). In this report it is describe the sampling strategies and the methods used only in the subproject GESA.

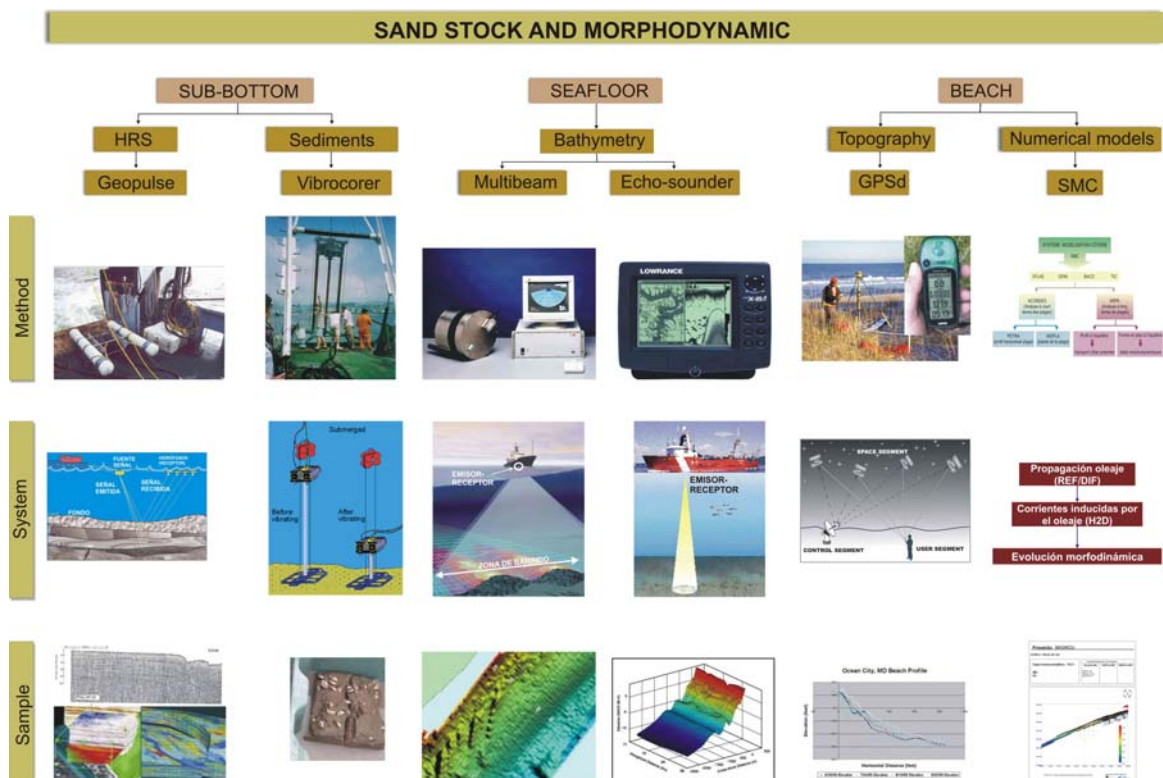


Figure .3. Synthesis of the methods used in the Gesa subproject.

1. Field work

The field work includes the acquisition of topographic, bathymetric, geophysical, and sedimentological data in the area of Masnou, during different surveys.

Topography and bathymetry

Four topographic and bathymetric surveys have been proposed in the Masnou area (fig. 4):

- The first one was performed before the dredge and nourishment. It was on march'06 and covers an area of 12 km² in front of the Masnou harbour and beach located at the southern part of the port.
- Second one was designed just after the nourishment and the most extensive dredge activities (june'06). It was planned in the same area of the previous one for the monitoring of the study area.
- The third survey was planning with two purposes, the cartography of the infralittoral wedge and the monitoring of the dredge area. In this way, the survey area extends from Premiá to Masnou and from the coastline to 35 m depth. It has been performed on november'06 (6 months after dredge and nourishment).
- The last cruise has been designed in the same area that one year. It was developed after dredging (may'07) covering the same area that the last one.

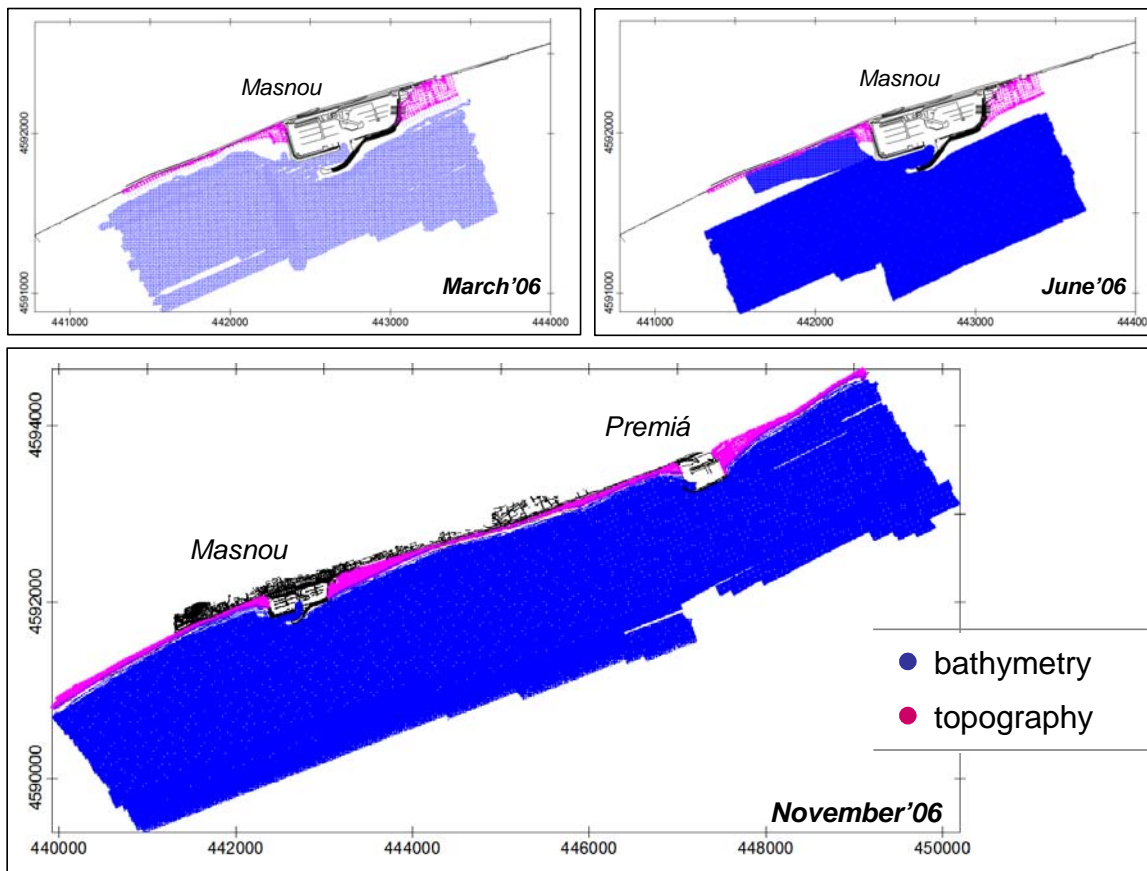


Figure 4. Bathymetric and topographic surveys.

The three first surveys have been performed and the data have been analyzed during the phase B. The last survey has been developed on May and the data are being processed.

The methods used in these surveys comprise the multibeam sounder, an echosounder and a dGPS. The multibeam is used in the nearshore area, from -35 to -1.5 meters. The bathymetric data in the shorezone between the coastline and 1.5 m depth was collected by using an echo-sounder and a dGPS.

High resolution seismic data

The seismic plan comprises 2 working areas around the Masnou area. The first one (Fig. 5) has as main target to characterize the morphosedimentary evolution of the infralittoral sector around Masnou. The second one (Fig.6) has the aim of monitoring the dredge area close to the breakwater and entrance of Masnou port. A total of 115 km of

seismic lines has been planned, which are parallel and perpendicular to the structures previously observed in the multibeam bathymetry. The design of this seismic net will permit to characterize the existing sedimentary bodies and their lateral variability.

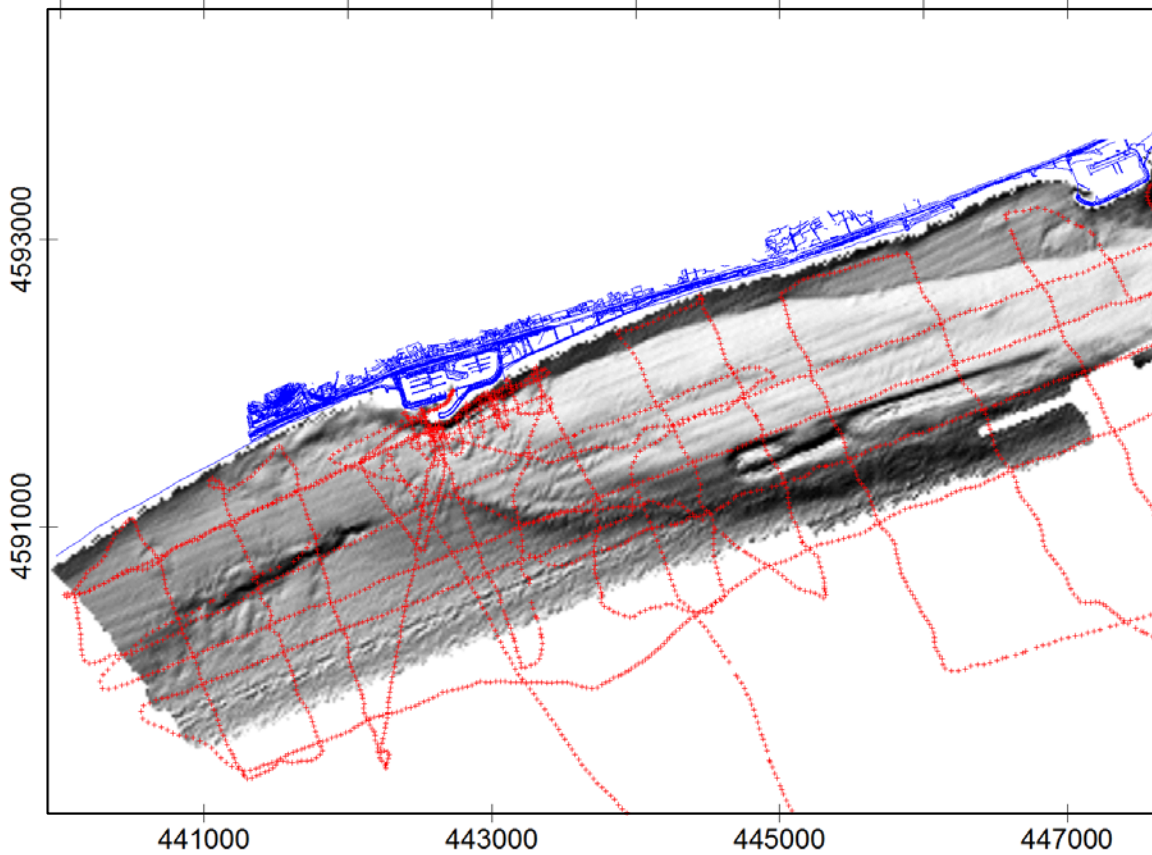


Figure 5. Seismic net projected to characterize the morphosedimentary evolution of the infralitoral sector around Masnou.

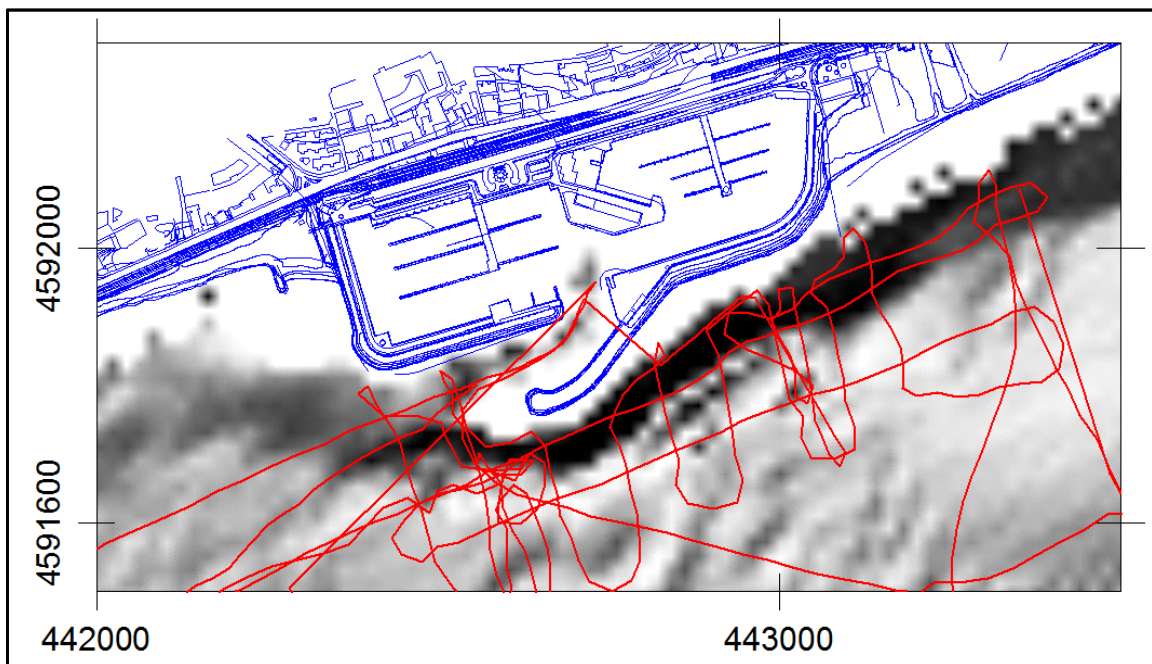


Figure 6. Seismic net projected to monitoring the dredge area close to the Masnou Port.

High resolution seismic profiles have been used to characterize the littoral prism (thickness, extension, volume) of the study area, and the GeoPulse Boomer System has been chosen (Fig. 7). It is a widely seismic system used for high resolution, deep penetration profiling in both deep sea and shallow coastal environments. GeoPulse offers a flexible high resolution solution and it also provides up to three times the acoustic energy of conventional profiling systems while operating in very shallow water and in high noise environments.

The seismic system characteristics and its methodological test and evaluation are described in the OpTIMAL phase B report. The system includes different parts (Fig. 7):

- An acoustic source Boomer plate mounted on a Catamaran (Fig. 7A). The GeoPulse sound source produces a high energy pulse by the action of a unique vacuum controlled electromechanical “plate”.
- GeoPulse Hydrophone (Fig. 7B). The hydrophone array receives the returned signals. The hydrophone contains twenty elements.
- GeoPulse Power Supply (Fig. 7C). The GeoPulse employs a solid state high voltage switching device which offers higher efficiency, very high reliability and excellent repeatability.
- GeoPulse Receiver (Fig. 7D). It receives the acoustic return from the hydrophone. It gives the essential processing and control functions for analogue data enhancement.



Figure.7. The basic seismic system includes different parts: (A) Boomer plate mounted on a Catamaran, (B) Hydrophone, (C) Power Supply, and (D) Receiver and EPC graphic recorder.

Data from the GeoPulse Receiver can be displayed directly onto a wide variety of industry standard graphic recorders.

According to the results of seismic cruise, some Van Veen grabs samples, will be used to get a preliminary test of what kind of sediment is present in the areas worked. Both information, seismic and grab-samples will determine the final position of long-sediment cores (vibrocores).

Sediment samples

The collection of sediment samples includes the beach surficial samples and the nearshore samples (grabs and vibrocorers). The beach samples have been collected in two different periods: December 2006 and May 2007. During the first one (December 2006), the samples were collected from the beach at the northern and southern of Masnou (fig. 8). These samples allow to characterize the sand of the beaches closed to the harbour.

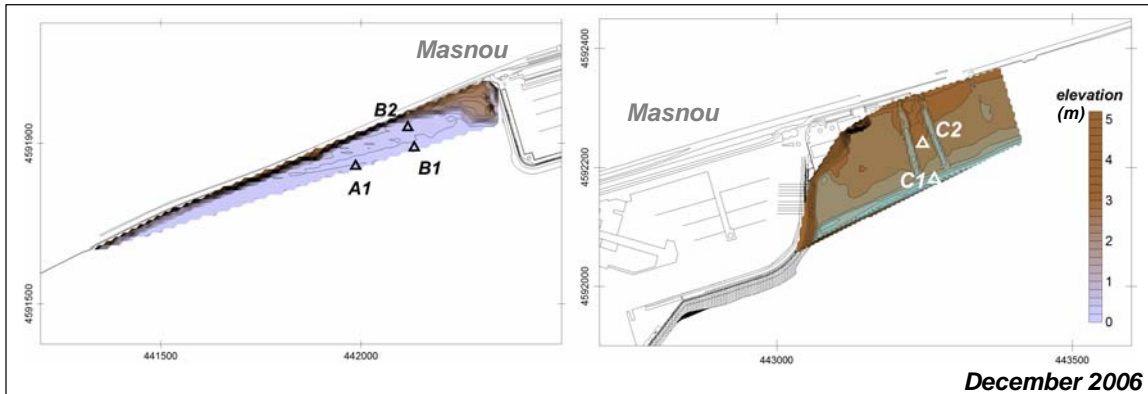


Figure 8. Sediment samples (A1, B1, B2, C1, C2) collected in the beach, close to the Masnou harbour, in December 2006.

During the second one (May 2007), new bottom samples were taking in may for using in the morphodynamic model. In this survey, it has been collected bottom samples from the southern beach of Premiá to Masnou (fig. 9).



Figure 9. Sediment samples collected in the beach (may 2007) in the coastline Premiá-Masnou

Nearshore sediment samples have been collected using a vibro-coring device and a grab (Fig.10). The type of collecting equipment chosen depends on site location, analyses to be performed and study goals. The sampling strategy designed in this project has been the following.

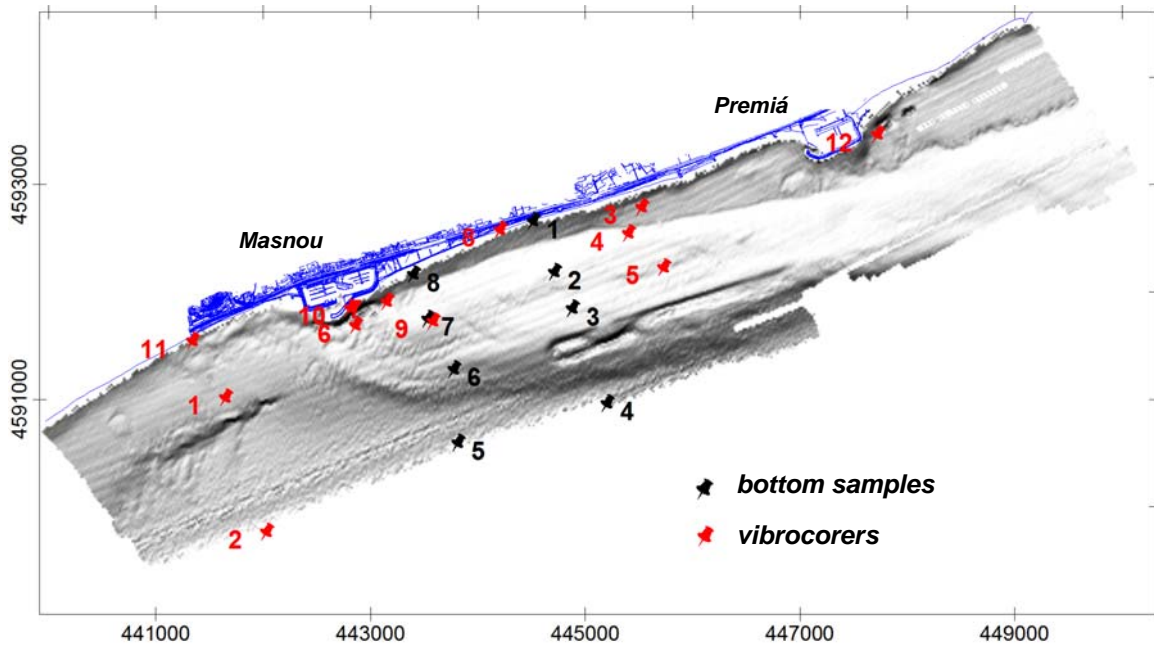


Figure 10 . Location of bottom samples and vibrocorers.

It was planned a grid of grab samples for the seafloor characterization and for using in the numerical model. They have been collected using a Van Veen grab (Fig.11). It allows recovering the most superficial sample of sediment. This sediment sampler has a clam shell-type scoop setup. Although it tends to disturb the sediments, it is simpler to operate. It can extract samples up to 20 centimetres deep within a sampling area of 0.1 square meters.

The sediment corer sampling strategy has been planned from the analysis of bathymetric and seismic data. It has been collected 12 samples in the area from Premiá to Masnou using a vibrocorer.

The Seabed vibrocorer (Fig. 11) is designed to obtain cylindrical cores in soft, cohesive soils at a maximum depth of 50 meters. After the unit is placed on the seafloor (Fig. 11), the electrical vibration head drives the core-barrel containing the PVC core-liner into the seafloor. The stationary piston system assists in the intrusion of seabed sediment into the barrel with minimum disturbance. After recovery the vibration unit the core can be rotated to a horizontal position to facilitate the removal of the liner with the sample (Fig.11). The standard range of vibrocorers includes 3, 4 and 5 meter frames.

The basic Vibrocorer system consists of:

- Thermally galvanized frame with guiding posts, steel wires and tensioners
- Vibration unit in swing frame with barrel adapter
- Containerised control unit
- Cable on reel (60 m. standard)
- Stationary piston system with penetration indicator
- 3, 4, or 5 m. core barrel

2. Work on desk

The work on desk includes the analysis of topo-bathymetric and geophysical data and the application of numerical models for wave propagation in the study area.



Figure 11. Image of a Van Veen grab and deploy of vibrocorer. After recovery, the vibrocorer can be rotated to a horizontal position to facilitate the removal of the liner.

Analysis of topo-bathymetric data

The analysis of topographic and bathymetric data includes the elaboration of bathymetric maps, the morphometric analysis, the extraction of bathymetric profiles and the evaluation of volumetric changes between different periods.

The bathymetric map has been made from the multibeam data using the nearest neighbour as interpolation method. The topography of the beach is obtained from the dGPS data. One of the improvements of this project in relation to coastal management is the continuity in the topographic data. The beach topography is completed by bathymetric data without any blank area between them. This is important in the beach morphodynamic analysis.

The periodical bathymetries allow evaluating the volumetric changes in the study area. Cut and fill volumes between consecutive surveys show the net accumulation and erosion.

From a morphological point of view, the analysis of topographic features is a well-established field. Morphometric analysis has long been applied in different studies (Frisch, 1997; Radoslav, 2002; Santero, 2002; Jordan, 2004). In this context the results of the morphometric analysis of the dredged area (slope, terrain aspect and profile curvature maps) show the changes in the trench and sand pits along time.

Slope and terrain aspect maps have been generated and analysed based on the bathymetric grid. The Terrain Slope calculates the slope at any grid node on the surface. It is reported in degrees from zero (horizontal) to 90 (vertical). For a particular point on the surface, the Terrain Slope is based on the direction of the steepest descent or ascent at that point. This means that across the surface, the gradient direction can change. Grid files of the Terrain Slope can produce contour maps that show the isolines of the constant steepest slope. The Terrain Aspect calculates the downhill direction of the steepest slope (i.e. dip direction) at each grid node. It is the direction that is perpendicular to the contour lines on the surface, and is exactly opposite to the gradient direction. Terrain Aspect values are reported in azimuth, where 0 degrees points due North, and 90 degrees points due East.

Analysis of geophysical data

The seismic data has been interpreted in three steps: (1) identification of unconformity surfaces; (2) definition of seismic units of the infralittoral wedge; (3) description of seismic facies.

Unconformity surfaces have been used to define the seismic units in the present analysis. The configuration of the unconformities and conformity surfaces, and the nature of the bounding reflectors of these unconformities have been used to interpret depositional events. The term "unconformity" is used to define discordance surfaces

caused by nondeposition, weathering or erosion that separate groups of strata with no continuity in deposition between them, and that only in some cases may coincide with sequence boundaries (Mitchum, 1977). A “seismic facies” is defined, using Mitchum’s original definition, as any seismic attribute that distinguishes one succession of reflection events from another.

Application of numerical models

The Coastal Modelling System is for the simulation of wave propagations from indefinite depths towards the coast line of Masnou area. The wave climate data have been compiled during the phase A of this project. Different scenarios of wave generation and propagation were simulated from the data. The methodological approach designed for the application of numerical models during the phase B is described in the OpTIMAL report of phase B.

The wave climate analysis shows four scenarios of wave conditions. The strongest waves in the area shows NE to E predominant directions and significant wave about 9m (table 1).

Wave direction	Maximum waves			Mean waves	
	ENE	SSW	E	ENE	SSW
Hs (m)	3.5	3.5	3.5	0.5	0.5
T (s)	9	9	9	4	4

Table 1. Wave forcing scenarios defined from long time series of wave data.

These scenarios are considered in the morphodynamic analysis of the nourished beach located at the northern and southern of the Masnou port. The first results of the application of hydrodynamic model are presented in the OpTIMAL phase B report. In this report it has been summarized the most representative ones in the following section.

3. Work on laboratory

The sedimentological data consist in 20 sediment samples collected on the beach; 8 bottom samples and 12 vibrocorders collected on the nearshore. The analysis of these sediment samples is the same on all of them.

Sediment texture

Sediment texture analysis of samples is performed using a coulter counter (Shideler, 1976), state-of-the-art instrumentation that employs laser diffraction to measure the size distribution of sedimentary particles. The utility of the coulter is the high reproducibility of measurements, acquisition of results within less than 15 minutes for each sample, ability to accurately and quickly provide quantitative measure of extremely small grain-size fractions, and customizable data output.

Prior to analysis bagged samples are shaken, stirred, and mixed to homogenize the sediment within the bag and break apart any clay and or sand clumps. An aliquot of sediment to be analyzed is then placed on a petri dish and mixed into slurry in order to break apart any remaining cohesive clay clasts as well as separate major shell fragments from the siliciclastic sample portion. Approximately 20 to 25 grams of each sediment sample is then added to the instruments water-filled containment vessel where the sediment particles become entrained within the circulating fluid. Following the addition of the sediment the sediment-water mixture is sonicated for 8-10 seconds to further disseminate any remaining cohesive clay particles. The sediment and water is then circulated through a laser-light beam; scattering of the laser light as it passes through the sediment water mixture is recorded in detectors mounted opposite the laser source. Recorded diffraction patterns reflect the size distribution of the sediment

because of an inverse relationship that exists between particle size and laser-light scattering.

Textural parameters (mean, standard deviation, skewness, and kurtosis) are calculated from the coulter counter data output using moment measurements.

Composition

Sand fraction components are identified using a binocular microscope. The composition identified and counted includes the following components: biogenic components (mollusc, gastropods ...) and terrigenous (quartz, mica, feldspar, and others).

Carbonate

The carbonate content of the samples is determined using a Bernard calcimeter, according the method described by Vatan (1967). This method has been studied and developed by different authors (Hulseman, 1966 and Muller and Gatsner, 1971). Basically, the assay consists of quantifying the CO₂ released when the sample is treated with hydrochloric acid. In a closed system, under a constant pressure and temperature, and if there are no other gases involved, the quantity of CaCO₃² is directly proportional to the volumetric increase resulting from the release of the CO₂.

FIRST RESULTS

The first results obtained from the data acquired during the phase B has been presented in the IX Jornadas de Ingeniería de Costas y Puertos, in San Sebastián, on may 2007.

The bathymetric maps developed from the data acquired during the three first cruises show the evolution of the dredge and nourishment areas during six months after the activities. Because the dredge activities started on march, the incipient trench can be observed on the bathymetry (fig. 12A). It is an elongated trench of 800 m long between 4 to 7 meters depth. After dredging the bathymetry shows a trench is longer and deeper (fig. 12 B and D).

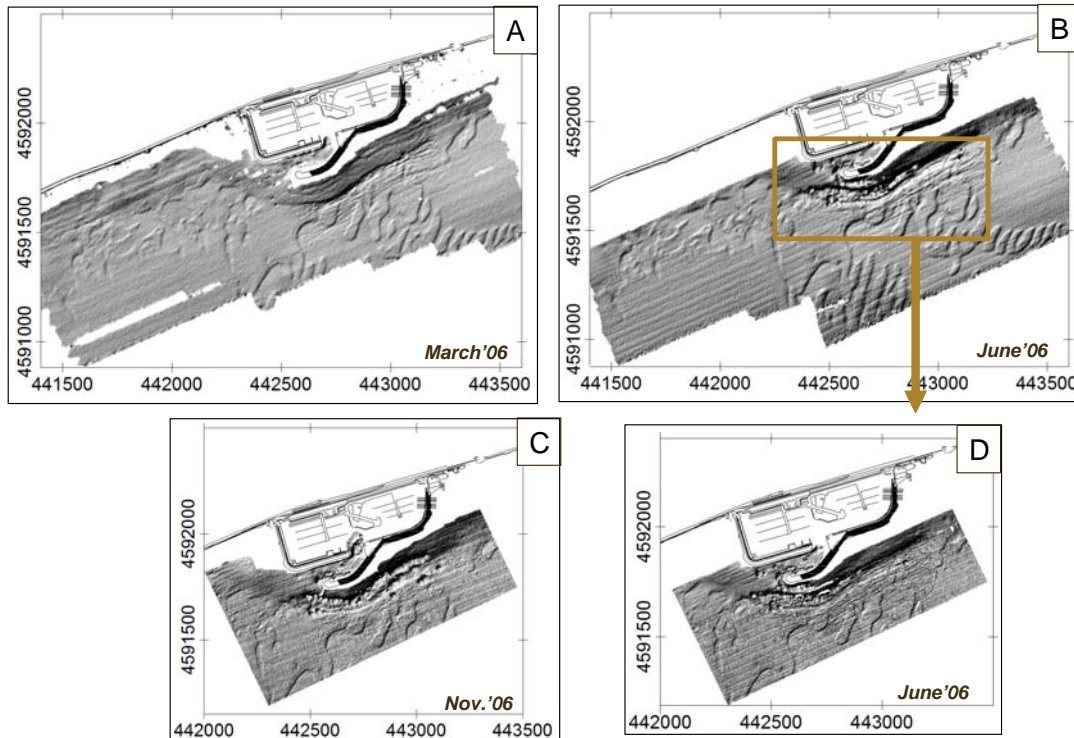


Figure 12. Bathymetric maps of the Masnou dredge area.

The infill of the trench and sand pits can be evaluated from the bathymetries of June (just after dredge) and November (5 months after). Some parts (sand spits and the southern of the trench) start to infill although the dredge activities continued during summer (fig. 12).

The calculus between the bathymetries shows these results and the morphological changes in the trench (fig. 13A). The results between march (at the beginning of dredge activities) and june (just after main dredge activities) shows the morphology of the dredged trench. It is 800 m length and 4 meters depth, although it could reach up to 4.5-5 metres in some sand pits. The difference between november (6 months after dredge) and june reveals information about new dredge activities. New sand pits appears as result of dredge activities (see northern area in figure 13B), while the incipient infill begins in the southern part.

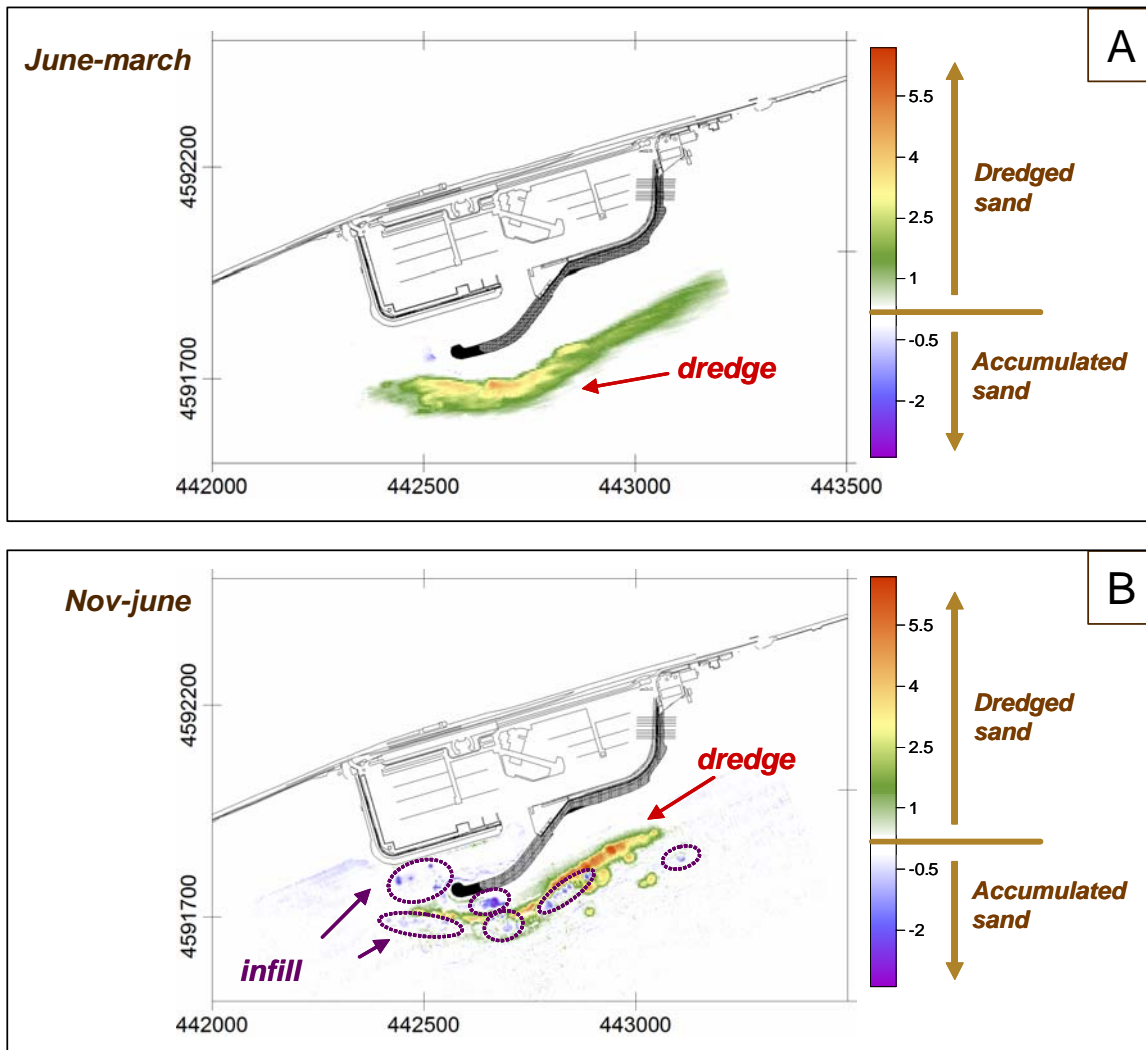


Figure 13. Calculus between consecutive bathymetries: (A) june-march and (B) November-June.

The vibrocorers collected in this dredge area allow characterizing the sand accumulated and the underlay sediments (fig. 14). The sand accumulated in front the harbour is similar to the beach. It is yellow medium to coarse sand composed by quartz. The underlay and surrounding sediments are finer and they are composed by mica (fig. 14).

The uppermost part of some vibros is highly disturbed due to the dredge activities and the incipient fill of sand pits.

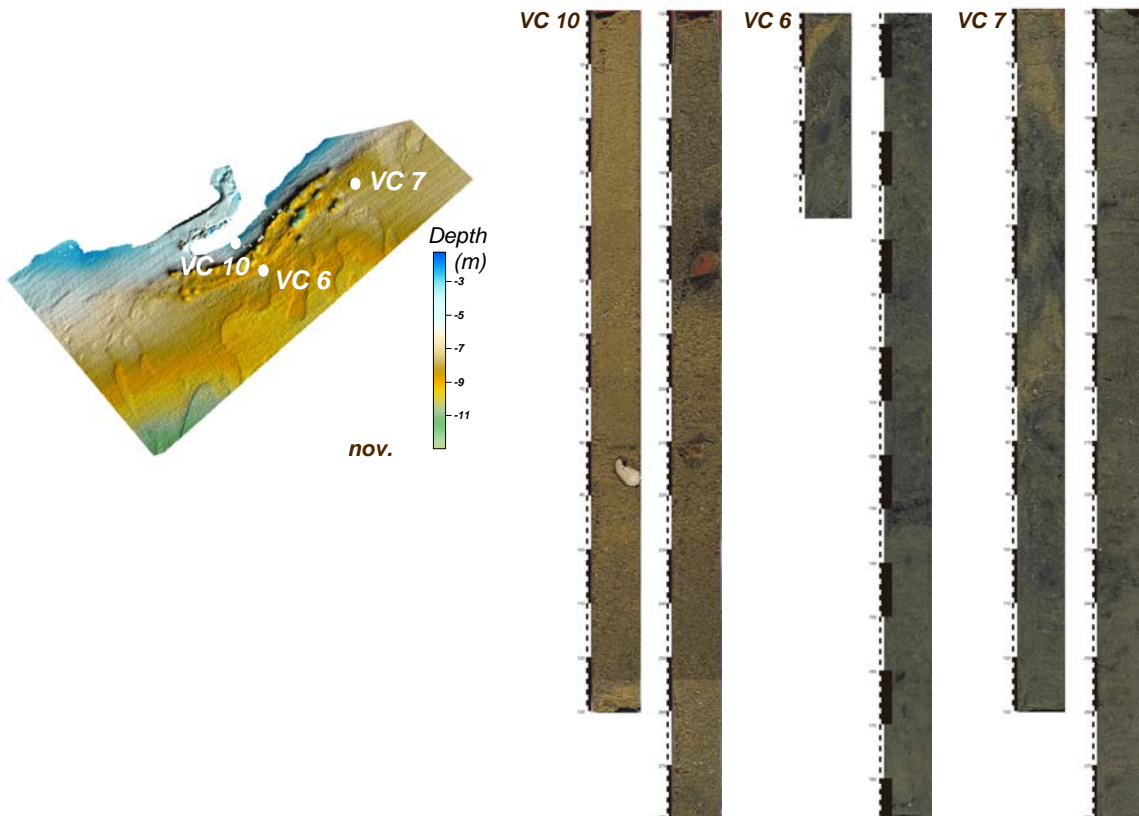


Figure 14. Vibrocoring collected in the dredge area.

References

- FRISH W. (1997) - Tectonic geomorphology. In *Proceeding of Fourth Int'l. Conf. on Geomorphology, Z. Geomorph. N.F. Suppl.-Bd.* 118 pp.
- HULSEMAN J. (1966) - An inventory of marine carbonate materials, *Journal of Sedimentary Petrology* ASCE 36 (2): 622–625.
- JORDAN G. 2004. Terrain modelling with GIS for Tectonic Geomorphology. Comprehensive. *Summaires of Uppsala Dissertations from the Faculty of Science and Technology*, 1031: 41.
- MITCHUM R.M. Jr. (1977) - Seismic stratigraphy and global changes of sea-level, part 1: glossary of terms used in seismic stratigraphy. In Payton, C.E. (Ed). *Seismic Stratigraphy-Applications to Hydrocarbon Exploration. AAPG Memoirs*, 26: 53-62.
- MULLER G., GATSNER M. (1971) - Chemical analysis, *Neues Jahrbuch für Mineralogie Monatshefte* 10: 466–469.
- RADOSLAV B. (2002) - Scale-dependent geomorphometric analysis for glacier mapping at Narga Parbat: GRASS GIS Approach. *Proceedings of the Open source GIS-GRASS users conference*.
- SANTERO F., TONIELL R., DE LAURO D., SIMIOLI A. (2002) - A GIS Application to study the influence of submarine topography and morphology on the development of nearshore benthic fauna of the Sorrento Peninsula (Southern Italy). *Littoral 2002, The Changing Coast. EUROCOAST / EUCC*:195-200.
- SHIDELER G.L. (1976) - A comparison of electronic particle counting and pipette techniques in routine mud analysis. *Journal of Sedimentary Petrology*, 42: 122-134.
- VATAN A. (1967) - *Manuel de Sédimentologie*. Paris (Technip.) : 397 pp.

**2. RAPPORT OF PHASE B:
UNIVERSITY OF BARCELONA – P2
MEASURE 3.3
GESA**

Serra, J. & Valois, X.

Introduction

In this phase B we made three different campaigns: cartography campaign, dredge campaign and vibrocorer campaign. The goal is know morphology and sandy volume of relict structures. Furthermore has been realized analysis of information obtain in previous phase.

River contribution to coastal equilibrium: Tordera and Maresme cell

The Tordera basin has a surface of 894 km² is controlled by geological setting and tectonic structure.

The climatic features basin is Mediterranean type subhumid maritime character; medium annual pluviometric is highest because is zone near sea. The balance interannual is highest. Therefore the average flow is 5m³/s, in storm moments flow is 200m³/s. The Tordera River is pluviotorrential character, with 1 or 3 avenues annuals. The Tordera River has a dominant transport characterized by coarse sand transported by bed load in minor proportion transport suspension and dissolution.

The sediments of the alluvial terrace are coarse sand granitic composition (Rovira, 2001).

The sedimentary balance of the river is determined by precipitation, erosion, temporal storage and the arid extractions. The annual volume sediments calculate in the final part of the river is the 40.000m³ (Rovira, 2001). A potential contribution oh the 200.000m³ of sediment, results are similar than results obtains by drift potential transport, to range 80.000 or 200.000 m³/year (Serra & Montori, 2003).

The value calculated this transport has calculated the relict deltas lobes on the extern shelf, these is a regression during the last level sea rise (Diaz & Maldonado, 1990). This difference is caused by climatic changes and anthropogenic exploitation resources.

Beach cartography

The interpretation coastline evolution has been done realized three cartography campaigns, later compare results with precedents data. We divide study zone in three, sector North of delta (Sabanell, beach Blanes), Tordera delta s.s and sector South of delta (Malgrat-Sta. Susana beach). In sector north there is erosion trend (2m/year), in a delta zone erosion trend (7m/year) and finally sector south is an accretion trend (2m/year). The campaigns observed seasonal changes. In fig.1 we can see evolution coastline, superposed results of three campaigns. In fig.2 there are results of three cartography campaigns, are the 3D simulation by Surfer 8.

Learning from shelf relict and coastal bodies

For geophysical methods, Side Scan Sonar or Seismic methods (UNIBOOM), there has been possible the study of the morphology of the delta of the Tordera. Three relict structures have been recognized on the shelf. The ancient delta is D-I that is a to depth of 50 meters and 9.000 years age, the second delta D-II is a to depth of 30 meters and 7.500years age, and in last place third delta to a depth D-III is a to depth of 15 meters and the present delta D-IV (fig.3). These relict deltas are formed in different eustatic conditions than present situation. The relict deltas presence has served to stratigraphic interpretation of the delta Relict deltas is analyzed by high resolution bathymetry and seismic profiles. The correlation with age to delta is by interpolation of

Aloïsi curve of the Occidental Mediterranean. At present we analysed the Vibrocores results and finally we will do datation and interpretation of structures in a prodelta Tordera.

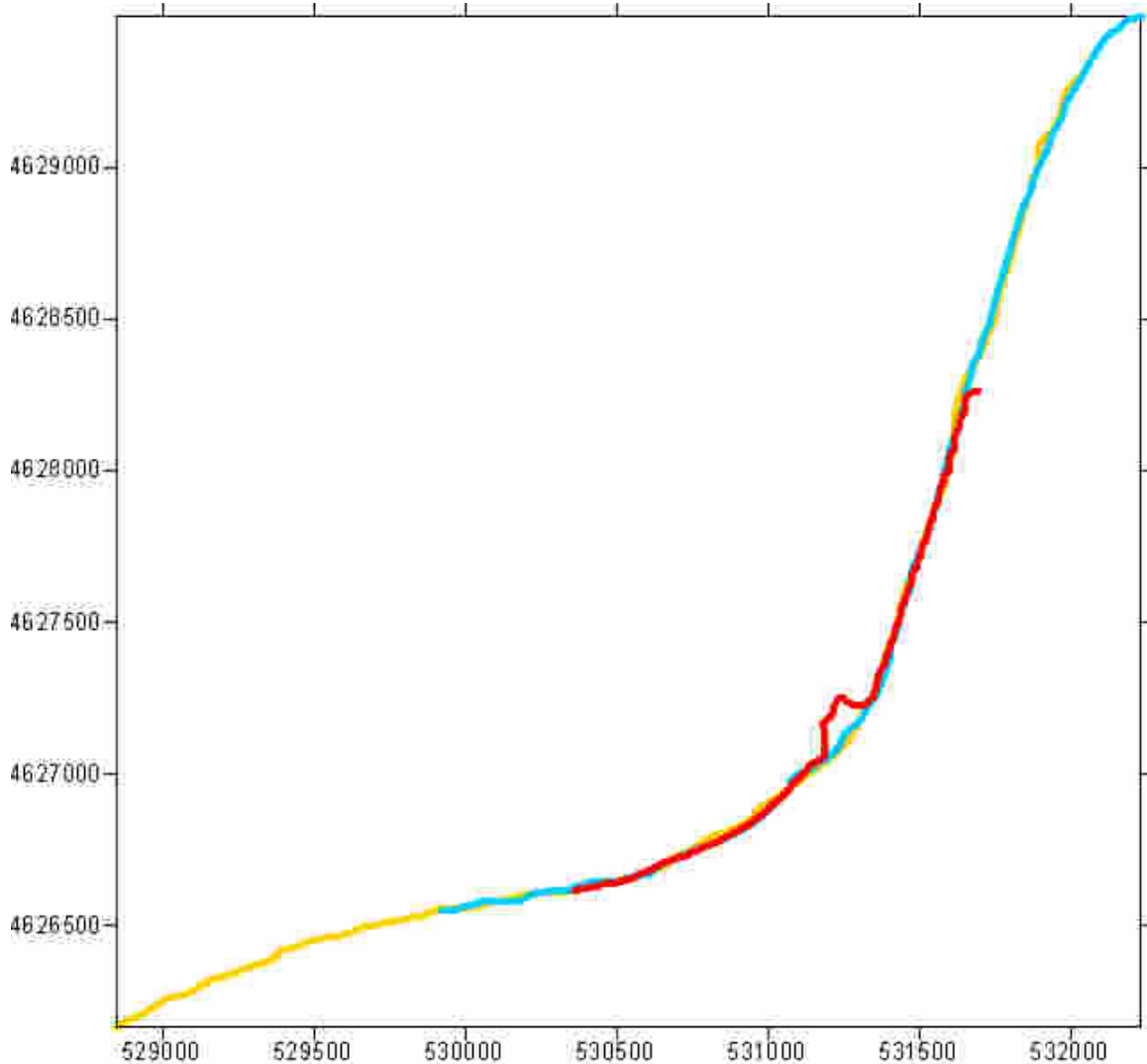


Figure.1. Coastline evolution in a Tordera delta. In colour yellow is a October (2006) campaign, in blue is a December (2006) campaign and finally in a red is a April campaign (2007).

Present delta regimen and prograding rate needs much more volume of sediment for surface unit because it's present new base level depth. This important difference between present delta evolution and that of few centuries ago were base level was D-II top at 35m depth can explain drastic changes in the coastal cell sedimentary transport and equilibrium giving a general erosive trend. The negative Maresme cell sediment balance has been attributed until now to human activity. Present needs of marine sand for beach nourishment purposes give an important value to the stocked sand on those relict sedimentary bodies.

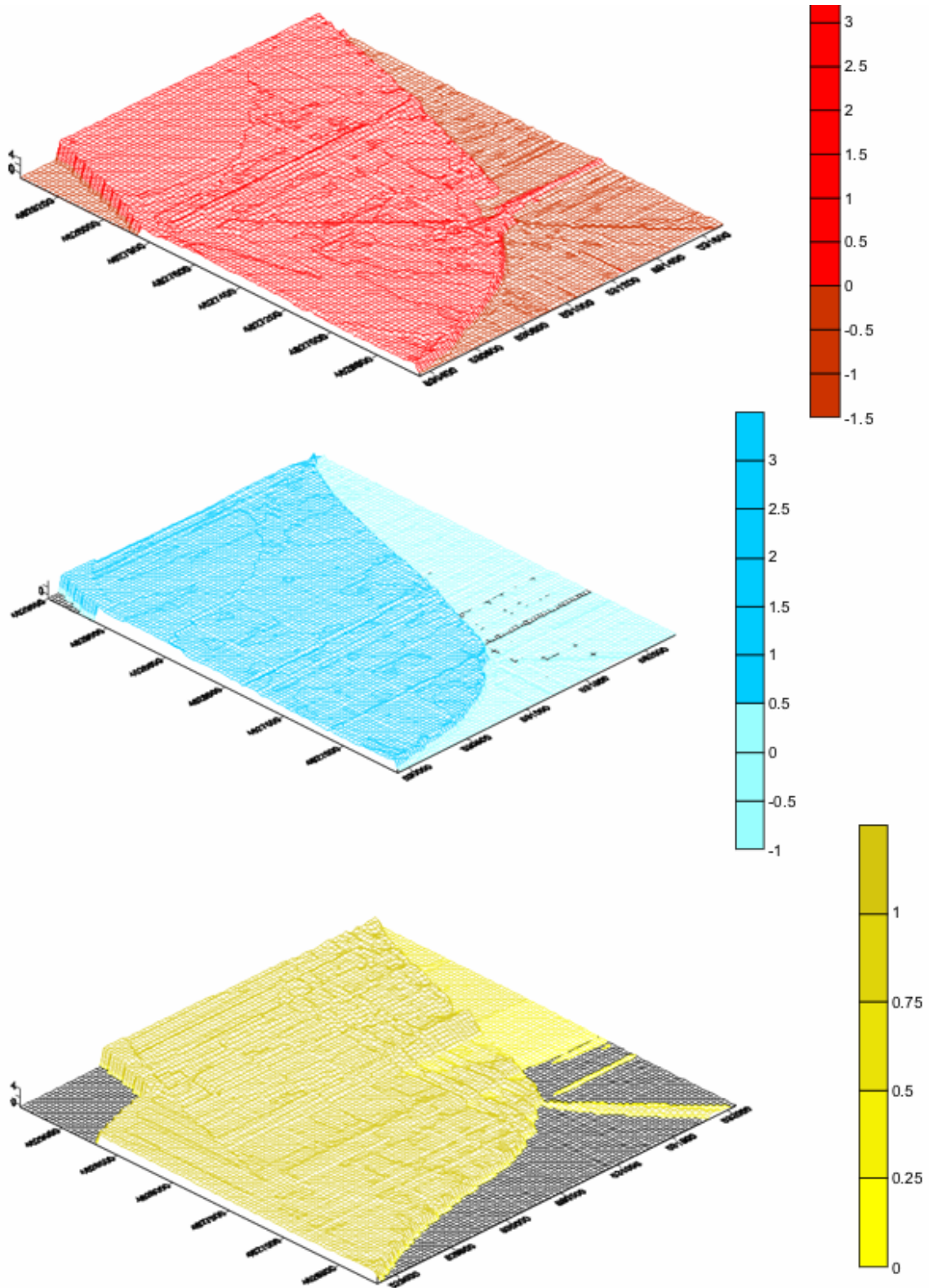


Figure 2. 3D image of cartography campaigns.

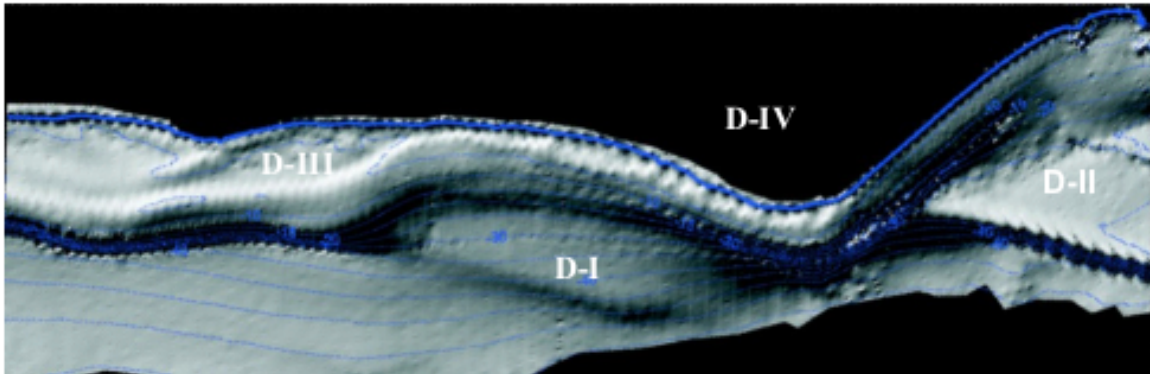


Figure 3. This picture is a high resolution bathymetry and gradient map, MMA. Shows three relict delta lobes (D-I, D-II, D-III) and present D-IV, modified to Hitdma 2002.

Sand resources on prodelta bodies.

The information obtained by bathymetry complemented by SSS campaign it shows accurately of the distribution of the bottom of delta, the dynamics limits and presence gravitational episodes. We have to emphasize the zone of the emissary desalination Tordera it does constitute the most important point for being in a zone of instability (fig.4).

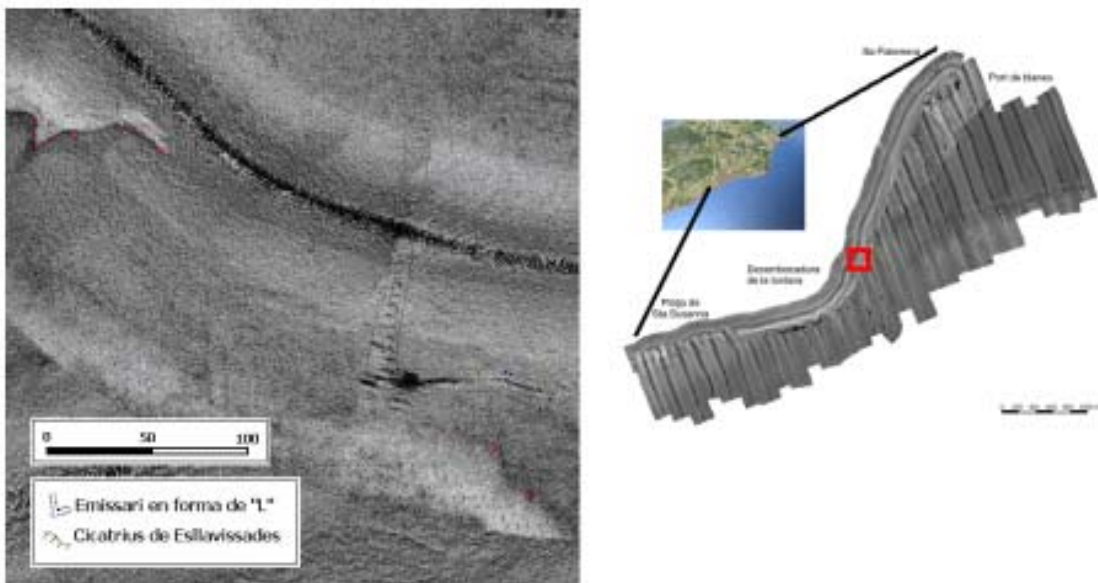


Figure 4. Image SSS scar landslide and emissary.

The Seismic campaign has studied the zone morphology, structure and quantified sand volume in relict lobes. Has been realized 4 profiles in delta zone defined from the study bathymorphologic (fig.5). The result obtained in the profiles shows us the structure of the different units that shape the delta and the existence of internal visible discontinuities only with this type of analysis.

The seismic lines show typologies of sequences depositional that correspond deltaic deposits: progradations, toplaps, onlaps, downlaps that facilitates the genetic interpretation.

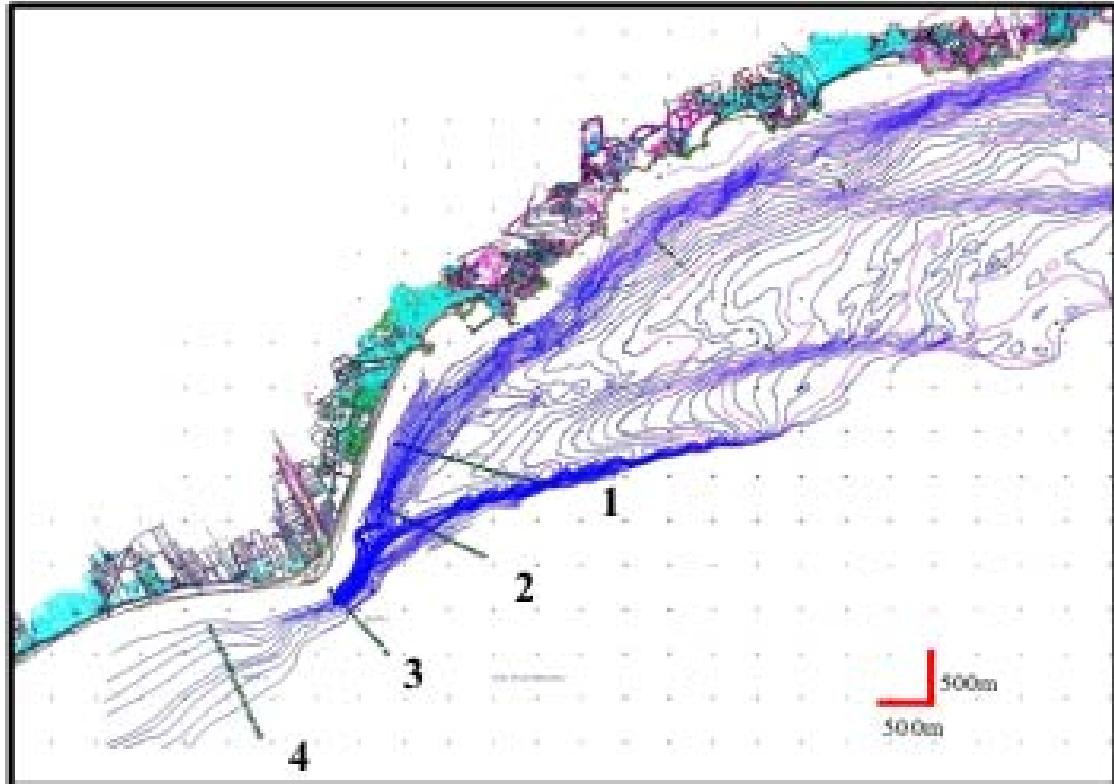


Figure 5. Situation of the seismic profiles realized in the delta of Tordera.

Description of the seismic profiles

Profile 1: The materials nearest to the coast have a few thicknesses of 30m (Holocene materials). The plane situated in the deltaic slope also it has 30 meters in the most external zone. In the zones placed in the base of the talus there are chaotic sediments because landslide. The second slope passed 30 to 60 m in less than 200 meters, with angle of 10° . The profile show different levels of estratigraphic construction (fig.6).

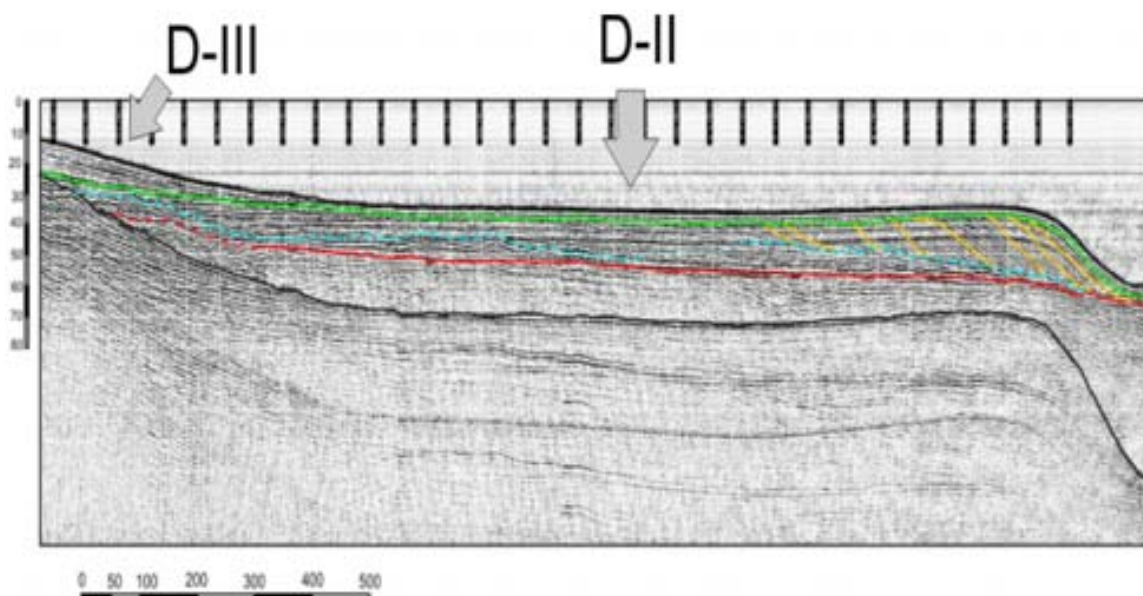


Figure 6. Profile 1 (north hemidelta of the Tordera).

Profile 2: This profile begins with the present slope very near to the present coast, where we observed the previous plane; both units limited by the two slopes do not have any more than 300 meters of length in the profile (fig.7).

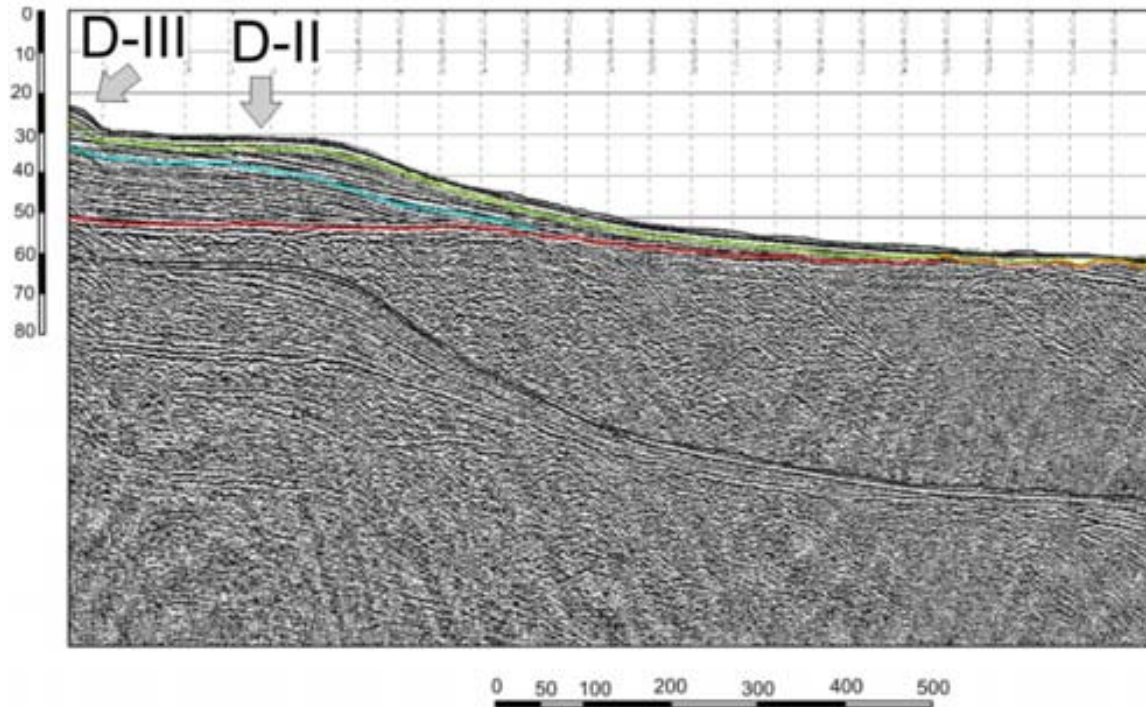


Figure 7. Profile 2 (north hemidelta of Tordera, near deltaic front).

Profile 3: This profile is in front the mouth of the Tordera River (fig.8); this characterized a high gradient 20°. We can quantify relict deltas in a zone. In this profile the materials of the present delta are in 60m depth whereas on the coast are 30 m depth above relict structures.

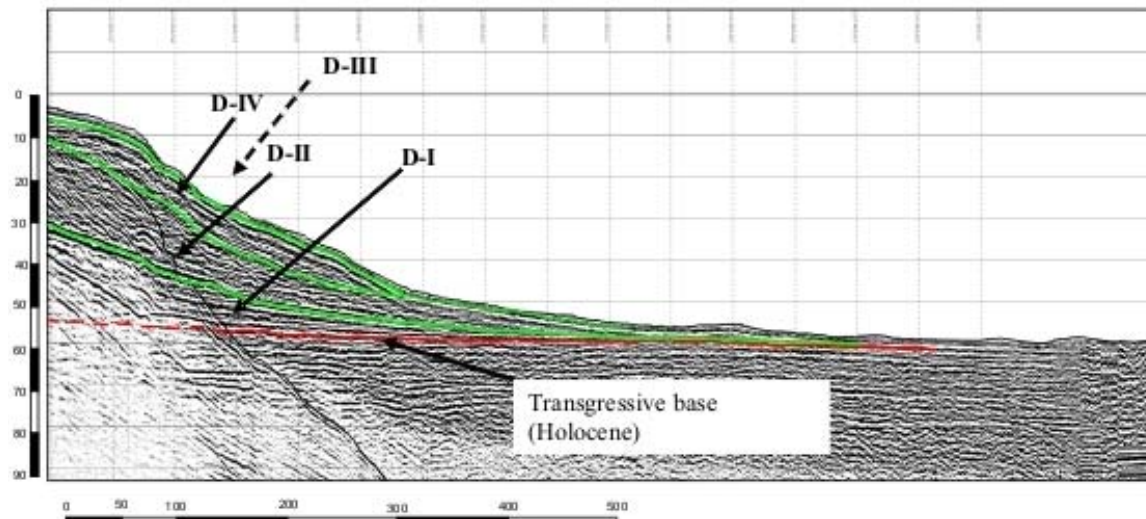


Figure 8. We can see seismic profile 3, its structure interpretation. In this profile we can see the relict deltas in a Tordera zone.

Profile 4: Profile realized to the south mouth delta Tordera where are observed escarpment that had been smoothed (fig.9). The zone nearest to the coast the materials

are 30 m depth whereas far the coast have a 3-4m above relict structures. In this profile is observed a structure of relief of channel parallel to the line coast to approximately 20 meters. These sediments of the replenishment to channel correspond to a former channel of the Tordera River when the Sea Level Rise was 80 m upper present situation.

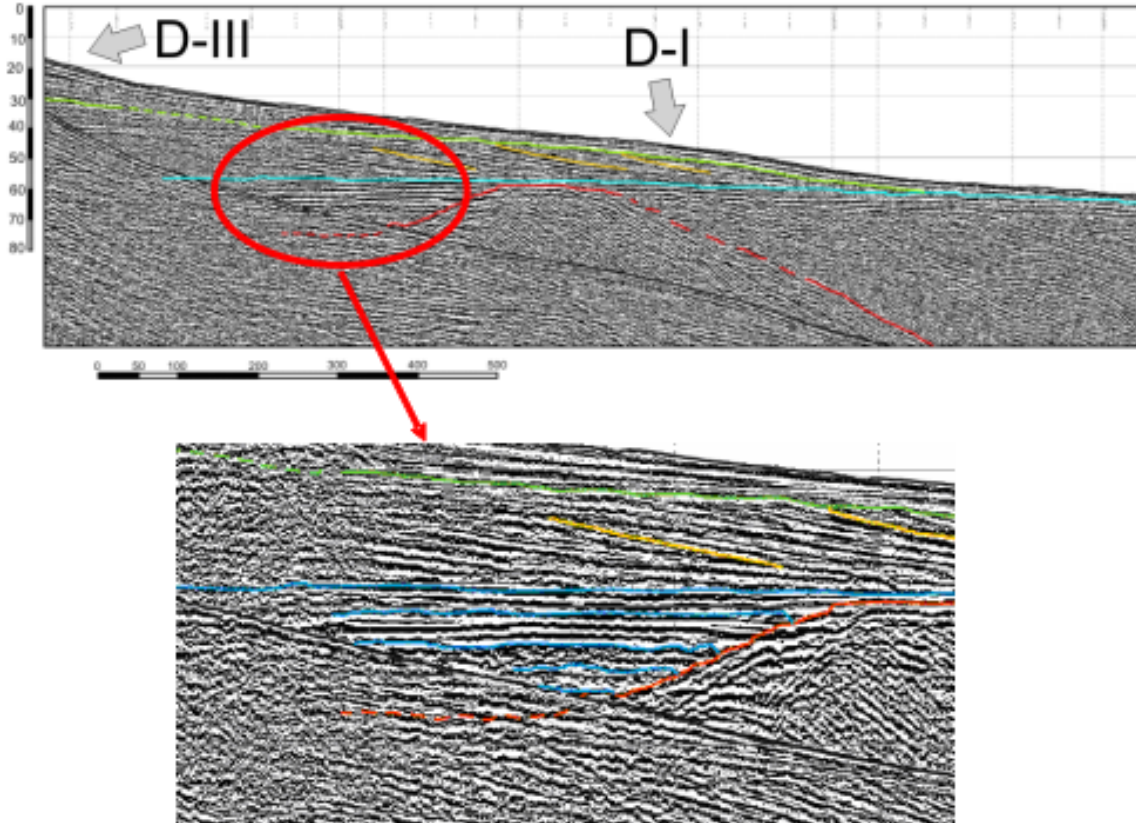


Figure 9. Profile 4, detail of the profile 4 where we can see the paleochannel and the replenishment by transgressive sediments above are developing deltaic sequences present.

Also we realized a dredge campaign in Tordera delta zone. There have been realized six profiles perpendicular of coast (fig.10). The goal this campaign is to characterise the material and know composition of sand (Tab.1). We have realized sedimentology and visual analysis of samples and % carbonate. The results give coarse sand, a granitic composition these factors are valid to analyse the structures relicts in a Tordera zone.

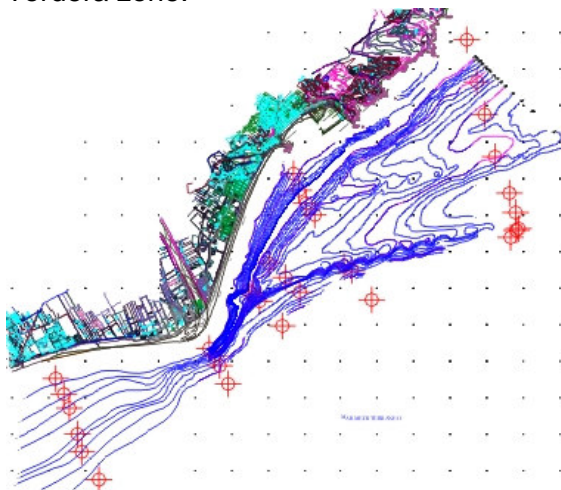


Figure 10. This map of situation dredges profiles.

Dredge campaign April 2007								
	X(WEST)	Y(NORTH)	DEPTH (m)	MODE	Median	<63 µm	% CaCO ₃	Comments
07 TD/1	Sta. Cristina beach 170°							
07 TD 1-1	485825	4612195	58,5	223,4	313,6	5,79%	54,55	Transgressive surface
07 TD 1-2	485904	4612293	50	648,2	718	1,78%	30,39	Talus D-II
07 TD 1-3	485934	4612316	39	471,1	548,3	2,16%	25,4	
07 TD 1-4	485893	4612536	40	1091	913,4	4,87%	45,33	Plane D-II
07 TD 1-5	485810	4612800	42,7	993,6	778,6	17,00%	63,76	
07 TD 1-6	485612	4613300	33,5	340,2	995,6	6,12%	42,34	
07 TD 1-7	485470	4613879	34,8	1091	1044	0,81%	12,2	Littoral prism
07 TD 1-8	485363	4614324	29,5	156,6	824,7	0,89%	4,98	
07 TD 1-9	485227	4614900	15	429,2	411,3	0,72%	5,48	
07 TD/2	Palomera 330°							
07 TD 2-1	483929	4611341	59,5	1909	211,6	12,50%	41,1	Transgressive surface
07 TD 2-2	483660	4611745	50	684,2	611,1	9,26%	38,36	Talus D-II
07 TD 2-3	483550	4611798	30,5	684,2	717,9	1,76%	25,4	
07TD 2-4	483367	4612095	32,5	993,6	914,1	2,31%	18,93	Plane DII
07TD 2-5	483132	4612503	19,5	140,1	178	4,98%	15,69	
07TD 2-6	483013	4612664	25	153,8	171,3		3,49	Littoral prism /D-IV
07TD 2,7	482915	4612840	19	153,8	171,3	3,20%	1,74	
07TD 2,-8	482842	4613067	12,5	168,9	201,6	2,06%	1,74	
07TD/3	Sabanell south							
07TD 3-1	482690	4610984	56,2	140,1	157,8	10,00%	13,7	Delta Front D-IV
07TD 3-2	482377	4611321	36	127,6	149,3	9,46%	3,24	
07TD 3-3	482265	4611429	28	1091	1059	0,84%	2,74	
07TD 3-4	482227	4611467	19,5	905,1	890,9	0,28%	0,25	
07TD3b-5	482508	4611836	29,5	1091	962,4	2,13%	0,75	
07TD3b-6	482735	4611645	30	623,3	648	1,93%	4,48	
07TD3b-7	482928	4611445	49,7	153,8	190,3	10,40%	17,68	
07TD/4	Tordera Front							
07TD 4-1	481949	4610190	58,3	429,2	235,3	8,47%	2,24	Talus D-IV
07TD 4-2	481832	4610439	47---49	429,2	410,5	3,73%	2,24	
07TD 4-3	481769	4610577	31	623,3	586,8	1,51%	1,99	
07TD 4-4	481692	4610674	10---9	567,7	583,6	0,34%	1,99	
07TD/5	Malgrat Z1 a 335°							
07TD 5-1	480186	4608880	56	116,3	110,8	27,10%	8,97	DI/D-IV
07TD 5-2	479989	4609210	45	684,2	611,1		2,49	
07TD 5-3	489892	4609503	35	116,3	118,9	16,80%	1,99	
07TD 5-4	479782	4609857	25	116,3	123,6	12,70%	1,74	
07TD 5-5	479707	4610051	14	429,2	400,4	0,75%	0,5	
07TD 5-6	479596	4610263	4	824,5	674,5	0%	2,49	
07TD/6	Búnker							
07TD 6-1	475848	4608427	4	623,3	585,3	0,13%	0,75	Spit
07TD 6-2	475932	4607752	2,5	623,3	654,3	0,08%	1,49	
07TD 6-3	476213	4707480	41,7	517,2	445,8	8,66%	3,24	
07TD 6-4	476235	4607552	29	905,1	843,5	1,20%	1	

Table 1. In this table sees results analysis textural, compositional of dredge campaign

Finally we realized a Vibrocoring campaign to analyze the chronology of the sedimentary record. At present we have studying this cores and have an interpretation (phase C).

Interpretation and chronology of the deltaic structure

The interpretation of the seismic profiles with the bathymetric information previous confirms deltaic bodies in the shelf. These deltas were formed in the last glacial stadium does 18 Ka with a marine level of 110 m for below of the present level (<6Ka, Holocene deltas). We have recognized three relict deltas in the zone by seismic

campaign. Together a Seismic campaign it has been realized a cartography and dredge campaigns with goal to observe the changes in sand delta. Tordera delta and spit have at least a volume of sand 38 millions of cubic meters (Serra. J. & Valois, X., 2007).

The delta D-I is possible observed by profile 3 and 4, it presence indicates growth to us it south is it direction and it's observed by bathymetry. The delta D-II is visible in the profiles north hemidelta where we observed that it finished in an extensive plane. A Sea level Rise could be created of the delta D-III. When came present Sea level delta was formed.

The chronology of deltas is doing by correlation with curve Aloïsi (1986) Mediterranean Occidental information (fig.11). These values will be corroborating by analysis of datation testimonies vibrocorer.

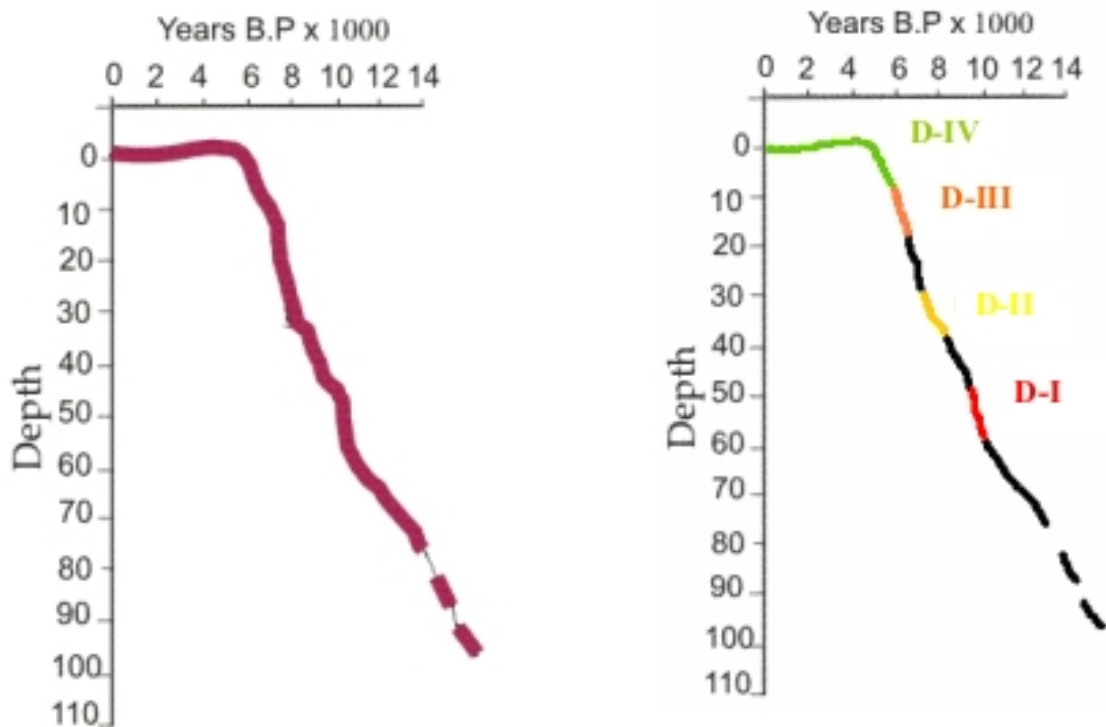


Figure 11. We can see the Aloïsi Curve (1986) to Mediterranean Occidental with interpretation and correlation with relict deltas.

Finally by interpretation seismic profiles and bathymetry Tordera delta D-II and present spit have at least a volume of sand of 38 millions of cubic meters.

References

- ROVIRA, A. (2001) - Balanç sedimentari i dinàmica fluvial en un riu de règim hidrològic transitori. (tram final del Tordera). Tesi doctoral. Univ. De Barcelona.
- SERRA, J., MONTORI, C.(2003) - Morphology and sedimentary processes of subaqueous Tordera River Delta (NW Mediterranean). Coastal Sediments 2003, proceedings.
- SERRA, J., VALOIS, X., PARRA, D. (2006). Estructura del prodelta de la Tordera (Costa del Maresme, NO Mediterráneo) a partir del anàlisi sísmico de alta resolució. Sociedad Geológica Española. En prensa.
- SERRA, J. & VALOIS, X. (2007) -Sand budget on Holocene relict delta Tordera bodies and spit (Maresme coast, NW Mediterranean). 2ond International Conference Coastal Conservation and Management, 225:226.



- SERRA, J & VALOIS, X. (2007) - Evolución de la costa del delta del río Tordera durante el último ascenso eustático (Holoceno). IV Reunión de Geomorfología Litoral. Investigaciones recientes (2005-2007), 61:64.
- SERRA, J., VALOIS, X., VIDAL, J.R., MARTÍNEZ, H., SANCHEZ-HORNEROS, T., MARTÍNEZ, F. (2007) - Procesos litorales en el delta del Tordera: dinámica litoral, estabilidad e infraestructuras. IX Jornadas de Puertos y Costas. San Sebastián. 191:192.
- VALOIS, X., SERRA, J., MONTORI, C. (2006) -Coarse sand relict deltas processes and Sea level Rise: the Tordera delta (NW- Mediterranean). ISC 2006. Fukuoka. Japan, vol. A: 83pp.

**3. RAPPORT OF PHASE B:
UNIVERSITY OF BOLOGNA/DISTART - P3
MEASURE 3.3
GESA**

Lamberti, A., Martinelli, L., Merli, D. & Piemontese, M.

1. Research activities and problem

The objective of University of Bologna is to define the best methodology for nourishing the beach with sand dredged from port entrance channels.

In phase A the study site was selected. The works consist of the dredging at Porto di Cervia with nourishment in Milano Marittima. The idea of employing the dredged sand as nourishment is certainly a good example of coastal management. Indeed the works are necessary to allow navigation and the nourishment saves costs for waste disposal and is a benefit to beaches.

These works have been carried out in the period 14.04.07-31.05.07.

In phase B, the main task is to identify methods of analysis to be used in Phase C.

Such methods are presented in Section 2 of this document.

Actually UNIBO-DISTART virtually anticipated part of the activity to be carried out in Phase C. This happened because the same kind of works (dredged and nourishment), with the same technology, have been unexpectedly carried out in another site (Porto Garibaldi and Lido di Spina).

Such works, scheduled for year 2008, have been anticipated due to administrative reasons and have been monitored and documented in order to have a preliminary insight of the possible problems that will be faced in Phase C. The works and the relative analysis is presented in chapter 4. The main conclusions are drawn on the basis of a calibrated model, developed within eudrep project:

- The order of magnitude of the turbulent dispersion induced by releasing sand into water is 0.1 m²/s (a novel result here anticipated, that will be better supported in Eudrep project, Phase C);
- The order of magnitude of the expected losses during the works is 5%.

This preliminary investigation allowed a tests of effectiveness of the identified methods.

2. Techniques for possible design of dredging and nourishment

When planning coastal operations involving the transfer of sands, a crucial point is the definition of the strategies and techniques of transport. For example, in the northern Adriatic Sea there is no availability of big dredgers (i.e. With loading capacity of thousands of m³), for at least two reasons: the limited range of dredging and nourishment works during recent years, and the relative small water depth along the shore.

As a result, during the last decades beach nourishments were carried out with traditional methods, (i.e. the transport with dumpers), as the needed materials were obtained almost exclusively from quarries or pits. Delivering the sediments by land is also possible through pumping the desired mix of sand and water directly on the shore into a pipeline: this technique is commonly adopted to displace the sand if the beach to be replenished is stretched longshore.

The necessary dredging from the port approaching channels provides sediments which consist mainly of sands moved from adjacent beaches by longshore currents. Therefore, in more recent years, local administrations of Emilia-Romagna considered the possibility of using such material for nourishments. This solution partly eliminated the problem (and the costs) of discharging dredged sediments.

This possibility paved the way for a development of maritime transport of sand, which is surely the most practical solution, and sometimes the only one, when large amounts of sediments have to be delivered. Moreover, the great loading capacity of dredgers often determines littler costs per unit of volume of sand involved by the whole dredging-nourishment work.

2.1. Land transport

Lorries

Delivering sediments on land by dumpers or through a pipeline has evident disadvantages, consisting mainly of the impacts on the environment.



Figure 2.1. A dumper transporting sand (Picture by SARTI Spa)

As the loading capacity of a dumper is about 15-18 m³ (see fig. 2.1), a beach nourishment could be completed in thousands of trips: that is the reason why road transport may cause traffic congestion. In any case, the passage of such number of vehicles will cause structural damage on paved surfaces and a relevant atmospheric and acoustic pollution.

Pipelines

A pipeline is less disturbing although it constitutes a continuous obstacle along the beach; moreover, the presence of the pipeline will force the opening of a long yard, which is difficult to control and has a negative impact (see figure 2.2).

Moreover, a submerged pipeline can be efficiently used to “by-pass” a port approaching channel, when sediments have to be transferred from one side to the other of the port. This is the case of the works carried out between November 2003 and April 2004 at Porto Garibaldi, where the southern side (Lido degli Estensi), subjected to intense deposition of sand, was the source of material for the nourishment of the northern beaches (through a length of 6 km).

In this case, the amount of sand daily delivered was evaluated to be 1.800 ÷ 2.200 m³. Although the transport with dumpers could have been equivalent in terms of volume transferring rate, the by-pass of the port entrance through the existing roads had to be considered an impossible solution for evident practical reasons.

In conclusion, the main advantage of land transport is the possibility to have the nourishment sand directly on the shoreline. In particular, a pipeline allows to perform a more punctual and precise delivery of sediments, thus reducing the subsequent work of excavators and scrapers to obtain the desired profile. As the pipeline transfers a mix of sand and water, a further positive aspect of this method is the simultaneous washing away of the finest fraction of the sediments (see fig. 2.3).



Figure 2.2. Picture of a long pipeline during a nourishment at Lido degli Scacchi
(Picture by SARTI Spa)



Figure 2.3. A pipeline delivering diluted sand precisely where it is needed

2.2. Maritime transport

In general, maritime transport nearly eliminates the disturb on the existing coastal environment. Limits to this practice are represented by meteo-marine conditions.

In some cases, the presence of a dense fog during the morning hours heavily interfere with any kind of maritime operations; this happens, for example, in the northern Emilia-Romagna coastal zones during winter months, when nourishing works are most probably planned.

However, another restrictive limit is represented by the low water depth, particularly along the northern Adriatic Sea coastline, accentuated by the temporary low tide levels. In such cases the impossibility to get sufficiently close to the shoreline occurs: this fact emphasizes the need of new solutions.



Figure 2.4. A barge used for sediment transport along the coastline of Emilia-Romagna

Direct transport

Sands can be deposited offshore the eroded beach, in the so called “submerged beach” or pumped inshore.

In the first case, the constitution of a submerged berm does not have the only purpose of recreating the previously present amount of sediments, but also produces a physical interference in the interaction between the beach and the sea. In particular, lowering the water depth in front of the emerged beach means a dissipation of the wave energy at a greater distance from the shoreline, thus resulting in a reduction of the erosion mechanism.

However, applications of this method do not always provide evidence of the desired advantages: movements or losses of the deposited material may occur, reducing the effectiveness of the expected mechanism. In general, the prediction of the behaviour of nourishment sand on the submerged beach should be approached taking in account the dependency on many factors, including the following:

- the grain-size distribution of both the previously present and the added sediments;
- the morphology of the seabed;
- the directions and the distributions of longshore sediment transport;
- the presence of coastal defence structures and their interactions with the local currents;

More information about the design problems related to a nourishment that involves the submerged beach can be found in: BEACHMED, Technical Notebook - phase “A”, Chapter 5 (May 2004); BEACHMED, Technical Notebook – phase “C”, Activity 4 (December 2004).

An alternative solution is offered by the use dredgers that are adequately equipped with a pump station and are able to connect to a pipeline which delivers the mixture of sand and water to the eroded beach. The connection is made possible through the interposition of an offshore platform; then, structures supporting the pipeline at the water level are required. This method combines the advantages of maritime transport and the possibility to have the delivered sand directly on the shoreline.

Temporary deposit

The solution presented at the end of the previous paragraph could be particularly suited for the morphology of Emilia-Romagna coastal zones, characterized by low water levels at relatively large distances from the coastline. Being not disposable the types of dredgers described before, the construction company “Sarti Ing. Giuseppe & C. Spa” recently performed the nourishments at Lido di Spina and

Milano Marittima with a particular technique that consists of the temporary deposit of the dredged sand.



Figure 2.5. Dredging operations at the entrance of the port of Cervia

The exceeding sediments at the port entrance are dredged with a bucket mounted on a barge, in which the collected sediments are loaded; the barge has a storage capacity of 600/800 m³. During this work phase the barge is anchored with its own mooring piles, thus allowing in usual conditions the navigation of other boats coming in and out of the port (see fig. 2.5).



Figure 2.6. Deposition of sand into from the barge into the delimited area

The load is carried approximately 300 m offshore the eroded beach and is deposited using the same bucket into an area delimited by sheet pile walls, as illustrated in figure 2.6. From this area the adequate mix of sand and water is pumped and delivered onshore through a pipeline, while the barge comes back to the port entrance to continue the dredging. The repeated transport of a full load of the barge (2/3 trips per day) allows the completion of a 20.000÷30.000 m³ nourishment within a period of one or two winter months (including bad weather days).

The temporary deposit area is part of a “booster station” that includes:

- a supporting structure for the sand pump, which is moved vertically through an hydraulic hoist (see figure 2.7);

- a platform that provides the location for the pump's power pack and for a the data processing panel; from there, the polyethylene pipeline (D = 315 mm) conveys the diluted sand towards the beach.



Figure 2.7. The sand pump

All these structures are built on sheet pile walls and constitute an offshore yard, reached by the personnel by boat. The scheme of the “booster station” is illustrated in figure 2.8; a view of the maritime yard from the Milano Marittima nourishment site is provided in figure 2.9

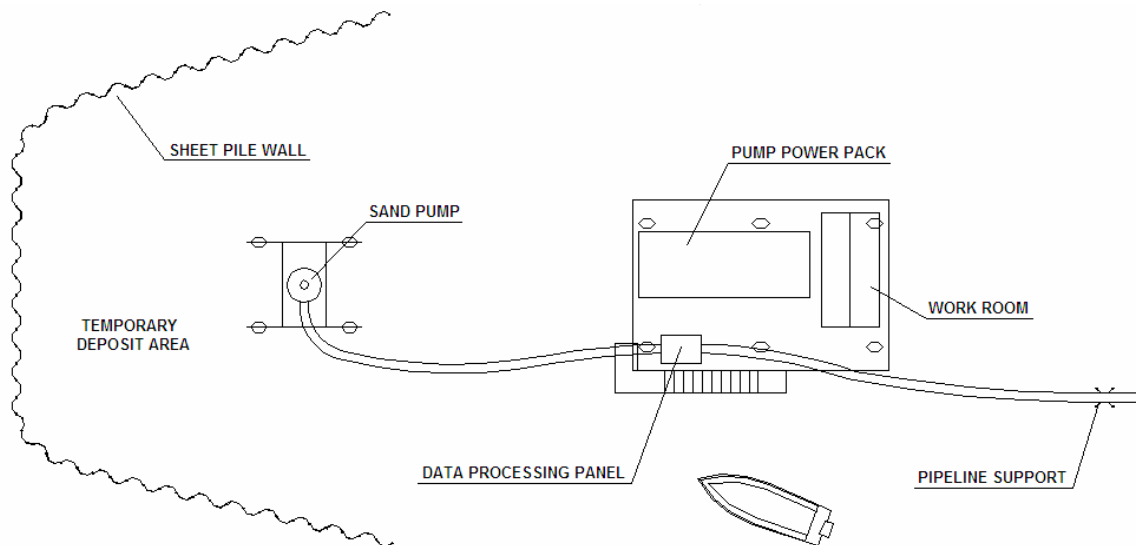


Figure 2.8. Scheme of the “booster station”

This method proved to be efficient, although it has the disadvantage of the turbidity introduced by the transfer of sand from the barge to the delimited area (see par. 4.1); further studies about the impacts of this phenomenon should be carried out, with particular reference to the implications on water quality and on the protection of marine fauna.



Figure 2.9. The “booster station” approached by the dredger (seen from the beach)

2.3. Further considerations

In coastal areas of Emilia-Romagna, the simultaneous presence of port entrances to be dredged and of growing or eroded beaches suggests the valorisation of littoral sediments moved by longshore currents.

Then, the dredged sand can be seen as a resource rather than a waste to be discharged or a fastidious result of natural transport processes; the purpose of that does not only consist of cost savings, but also of an integrated and more efficient coastal management. The predisposition of the “by-pass” of Porto Garibaldi (par. 2.1) and the combined dredging-nourishment cases presented below are clear examples of operations based on this point of view.

3. Case study: Cervia-Milano Marítima

The port of Cervia is located approximately where a convergence occurs between the north-directed and the south-directed sediment transport currents: that's why frequent dredging operations of its approaching channel are required.

The simultaneous lack of sand on adjacent beaches of Milano Marittima suggested in recent years the possibility to use such dredged material for nourishments of adjacent beaches (see table 2.1)

<i>Period</i>	<i>Amount (m³)</i>	<i>Destination</i>
1998	28.000	Offshore nourishment
May 2004	25.000	Offshore nourishment at Milano Marittima
January 2005	5.000	Offshore nourishment at Milano Marittima
April-May 2007	64.000	Nourishment at Milano Marittima

Table 3.1. Recent nourishment operations with sediments dredged from the port of Cervia

In relation to the dredging works at the port entrance, bathymetry data are available since December 2003. The last operation (April-May 2007) had the purpose of replenishing the northern 500 meters of the beach of Milano Marittima with 25.000 m³ of sand; before and after the execution, surveys of the port bathymetry and of the nourished beach have been carried out by the construction company who undertook the work.

3.1. Survey of the port entrance

Using a Topcon GPS instrumentation, all the measured points were defined in plan; reference to the mean water level (UTM-ED50 coordinates) was made with a tie to the benchmark n. 111051 (established by ARPA Emilia-Romagna at "Bagno Haiti", Milano Marittima).

The GPS instrumentation, which provides measurements in double frequency L1+L2 GPS/GLONASS, consists of two receivers:

- a Topcon Hiper Pro, used as "base" station, with a precision of 3 mm + 0.5 ppm (fig. 3.1);
- a Topcon GB500, used as "rover" station, with a RTK precision of 10 mm + 1.5 ppm.

The bathymetric data were obtained with a Sonarmite SM2BT echo sounder, which was directly connected to the computer equipped with a visualisation software (see fig. 3.2.). The whole instrumentation was set up on the boat used to cover the dredging area (300 m x 300 m).

The echo sounder performs an indirect measure of the water depth. The quantity directly measured by the instrument is the time needed by a sound impulse to reach an "obstacle", in this case the seabed, and to come back. The product between the measured time interval and the sound speed in water, assumed to be equal to 1500 m/s, provides the distance of the seabed from the transducer of the echo sounder, which is submerged. Adding to this value the vertical dip between the transducer and the water level, the real water depth can be obtained.



Figure 3.1. The Topcon Hiper Pro used as “base” station at the nourishment site of Milano Marittima

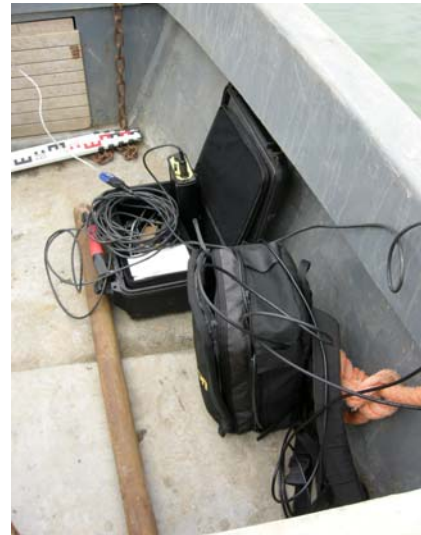


Figure 3.2. left) A computer collects the bathymetric data; right) Part of the echo sounder and of the GPS instrumentation



Figure 3.3. The bar supporting the “rover” station and the submerged transducer of the echo sounder

The GPS receiver is fixed at the top of the bar which also supports the transducer of the echo sounder, which is submerged (see figure 3.3). The echo sounder can measure 3 points per second; the horizontal position of two of them is interpolated, as the GPS receiver picks up its position only once per second.

Then, the collected data have been processed with the software Geopro Meridiana, to obtain the survey result on an AutoCAD LT 2006 .dwg file. Figure 3.4 illustrate the results.

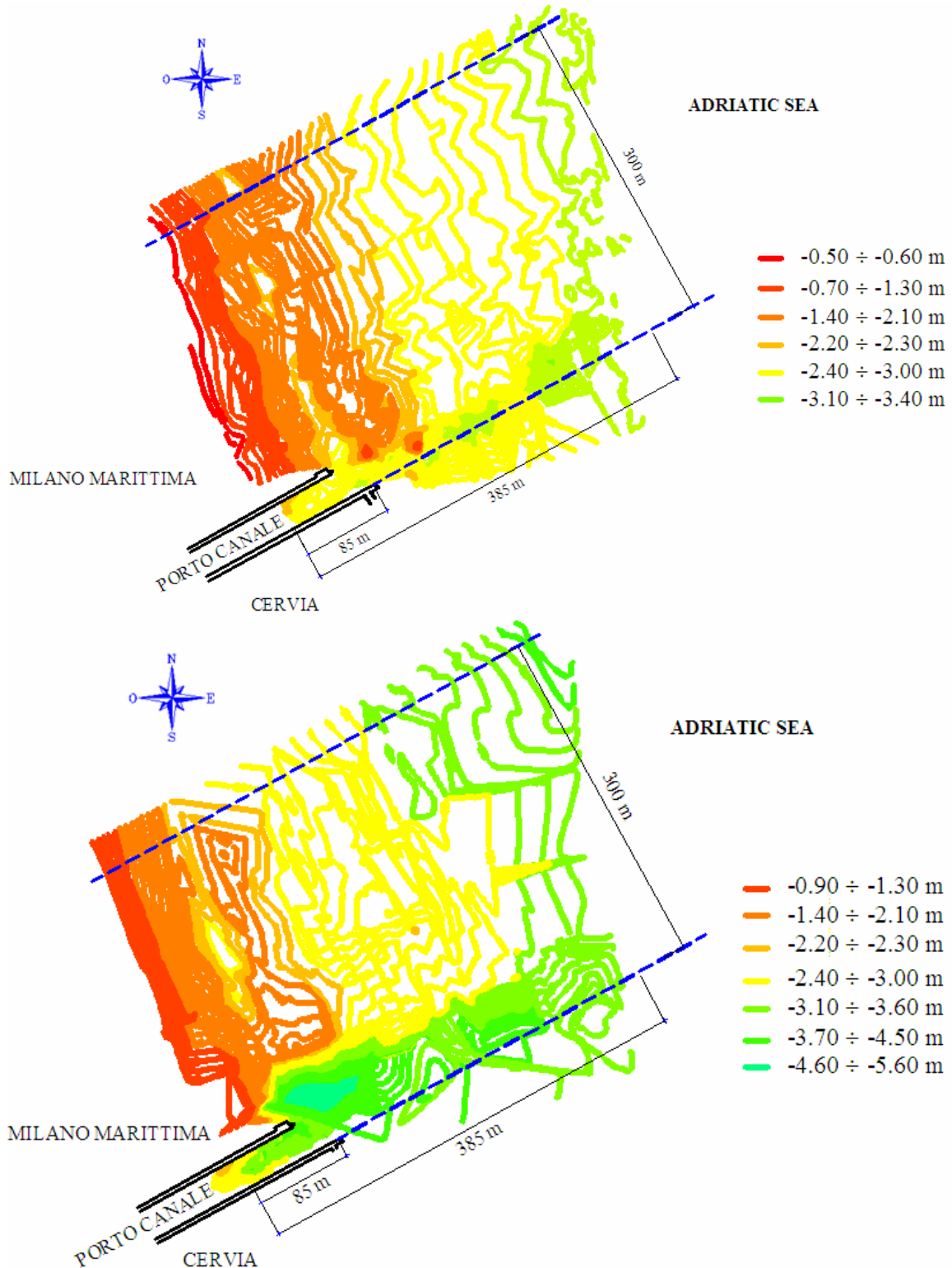


Figure 3.4. Top) Results of the survey before the dredging (13.04.2007); Down) Results of the survey after the dredging (1.06.2007)

The points captured on the emerged beach were selected at relevant locations (e.g. variations of the beach slope), and the surveys were made manually holding in a vertical position the “rover” station.

The bathymetric values for the submerged beach were obtained, at the end of the nourishment, with the Sonarmite SM2BT echo sounder previously described; in this case, the boat moved delineating the 11 established transversal sections. At the beginning of the operations the measures of water depth were carried out manually using a telescopic levelling stave and capturing points at regular distances.

4. Case study: Porto Garibaldi-Lido di Spina

For nourishment of Lido di Spina (February-March 2007), the “temporary deposit” method described in par. 2.3 was adopted. Figure 4.1 illustrates the locations of the dredged and of the nourished area; in this case, nearly 30.000 w dredged from a 600 m x 100 m area (see also figure 4.7).



Figure 4.1. Plan view of the dredged (Porto Garibaldi) and nourished (Lido di Spina) sites.

4.1. Considerations about the adopted method

During the execution of this work, a study was carried out about some aspects concerning the presence of an offshore “booster station” (Merli, 2007). In particular, the structural behaviour of the sheet pile wall was examined, and the diffusion of suspended sediments from the temporary deposit area was simulated.

Structural problem

Normally, the sheet pile wall which protects the temporary deposited sediments from the wave action is built 300 m offshore, at a water depth of approximately 3 m, needed by the barge to approach the “booster station”.

The wall height above the still water level allows the overtopping of high waves, since in this case the dredging-nourishment operations are expected to be interrupted. However, particularly in these conditions the wall could be loaded by relevant forces, mainly consisting of wave pressures.



Figure 4.2. Detail of the sheet pile wall

Considering the actual dimensions of the sheet piles (PU12, $L = 12$ m), a verification can be made of the wall structural resistance under the action of the maximum expected breaking wave, whose return period is estimated to be 1 year.

Calculating the pressures with formulas commonly used for vertical breakwaters, and referring to the scheme of figure 4.3, the verification failures for a pile at the center of the front wall of the structure.

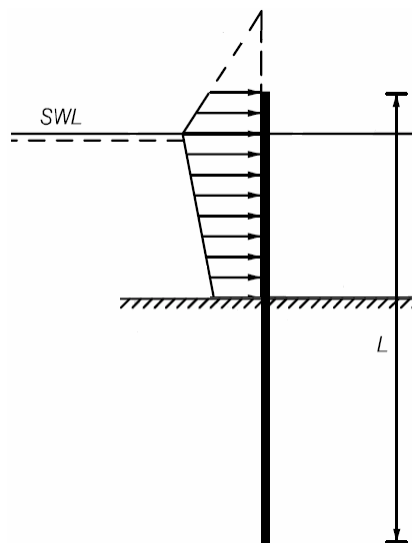


Figure 4.3. Scheme adopted for the calculation of wave pressure on the sheet pile wall

Possible solutions to this problem are:

- The use sheet piles with greater resistance (PU25) ;
- The interposition of a horizontal collaborating beam at the top of the front wall

The graph on fig. 4.4 shows the expected reduction of the maximum bending moment in a pile at the centre of the front wall when adopting the second solution:

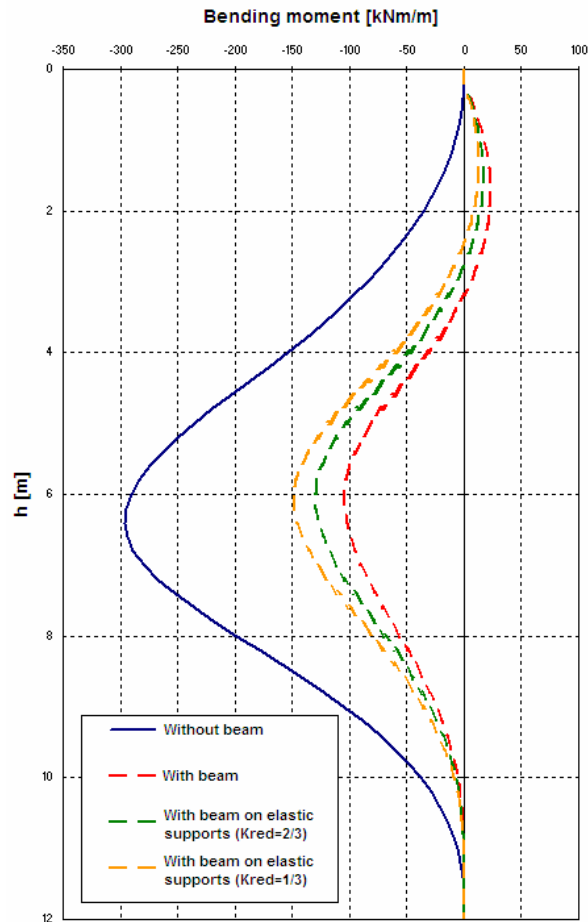


Figure 4.4. Graph of the bending moment on the pile in a pile at the center of the front wall, with different schematizations of the collaborating beam

Dispersion of sediments

The discharge of dredged sediments from the dredger to area delimited by the sheet pile walls, made through a bucket, leaves the finest part of the materials suspended immediately below the water surface. As a result, turbidity can be easily observed in the water surrounding the “booster station”.



Figure 4.5. Turbidity originated by the temporary deposit operations

With the aim of simulating this phenomenon, an experimental research was carried out in order to obtain a “turbulent dispersion” coefficient ε of the suspended particles.

Firstly, water samples were collected, at different positions and in different times, after a single release of sand in still water. Then, the concentration of particles was measured. Substituting these values into the analytical formula of bi-dimensional diffusion, an estimation of the ε coefficient was obtained, together with an estimation of the mass M of suspended particles. In particular:

- $\varepsilon \approx 0.1 \text{ m}^2/\text{s}$;
- $M \approx 5.5 \text{ kg/m}$ for a single release.

These values were introduced into a numerical model, implemented with the software COMSOL Multiphysics, which represented together the water circulation and the transport of suspended sediments.

The simulations were performed applying different wave condition, in terms of height and direction, covering an area that includes the nourished beach and the “booster station”.

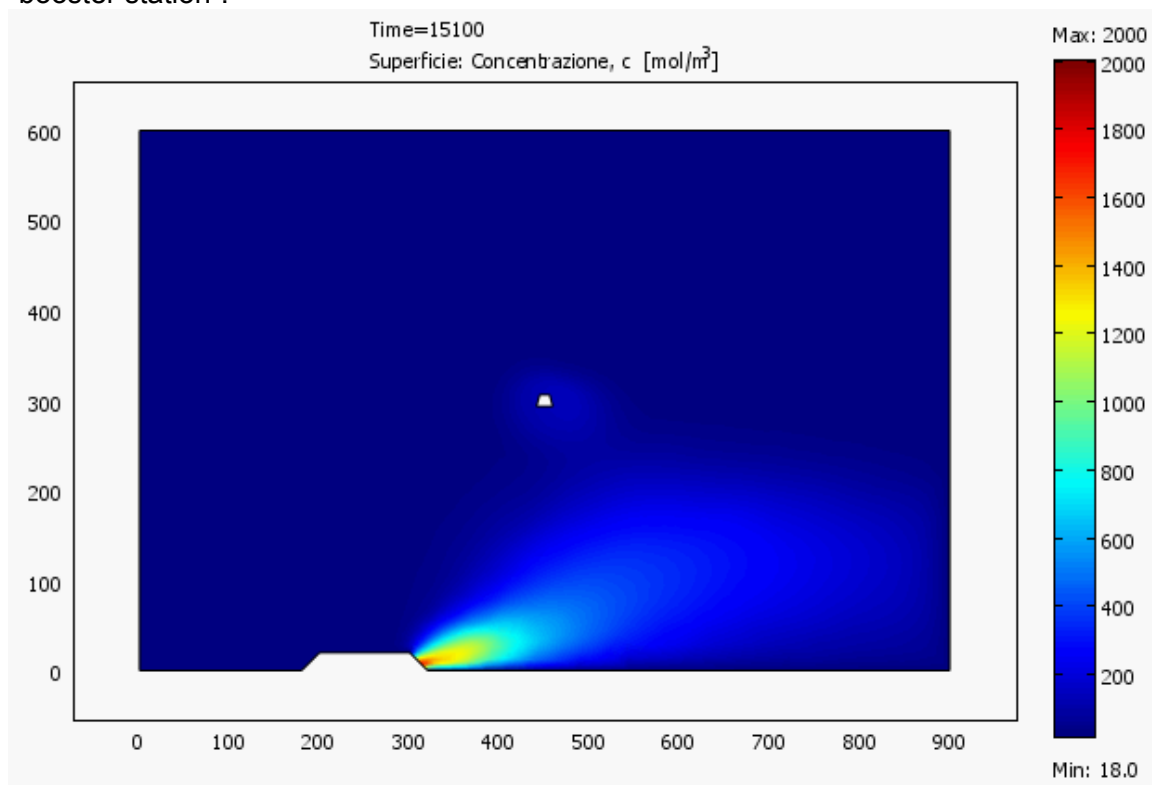


Figure 4.6. Difference of simulated concentration values between the shoreline (bottom) and the temporary deposit area (centre)

From other measurements, the amount of sand lost from the shoreline was evaluated to be nearly the 5% of the total amount involved by the nourishment. Then, the results of the simulation showed that, in terms of particle concentration, the turbidity generated around the temporary deposit area is evidently smaller than the turbidity which occurs near the shoreline (see fig.4.6).

However, considering the approximations of these simulations, the results here described may be the subject for further studies.

4.2. Available surveys

The surveys at the port entrance were carried out with the same methodology described in par. 3.1; the result of the survey is presented in fig. 4.7.

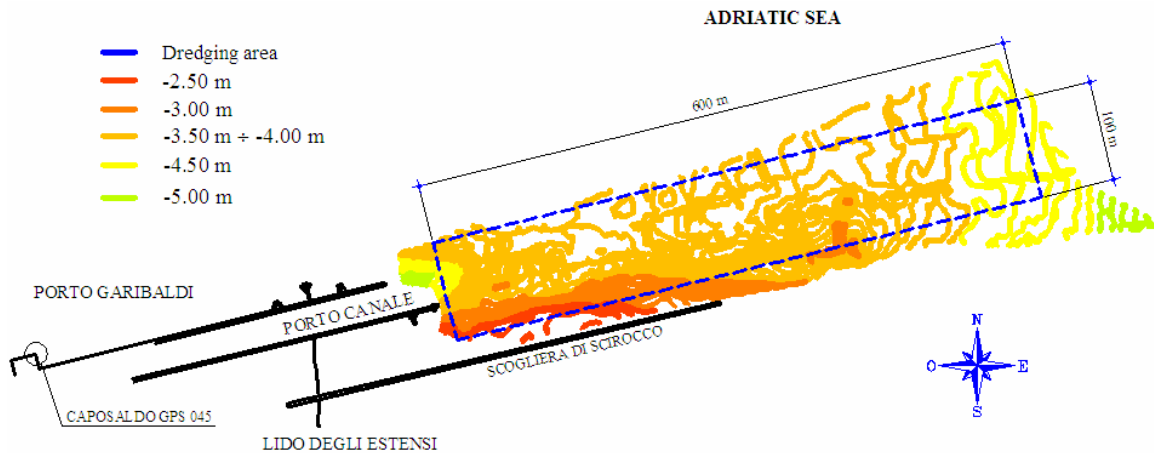


Figure 4.7. Bathymetry of the port entrance channel (30.01.2007)

5. Methodologies

The analysis of the bed evolution requires a detailed modelling. This allows for an evaluation of the relative importance of the many involved phenomena. The modelling alone is not sufficient: a final engineering interpretation, based on the essential quantitative simulation of the processes, will be required to propose different, more effective design schemes.

5.1. CAMS-DISTART

UoB is expert in the use of MIKE 21 software (see for instance Zanuttigh et al., 2005 or Zanuttigh, 2007). This tool, rather reliable in the hands of an expert, is then necessarily the main candidate for the simulation of the investigation of the morphodynamic evolution of the nourished beach.

MIKE 21 CAMS was built around standard modules of the MIKE 21 model suite and is based on an explicit forward-time integration scheme for bathymetry evolution (Zyserman and Johnson, 2002 and Zyserman et al., 2005). Execution is controlled by a shell, which also ensures the flow of information among the components of the modeling system. The evolution of the model bathymetry under a number of forcing processes can be simulated as the wave, current and sediment transport fields are calculated on the updated bathymetry.

MIKE 21 CAMS has been already successfully checked by the author (Martinelli et al., 2006) in representing erosions and depositions in laboratory tests on low-crested structures performed in a mobile-bed wave basin.

Specific problems

There is actually one concern about the possibility to model the coastal morphodynamic in presence of two different grain size distributions.

During the nourishment phase, it will be very important to establish the different grain size of the sand present in the original bed and in the nourished sand, which is dredged from the channel entrance. Such difference was not significant for the case of

Porto Garibaldi. Nevertheless, it is difficult to predict the effects of such difference.

Should this problem become relevant, a free source software described in the following will be used.

5.2. Community models

Community models are freely available computer codes that often include contributions from many researchers and, ideally, are widely tested and applied. The ideal modeling system includes well-documented open-source code; it also has an active group of users, test cases, software tools, and ongoing support by an institution or user group.

A coastal sediment transport model should implement peer-reviewed, process-based algorithms for circulation, sediment transport, and processes related to pollution, diagenesis, eutrophication, and turbidity.

Several approaches have successfully produced coastal sediment transport models: EcomSed was developed privately; SWAN and Delft3D have been purchased by the Office of Naval Research for broad use; and ROMS/TOMS has evolved through a collaborative process involving scientists from government agencies, academic institutions, and industry, with support from the National Ocean Partnership Program. As a specific example, the USGS, Rutgers University, UCLA, and the Virginia Institute of Marine Science have implemented bottom stratigraphy in the ROMS/TOMS model.

Updated sediment model to include stratigraphy and a couple of bedload transport formulations.

This model will be used to check differences in the sediment transport in presence of two grain size distributions.

5.3. Engineering

The engineering interpretation will be carried out by involving designers, owners of the facilities, local authorities, and deeply discussed with partners of GESA and engineers suggested by them. The exchange of experience from different geographical areas is expected make the difference with respect to other similar studies.

References

- MARTINELLI, L., ZANUTTIGH, B. AND LAMBERTI, A. (2006) Hydrodynamic and morphodynamic response of isolated and multiple low crested structures: experiments and simulations, *Coastal Engineering* 53 (4): 363-379.
- MERLI, D. (2007), "Execution of a nourishment with temporary offshore deposition of sediments: analysis of sand dispersion"
- ZANUTTIGH, B., MARTINELLI, L., LAMBERTI, A., MOSCHELLA, P., HAWKINS, S., MARZETTI, S. AND CECCHERELLI, V.U. (2005): Environmental design of coastal defence in Lido di Dante, Italy, *Coastal Engineering* 52 (10–11): 1098-1125
- ZANUTTIGH, B. (2007) Numerical modelling of the morphological response induced by low-crested structures in Lido di Dante, Italy, *Coastal Engineering*, 54 (1): 31-47.
- ZYSERMAN, A. AND JOHNSON, H.K. (2002), Modelling morphological processes in the vicinity of shore-parallel breakwaters, *Coastal Engineering* 45 (3–4): 261–284.
- ZYSERMAN, J., JOHNSON, H.K., ZANUTTIGH, B., AND MARTINELLI, L. (2005), Analysis of far-field erosion induced by low-crested rubble-mound structures, *Coastal Engineering* 52 (10–11): 977–994.

**5. CONTRIBUTION OF UNIVERSITÀ DI BOLOGNA/DISTART-P4
IN PHASE B
MEASURE 3.3
GESA**

PART 1. Accumulation of sediments in rivers associated with high hydraulic risk

Introduction

During phase A of the subproject GESA recent anomalous deposits of sediments in areas subject to hydraulic risk were identified in the Magra River watershed (northern Tuscany, Italy). During this phase of the project, a series of grain size measures have been carried out on these sites in order to characterize them.

Totally eighteen samples have been collected, two at each location of interest (Fig. 1), by using a sampler type box-corer, to the standard depth of 35 cm. The samples have been collected in the stream channel of the Magra River at the confluence point with the tributary torrent Aulella and in the channels of seven tributaries of the Magra River, i.e. Aulella, Bardine, Calcandola, Caprio, Lucido, Mangiola, Magriola.



Fig. 1 –Magra watershed, with locations where sediment samples have been collected.

Objective

The objective of this study is to analyse anomalous deposits of sediments that alter the normal hydraulic rivers efficiency creating risks for infrastructures and to understand if they can be dredged and eventually used for artificial beach nourishment.

Grain-size data and the degree of sorting are key parameters in a nourishment design. Any sand differences between the source of the nourishment and the natural sand should be then considered. Moreover, it is important to know how much mud will be brought onto the beach along with the nourishment sand, respecting a limiting value of 5 %. The first step is then to define the grading curves and composition of the selected sediment accumulation areas.

Methodology and procedure

Grain size charts are used to display the results of sieve and hydrometer tests. They are used to present the distribution of grain sizes in a soil or aggregate sample. The distribution of grain sizes larger than 0.075 mm (retained on the No. 200 sieve) is obtained by a sieve test, while the distribution of grain sizes smaller than 0.075 mm is

determined using a hydrometer test. The standard ASTM test used to determine the grain size of a soil or aggregate sample is D 422-63 (ASTM International).

The grain size distribution was calculated from sieve and hydrometer tests and presented as a curve on a semi-logarithmic plot. The ordinate of the graph is the percentage by weight of grains passing by the size given by the abscissa. Grain size is presented on a logarithmic scale so that soils with the same degree of uniformity have the same shape of the distribution curve regardless of their positions on the graph.

The sieves that are used to determine the soil's grain size distribution were selected as a function of the characteristics of that particular soil. The sieves opening size (in millimetres) used in the analysis are reported in Tab. 1.

Sieve opening sizes [mm]												
0,06	0,02	0,075	0,177	0,425	1,00	2,00	4,00	8,00	19,00	37,50	50,00	75,00

Table 1. Sieve opening sizes used in the analysis

Sieve analyses

A representative sample has been first selected and weighted. The soil has been broken into individual particles by crushing with either the fingers or a rubber-tipped pestle. The weight size of the sample which is considered to be representative is dependent upon the fragment of maximum size that has to be analysed.

An initial washing of the soil has been carefully conducted to avoid any damage to the sieve or lost of soil by splashing the material out of the sieve. The soil has been washed through the sieve using tap water until the water runs clear. Using a wash bottle, the residue has been (i) carefully backwashed into a large porcelain evaporation dish, (ii) decanted of the excess water as long as possible in order to ensure that none of the sample got lost in the process. The remaining soil-water suspension has been oven-dried for 16-24 hrs.

The sample has been removed from the drying oven, a watch glass was placed on the top of the evaporation dish and the dish and the content were allowed to cool to room temperature. The weight of the sample was recorded and the sample has been passed through the stack of sieves.

Once placed the sieves in a stack of increasing sieve number with the largest opening on top, and the pan on the bottom, the shaker has been working for 10 minutes, then the sieve stack has been removed disassembling it.

Each sieve (and the pan) have been massed with its contents. In this way the sieves' masses and the amount of soil retained by each sieve are already known. The grading curves could be then derived.

The percentage of soil retained on the n^{th} sieve (R_n) is given by eq. [1]:

$$R_n = \frac{100 \cdot M_r}{M_{\text{tot}}} \quad [1]$$

The cumulative percentage of soil retained on n^{th} sieve (C_n) is given by eq. [2]:

$$C_n = \sum_{i=1}^n R_n \quad [2]$$

The cumulative percentage of soil passing through the n^{th} sieve (P_n) is given by eq. [3]:

$$P_n = 100 - \sum_{i=1}^n R_n \quad [3]$$

Hydrometer tests

The distribution of particle sizes smaller than 0.075 mm has been determined by a sedimentation process, using an hydrometer (Buoyocoz, 1928).

The hydrometer test is an application of the Stokes Law, which basically states that larger particles have a higher settling velocity than fine particles that remain in suspension for a longer time. The time at which the hydrometer readings are taken, indicates the size of particles in suspension, while the reading on the hydrometer provides the amount of that size.

The sample has been (i) weighted out, (ii) placed in a 250 ml beaker, (iii) covered by 25 ml of sodium hexametaphosphate, (iv) stirred and allowed to soak at least 16 hours. At the end of the soaking period, the sample has been dispersed by transferring the complete sample to the dispersion cup and then stirred for a period of 1 minute using a stirring apparatus. Immediately afterwards, the solution has been transferred to the sedimentation cylinder and distilled water has been added up to the mark of 1000 ml. The cylinder has been shaking and after 10 minutes the hydrometer takes measures at the time indicated in Tab. 2 (measured from the beginning of the sedimentation process).

The percentages of sediments of each size are obtained with graduated scales from a linear interpolation between the density values read by the hydrometer and the measure times.

Times of measure (with respect to the beginning of the sedimentation) [min]						
2	5	15	30	60	250	1440

Table 2. Times of measure in the hydrometer tests

Results and discussion

Results of the sieve analyses and hydrometer tests are summarised in grading curves. In Tab. 3 percentage of gravel, sand and silt/clay are reported at each analysed site in the watershed and for each of the samples collected at the sites.

Fraction Sample	Gravel [%]		Sand [%]		Silt/Clay [%]	
	C1	C2	C1	C2	C1	C2
Aulella T., Pallerone	70,754	70,968	27,963	29,032	1,283	0,000
Bardine T., Pallerone	66,846	73,644	32,032	24,332	1,122	2,024
Betigna T., Casa Corvi	90,668	88,969	19,332	11,031	0,000	0,000
Calcandola T., Sarzana	76,738	93,688	18,242	5,282	5,020	1,030
Caprio T., Scorcetoli	91,839	82,658	8,161	17,342	0,000	0,000
Lucido T., Gragnola	67,668	75,002	32,332	22,012	0,000	2,986
Magra R.- Aulella T. confluence	80,978	73,038	19,022	26,962	0,000	0,000
Magriola T., Mignegno	90,668	83,865	9,332	16,135	0,000	0,000
Mangiola T., Mulazzo	83,948	85,018	16,052	14,982	0,000	0,000

Table 3. Sieve analysis of samples collected within the River Magra watershed

The grading curves obtained at each location and for each sample are reported in Fig. 2. The ordinate of all graphs represents the passing fraction (%) by the size (mm) given by the abscissa.

The prevalent fraction in all analysed samples is given by coarse and medium sand and gravel. Pebbles and boulders are often present, but they are included in the gravel fraction.

The coarse ruditic fraction percentage decreases moving downstream, the corresponding values lying between 94% and 67%.

The arenitic fraction percentage increases moving downstream, with values between 5% and 32%. The clay/silt fraction is very poor in all samples, the percentages ranging from 1% to 5% with an increasing trend moving downstream.



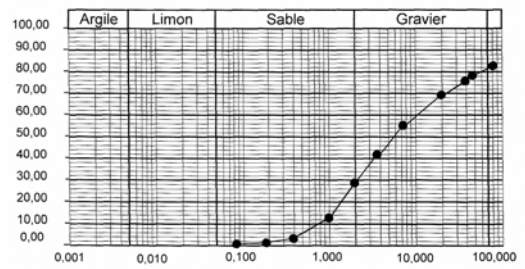
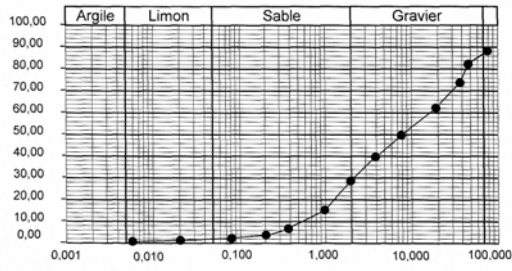
The lithological types represented in the coarse fraction are: gray sandstone of the “Macigno Formation”, marly limestone. In some cases, coral limestone of the Scaglia Rossa Formation (meaning “red scale or flake” despite the white colour of this formation and its massive bedding found) and rare pebbles of Serpentine marble can be distinguished.

The mineralogical phases represented in the fine fraction are: quartz aggregates, phyllosilicates, pheldspates, calcareous spar crystals, silt and clay aggregates.

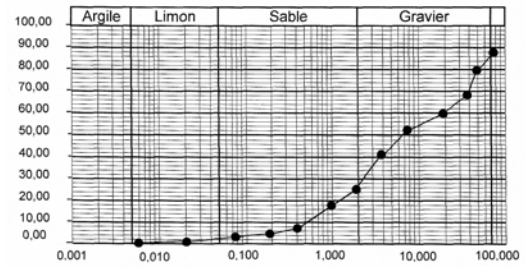
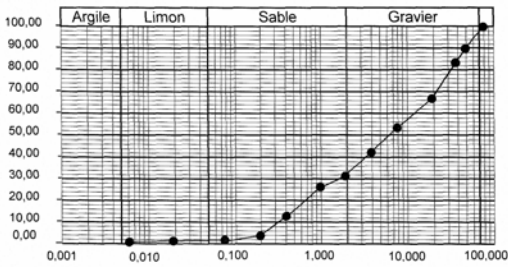
Conclusions and expected future results

The granulometric characteristics of the analysed samples may represent a possible source for small beach nourishment projects, where the primary goal is to increase the width of the beach in order to improve the protection from sea storm damages and increase the value of the beach as a resort (Essink, 1998). In fact, the stability of sediments placed on a beach is directly related to the grain size. In particular, nourishment material that is finer than the natural may move quickly off the beach. On the other hand, coarser material better absorb wave energy and it is generally more stable, but may affect the recreational use of the beach and its aesthetic value. Consequences of dredging of the analysed sediment accumulation areas and possible performance as a nourishment material has to be then carefully addressed and is one of the main goal of the forthcoming phase of the project.

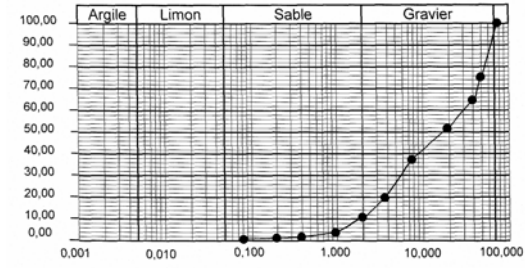
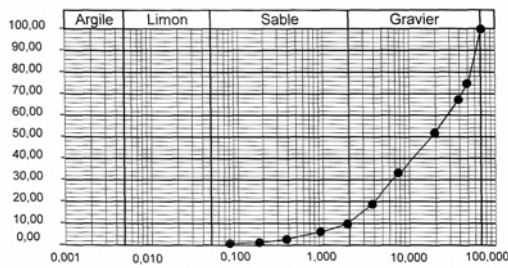
Aulella T., Pallerone



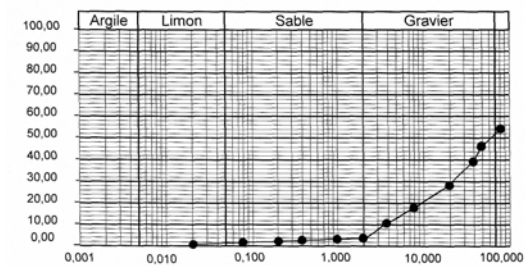
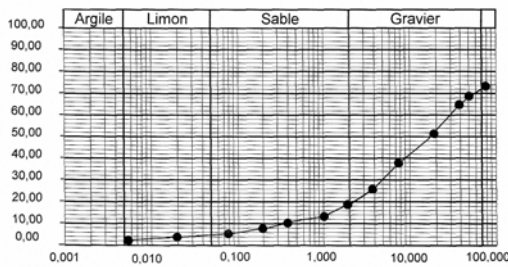
Bardine T., Pallerone



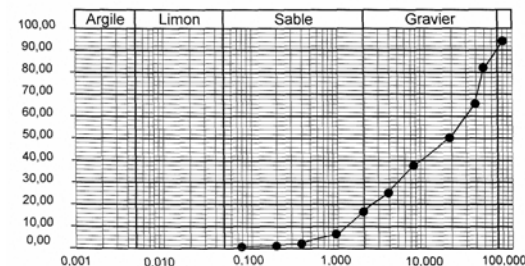
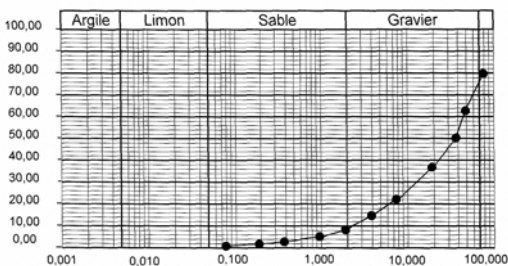
Betigna T., Casa Corvi



Calcandola T., Sarzana



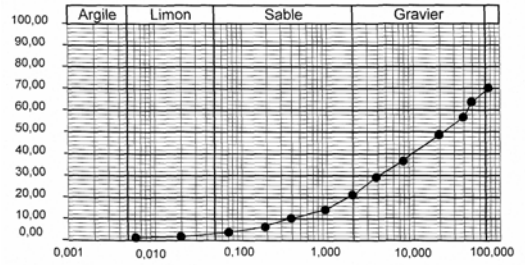
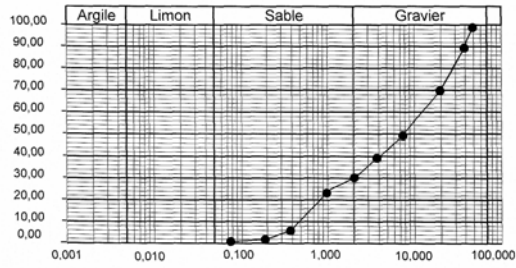
Caprio T., Scorcetoli



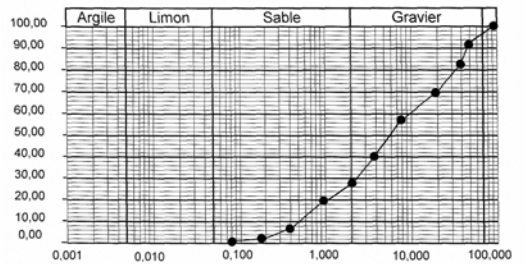
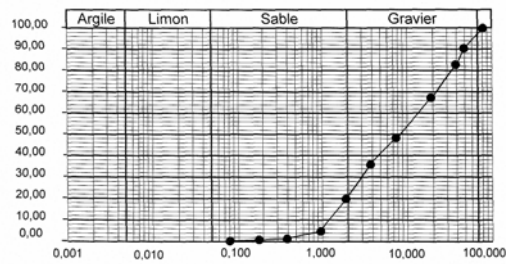
Continued...

Continued ...

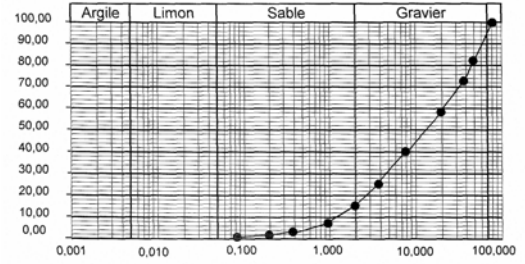
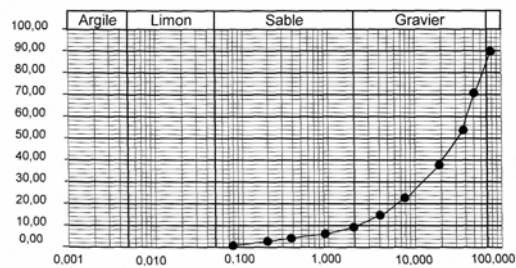
Lucido T., Gragnola



Magra R.- Aulella T. confluence



Magriola T., Mignegno



Mangiola T., Mulazzo

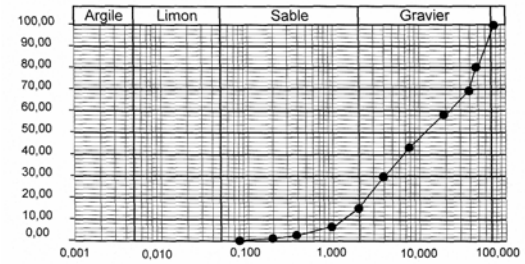
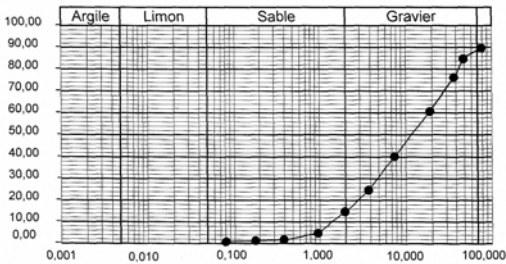


Figure 2. Grading curves obtained at each location for each sample (C1 right, C2 left)

PART 2: Quantification of sedimentary stocks intercepted by harbours

Introduction

Harbour structures, e.g. breakwaters, intercept sediments partially modifying and blocking the natural flow of the littoral current. The most common effect is an accumulation area up-drift and an erosion area down-drift. Under some circumstances, the accumulated sediments build a sedimentary stock which can create problems to the ships that are approaching the harbour, by reducing the water depth close to the access channel, and may represent a source of sediments for nourishments. It is then important to quantify the availability of such sediments and how they can be managed and further used. Available volumes and their future prediction should be known for an effective plan of activities in the area.

Objective

After collecting wave data and bathymetric surveys (Phase A of the GESA subproject), a procedure to estimate the sedimentary stocks around the major Tuscan harbours (Marina di Carrara, Viareggio e Livorno) has been set up, by analysing old and most recent bathymetries. A similar approach has been followed for the evaluation of shoreline movements in Japan (Tanaka et al., 2006). Final output of the analysis is a prediction of accumulation volumes per year. If the accumulated sediments are of a non-negligible amount, hypotheses on their further use is analysed. In particular, consequences of dredging have to be assessed if artificial nourishment by using the accumulated sediments is planned.

Methodology and procedure

The collected bathymetries (Tab. 4) are of two types: (i) old surveys (before the 80's) from ships producing a hard copy map with water depths and integrated with the position of the shoreline and (ii) recent surveys (after the 80's) with the single beam technique producing a digitalized map of water depths and position of the shoreline.

Carte	Anno	Tipo	Scala	Profondità minima [m]	Profondità massima [m]
Livorno	1881	Survey from ship	1:20000	0.8	27.0
Marina di Carrara	1954	Survey from ship	1:10000	0.4	15.6
Livorno	1976	Survey from ship	1:25000	1.3	39.0
Marina di Carrara	1977	Survey from ship	1:5000	1.1	13.2
Viareggio	1997	Single beam	-	0	10
Livorno	1997	Single beam	-	0	10
Marina di Carrara	2001	Single beam	-	0	10
Viareggio	2005	Single beam	-	0	10

Table 4. Bathymetric surveys that have been analysed

The first type is not georeferenced, but the position of the collected points is identified with respect to some reference points, which are known and fixed over time (e.g. churches, squares, rivers, harbours), whilst the second type is normally given in UTM or Gauss-Boaga coordinates. Moreover, the two types provide the water depths with a different elevation zero reference (Table 5).

As a first step, the georeference of the old maps with the error estimate was then necessary. After digitalising the old maps, reference points were selected and their positions in Gauss-Boaga coordinates were detected by using the topographic maps of the Region Toscana (Table 5). At least three points have been selected for each map.

The errors associated to the georeference of the maps have been calculated in two ways. Errors are however related to the difference between the coordinate of the reference point in the topographic map of the Region Toscana, which are assumed correct, and the coordinates of the corresponding point in the map.

LIVORNO					
1881			1976		
Point location	X	Y	Point location	X	Y
Torre del Marzocco	1605335	4824549	Torre del Marzocco	1605335	4824549
Faro, Darsena Morosini	1604208	4822928	Faro, Darsena Morosini	1604638	4822032
Calambrone	1604621	4822844	Porticciolo di Ardenza	1604206	4821927
Bocche d'Arno	1604638	4822032	-	-	-
CARRARA					
1954			1977		
Point location	X	Y	Point location	X	Y
Colonia FIAT	1581593	4877612	Torrente Palmignola	1578699	4877162
Marina di Carrara	1583365	4875556	Shoreline	1580410	4878027
Faro molo di Levante	1583605	4875738	Shoreline	1581640	4877341
-	-	-	Shoreline	1583052	4875872

Table 5. Reference points to georeference the old maps

A first estimate of the error is simply the average of relative errors (ϵ_i) calculated at each reference point (N_p):

$$\epsilon_1 = \sum_{i=1}^{N_p} \epsilon_i; \quad \epsilon_i = \sqrt{\epsilon_{x,i}^2 + \epsilon_{y,i}^2}; \quad \epsilon_{x,i} = \frac{|X_{CTR,i} - X_{map,i}|}{X_{CTR,i}}; \quad \epsilon_{y,i} = \frac{|Y_{CTR,i} - Y_{map,i}|}{Y_{CTR,i}} \quad [6]$$

A second estimate is the ratio between the average of absolute errors (ϵ_i) calculated for each reference point (N_p) and the maximum distance between two reference points (d_{max}), which represents an indication of the size of the domain:

$$\epsilon_2 = \frac{\epsilon}{d_{max}}; \quad \epsilon = \sum_{i=1}^{N_p} \epsilon_i; \quad \epsilon_{x,i} = |X_{CTR,i} - X_{map,i}|; \quad \epsilon_{y,i} = |Y_{CTR,i} - Y_{map,i}| \quad [7]$$

In both cases errors are limited and normally lower than 0.5%. In Tab. 6, a summary of the errors calculated with both eqs. [6] and [7] are reported.

Map	Relative error [%]	Error over distance [%]
Livorno 1881	0.10	0.35
Carrara 1954	0.17	0.09
Livorno 1976	0.16	0.41
Carrara 1977	1.71	0.39

Table 6. Errors in the georeference of old maps

As a second step, all maps have to be referred to the same elevation zero reference for water depths. The analysed bathymetries were collected in different periods by different techniques and have been referred to a variable elevation (Tab. 7). The bathymetries collected with the single beam technique are all referred to the Zero I.G.M. 1954, while the old surveys were not. A correction of the water depth values was necessary and they have been all referred to the Zero I.G.M. 1954 (Tab. 7).

After these two first steps, comparable bathymetric domains from all maps could be generated. For each harbour a common area of analysis, where sediments may be accumulated, was selected: north of the harbour for Marina di Carrara and Livorno and south of the harbour for Viareggio. Bathymetries were obtained through interpolation. In Fig. 3, the generated bathymetries for the harbour of Livorno from the map of 1976 is shown. Similar results are obtained for the other maps.

Reference	Time	Survey	Reference	Correction
		Livorno (1881)		
Zero I.I.M.	-	Carrara (1954)	Zero I.I.M.	+20
Zero I.G.M.	1897-1954	Livorno (1976)	Zero I.G.M.	0
Zero I.G.M.	1954-today	Carrara (1977)	Zero I.G.M.	0

Table 7. Reference levels for water depths and corrections applied to old maps

The volumetric variations have been calculated taking the difference between two bathymetries.

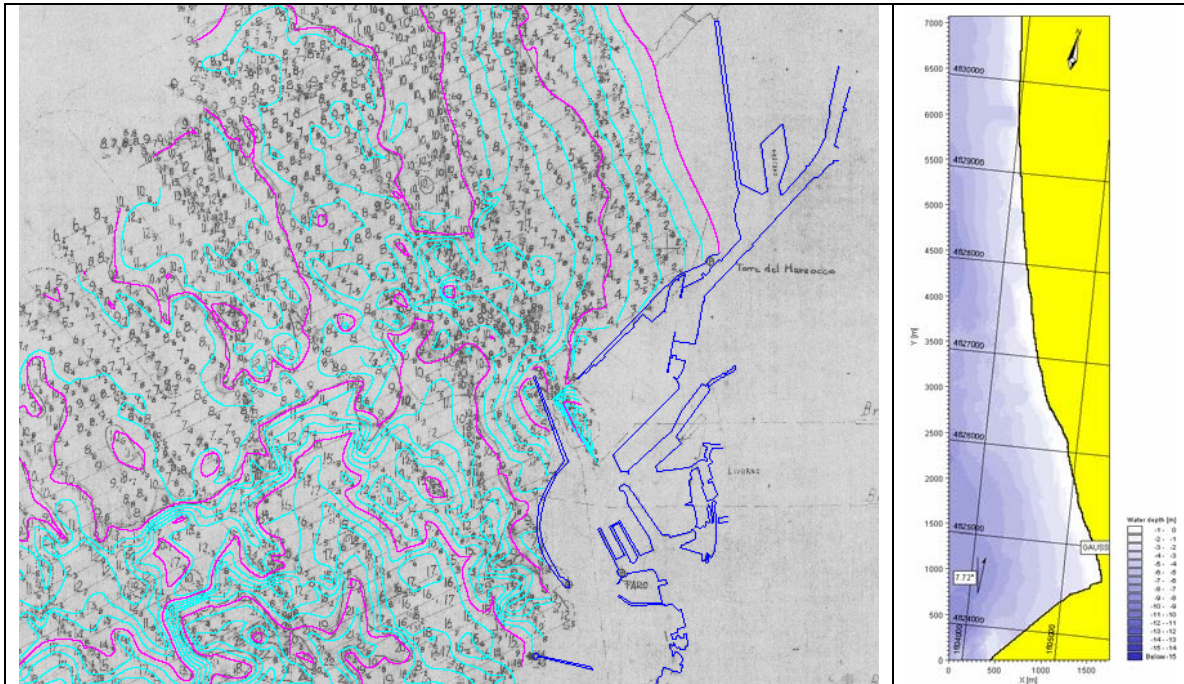


Figure 3. Generation of bathymetries from old maps.

Results and discussion

Differences in elevation throughout the analysis domain are obtained and visualised (Fig. 4-6). In order to better understand the volumetric variations over the distance from the harbour, the bathymetric domain is divided in strips that are 500 m wide (Y direction) and the partial variation volumes are calculated for each strip.

Harbour of Marina di Carrara

Three bathymetric surveys (1954, 1977, 2001) were available for the harbour of Marina di Carrara (Fig. 4).

Between 1954 and 1977 there is an accumulation of sediments in the first 1500 m north from the harbour of about 250000 m³, but localised erosion areas are detected between 2000 m and 3500 m (Fig. 4a,c). The accumulation trend is also confirmed by the by-pass system that was installed just at the harbour secondary breakwater in the 70s. This trend seems to change in the period 1977-2001, where erosion is generally observed along the analysed coast, although a small accumulation is present at the shoreline in the first 1500 m north from the harbour (Fig. 4b,d). In this area, there is a movement of part of the sediments on-shore, but also a generalised lost of material from the submerged beach of about 350000 m³, while from 2000 m and 3500 m, also the shoreline is eroding and in fact in this period the beach has been protected with a system of emerged groins.

These results qualitatively show that there is probably in the area a lack of material transported by the littoral current southward. The harbour in this case does not

intercept a significant volume of sediment feeding a sedimentary stock. Moreover, as a consequence of the poor availability of sediments, beaches that are south of the port are mainly not eroding because of the harbour.

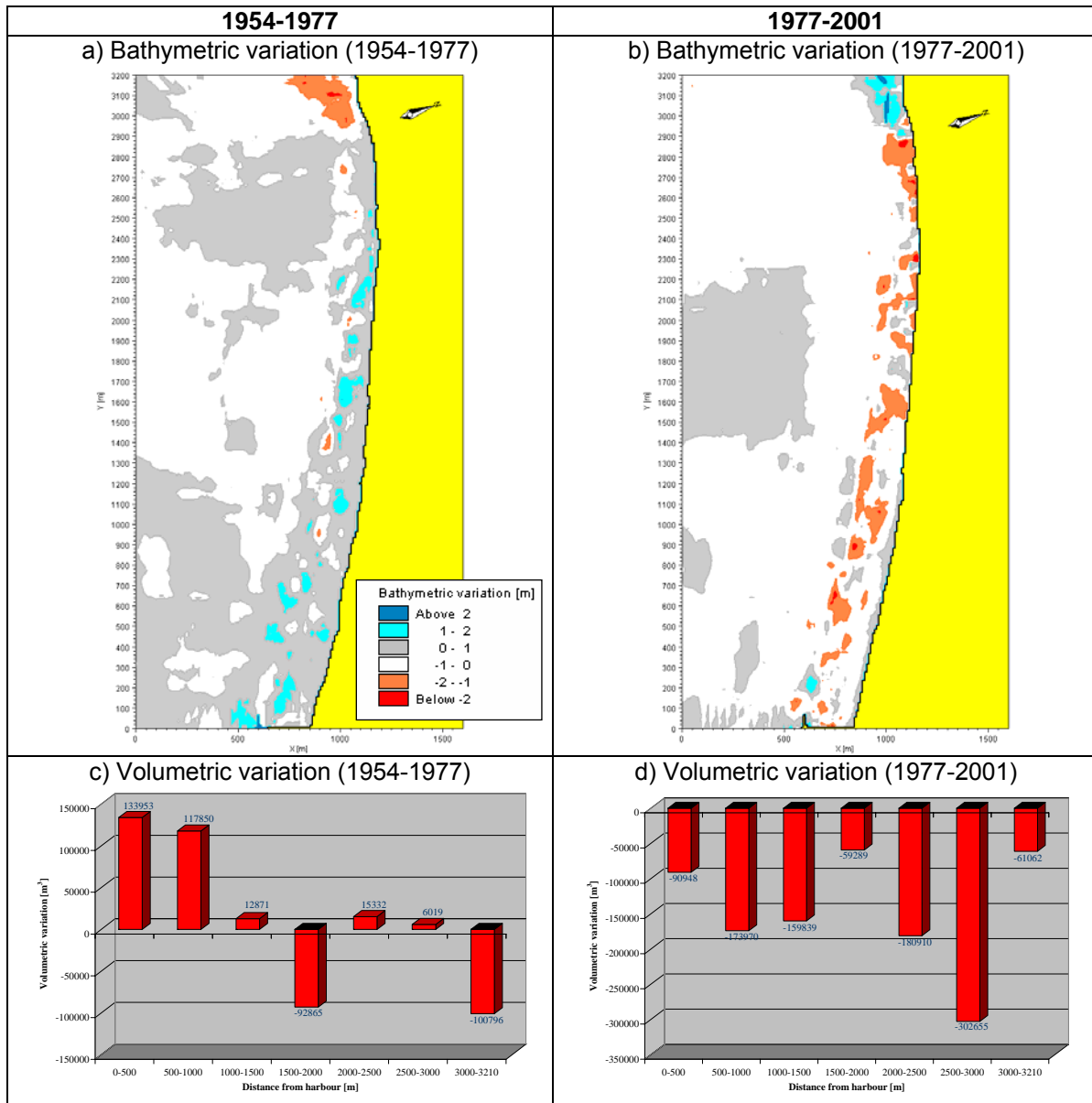


Figure 4. Bathymetric evolution and accumulated volumes (Marina di Carrara)

Harbour of Viareggio

Two bathymetric surveys (1997, 2005) were available for the harbour of Viareggio (Figure 5).

During the analysed period, there is a non negligible accumulation of sediments of about 140000 m³, especially localised in the submerged beach in the range of the sand bar movements, but an accumulation of sediments is also present onshore the bar (Fig. 5a). Moreover, due mainly to the different seasonal period of the surveys, the bar has in the two bathymetries a different position and a strip of erosion is followed by a strip of accumulation. In particular, the bar in the 2005 survey has moved seaward (Fig. 5a).

The results indicate that a sedimentary stock of small size is nourished by the littoral current northward directed and that the harbour partially blocks the material. Although the analysed period is short (9 years), the calculated volumes may be integrated with dredging volumes relative to the same area and available in the period

1980-2001, which indirectly are a measure of the accumulated sediments. The harbour of Viareggio is a good candidate for further application of management of the available sediments.

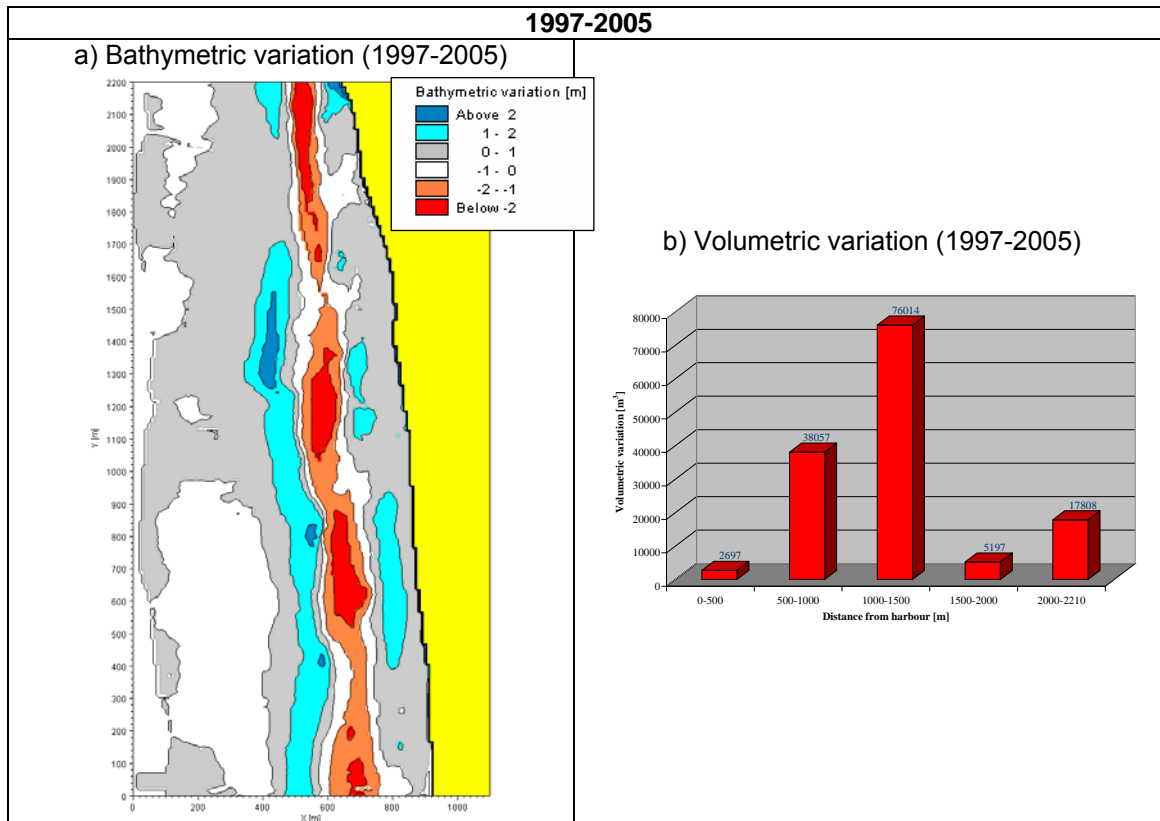


Figure 5. Bathymetric evolution and accumulated volumes (Viareggio)

Harbour of Livorno

Four bathymetric surveys (1881, 1976, 1997 and 2002) were available for the harbour of Livorno (Fig. 6). The obtained results in the period of 1881-1976 are not presented because a severe erosion throughout the area is obtained in contrast with observations. The reason of such unrealistic results is probably due to the zero reference elevation used for the most ancient map (1881). The map of 1881 was then discarded from the discussion of the results. In the period 1976-1997 there is a generalised accumulation of sediments of 700000 m³ in the first 3000 m north of the harbour. In particular, in the first 500 m over the harbour there is a consistent accretion of the shoreline, which is however almost stable further north. Around 3000 m north of the port there is a localised erosion area corresponding to a retreat of the shoreline. During the period 1997-2002, there is a change in the evolution trend of the bathymetries, similar to that observed for the harbour of Marina di Carrara. A generalised erosion of the submerged beach of about 700000 m³ in the first 3000 m north of the harbour, is observed throughout the whole analysis domain, although a part of the sediments has been moved on the beach and the shoreline shows an accretion trend in most of the analysed coast. Moreover, in this period, a depositing site has been built just north of the harbour, modifying the shoreline in the area. In both period an accumulation area close to the access channel at the north of the port is observed.

The obtained results seems to indicate that in the last years there has been a strong reduction in the sediments reaching and moving along the coast. The harbour does not provide a sedimentary stock. In this case, on the south of the harbour there is a rocky coast which naturally prevented from erosion problems.

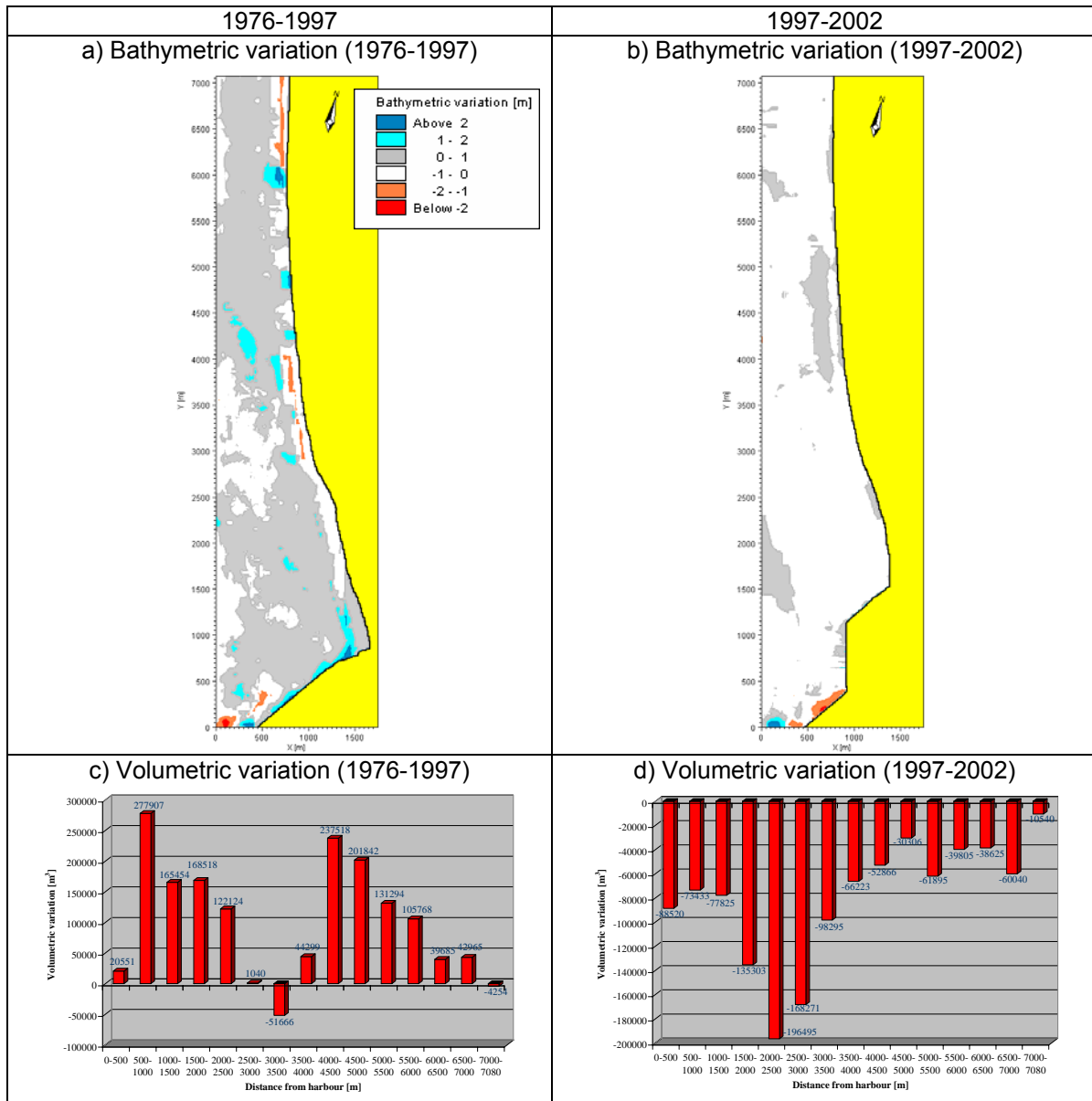


Figure 6. Bathymetric evolution and accumulated volumes (Viareggio)

Definition of sedimentary stocks

The analysed coastal areas don't include the access channel to the harbour and the seaward toe of the offshore breakwater, because the main goal of the study is more an estimate of the accumulated sediments on the beaches adjacent to the infrastructure than at the infrastructure. At present, all considered harbours experience accumulation of sediments in these areas, but apart from Viareggio, this is not the case of a sedimentary stock at the beaches that is growing over time. In some cases, as in Marina di Carrara, small volumes are dredged from the access channel and the material is normally carried and deposited seaward.

The total accumulated volumes between the most ancient and the most recent bathymetries and yearly accumulated materials are summarised in Tab. 8. The obtained values have been integrated with a prediction of the yearly sediment transport capacity (Kamphuis, 2000) calculated by applying a simple linear wave propagation model and available sediment transport formulae (Tab. 8).

The overall obtained results indicate that only south of the harbour of Viareggio there is the formation of a non-negligible sedimentary stock that can be exploited. In the case of Marina di Carrara, there is currently a lost of sediments especially from the

submerged beach, while in the case of Livorno there is a substantially stable bathymetry because accumulation and erosion are balancing, although the trend of the last years is going through erosion of the submerged beach.

Harbour	Marina di Carrara	Viareggio	Livorno
Period	1954-2001	1997-2005	1976-2002
Years	48	9	26
Distance from the harbour [m]	Volumetric variation [m]		
0-500	43006	2000	-68177
500-1000	-56119	48000	53495
1000-1500	-146968	71000	-20975
1500-2000	-152153	5000	33326
2000-2500	-165578	13000	-74371
2500-3000	-296635	-	-167231
3000-3500	-161858	-	-149961
3500-4000	-	-	-21924
4000-4500	-	-	184653
4500-5000	-	-	171536
5000-5500	-	-	69399
5500-6000	-	-	65962
6000-6500	-	-	1060
6500-7000	-	-	-17075
7000-7500	-	-	-14795
Totale	-935000	139000	45000
Totale/anno	-19000	17000	2000
Sediment transport capacity (CERC) [m ³ /yr]	1034527	513221	160601
Sediment transport capacity (Kamphuis) [m ³ /yr]	1576038	717990	292125

Table 8. Sediments accumulated at Tuscan harbours

The analysis of the harbour of Viareggio is based on a much shorter period than the other two harbours, but the observed accumulation trend is confirmed by the dredging data collected for this area. In fact, sediment dredging has been continuously performed all over the last 20 years.

An estimate of the accumulated volumes based on dredging data in the period 1980-2001 indicates a much higher accumulation (around 100000 m³/yr). The analysed bathymetries are however very recent and the shoreline in this area is currently close to the equilibrium due to the long period of sediment accumulation in the last decades. Moreover, sediment availability is decreased in the last years. Therefore, the accumulation rate has a decreasing trend over time if a continuous dredging of ad-hoc volumes is not operated.

A previous study on the Viareggio harbour (Aminti, 2005), based on a different methodology to calculate the yearly accumulated volumes, indicates a higher accumulated volume of sediments (around 65000 m³/yr). The estimate was derived from numerical simulations, by (i) propagating waves with a parabolic model to get the breaking angle at different sections spanning in the long-shore direction, (ii) applying the available sediment transport formulae (CERC, 1984 and Kamphuis, 1991) to get the littoral sediment transport and (iii) balancing the sediment transport between sections. The differences in the obtained results may be due to several reasons:

- (i) Uncertainties in the estimate of sediment transport discharges with available formulae (previous study);
- (ii) Calculation of the sediment transport capacity without considering the effective availability of sediments to be transported (previous study);
- (iii) Analysis of bathymetries over a limited time span (present study).

Proposals on how to use and manage sedimentary stock in Tuscany may be only discussed for the harbour of Viareggio

Conclusions and expected future results

The analysis of old and recent bathymetries around the major Tuscan harbours in order to detect and quantify the sedimentary stocks intercepted by the harbour infrastructures has generally indicated a poor availability of sediments. Apart from the concentration of sediments close to the access channel, only at the harbour of Viareggio there is a non negligible accumulation of sand along the southern beaches.

The prediction of the accumulated volumes, based on old and recent surveys, can be used to optimise the design of dredging volumes, further used to nourish suffering beaches.

During the forthcoming phase of the project, the volumes obtained for the harbour of Viareggio will be used to define several dredging scenarios. Consequences of dredging on the adjacent beaches will be simulated in terms of variation of the shoreline with the morphodynamic model CEDAS (see Activity 3).

PART 3: Modelling consequences of dredging on the adjacent coasts with morphodynamic models

Introduction

Dredging activities, especially if very close to the shoreline and in the active area of the beach, often characterised by bar migration, may have big effects on the adjacent beaches. These effects have to be predicted and addressed in the design and management of dredged volumes. Especially when there are not previous dredging experiences in the area under study, numerical simulations are required to predict morphodynamic changes induced by the dredging activities.

Objective

The study area is the coast around the harbour of Viareggio, where there is a sedimentary stock on the southern beaches (Activity 2) and the response of the coast to different dredging hypotheses may be verified. The main objective is to quantify the shoreline evolution as a consequence of several dredging volumes, through numerical simulations.

Methodology and procedure

The CEDAS software will be used to simulate the shoreline evolution before and after dredging. In particular, after testing the situation of no dredging, three dredging volumes are considered: (i) less than the accumulated, (ii) comparable to the accumulated, (iii) higher than the accumulated. Data on dredged sand are provided by the analysis of available bathymetries (Activity 2). The dredged volumes will be taken in the region of the submerged bar. Moreover, the possibility to also dredge some sediments at the seaward toe of the offshore breakwater of the harbour that shows reduced water depth due to accumulation will be also considered (Fig. 7).

The model will show the influence of dredging on the coast and how much the volume of dredged sediments affects the shoreline evolution.

Conclusions and expected future results

The simulations performed with the CEDAS software will provide the position of the shoreline over time. The results have to indicate: (i) if dredging volumes that are equal to the accumulated produces the observed accretion of the shoreline, (ii) if dredging volumes that are greater than the accumulated, alter the equilibrium of the beach inducing a higher or slower accretion of the shoreline or stopping the accretion tendency and (iii) if dredging volumes lower than the accumulated reduces the accretion rate because the beach is always close to its equilibrium.



Figure 7. Areas of dredging assumed for the application case of Viareggio

PART 4: Physical modelling of gravel beach profile evolution

Introduction

Gravel nourishments are sometimes preferred to sand nourishments because of the higher stability and capability to absorb the incoming wave energy (Aminti & Pranzini, 2000). Moreover, the use of gravel sediments accumulated within river basins due to natural or anthropic reasons for maintenance of beach nourishment is a promising strategy to manage sedimentary stocks of fluvial source.

Laboratory tests represent the best method to understand the underlying physical processes and to improve their prediction.

Objective

The main goal of the planned laboratory tests is to better understand and reproduce the cross-shore morphodynamics of gravel beaches under moderate and severe storm conditions, as a function of the sea parameters, the sediment size and the presence of a coastal defence structure altering the equilibrium of the natural beach. A gravel beach profile, reproducing the morphology of the beach immediately after a nourishment, is tested in the wave flume of the Civil and Environmental Engineering Department of the University of Florence (Fig. 7).

Methodology and procedure

A total number of 24 tests will be performed combining: (i) 2 mean sediment sizes, (ii) 6 wave attacks varying both wave period and steepness, (iii) pure beach nourishment and beach nourishment protected by a submerged structure.

The beach nourishment is realised over a sandy bottom with a slope of 1:20. Measurements during the tests include: (i) wave height at different locations along the wave flume, (ii) reflection coefficients from the beach, (iii) evolution of the beach profile and (iv) mean water pressures inside the swash zone of the gravel beach.

Data analysis has to indicate the relationship between the equilibrium final beach profile, the wave characteristic parameters, the sediment size and the presence of a submerged structure.

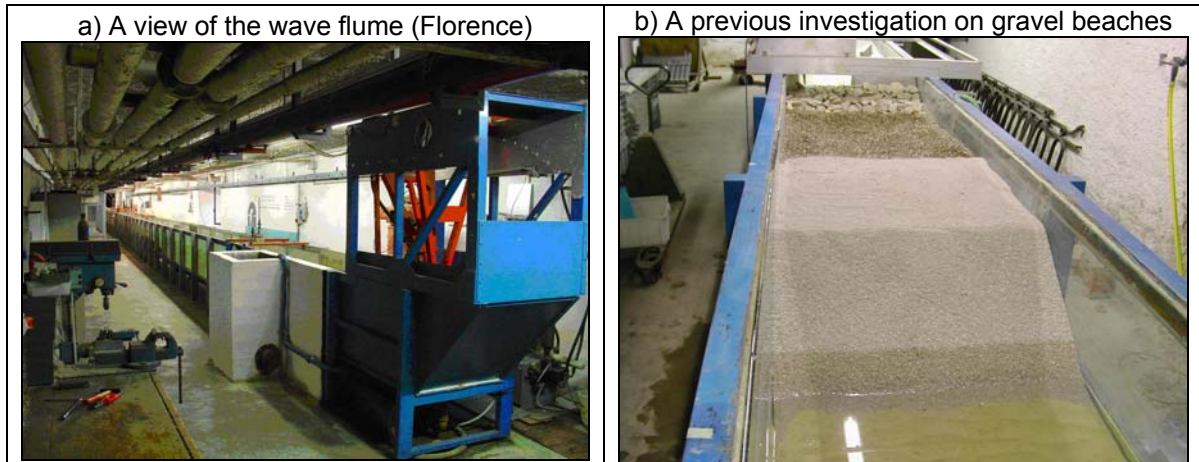


Figure 7. Wave flume (University of Florence) with a previous study on gravel beaches

Available formulae of the equilibrium profile, normally derived in case of no protection structures, will be also compared with the measured data, to test their prediction capability against the new data set.

Facilities and measuring devices

The wave flume of the Department of Civil and Environmental Engineering (University of Florence) is 47 m long, 0.8 m wide, 0.8 m deep (Fig. 7a). It is equipped by a piston-type wave maker, which can generate regular and irregular waves. Upper limits of the generated wave heights is approximately 20 cm at 1 Hz frequency. 16 acquisition channels are available to register signals from the installed measuring devices.

Resistive wave gauges are used to measure the water level over time, in order to derive at several location along the flume the spectral parameters, the wave height and the reflection coefficient. A bottom profiler is used to measure the beach profile. A video-camera will record all tests and information about the evolution of the beach profile over time will be derived by processing the images. In order have a reference measure for the beach profile evolution, a tape forming a grid could be put to the glasses of the flume lateral walls. Piezometers will be settled inside the core of the gravel beaches to measure the mean pressure in the swash zone.

Plan of the laboratory tests

Each test will take the time the beach profile reaches its equilibrium. The video-camera will record the whole test. Tests will be performed according to the following order: (i) first gravel size, no submerged structure, all waves, (ii) first gravel size, submerged structure, all waves, (iii) second gravel size, no submerged structure, all waves, (iv) second gravel size, submerged structure, all waves. After each test the beach profile is shaped at its initial configuration, assumed immediately after the nourishment. In Fig. 8, a section of the wave flume with a layout of the experiments is schematically shown.

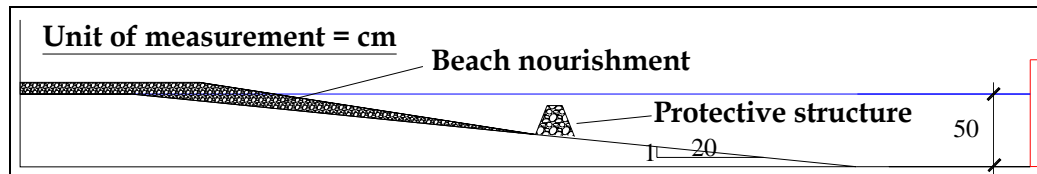


Figure 8. Section of the wave flume with the layout of the experiments

Conclusions and expected future results

Two main results are expected from the laboratory tests: (i) understanding the influence of a submerged structure on the time needed to reach the equilibrium and the equilibrium shape and (ii) measuring the reflection coefficient over time at the beach in order to understand the relation between the evolution of the profile toward the equilibrium and the energy that reaches the beaches estimated through the amount of wave reflection. These two aspects are in fact normally neglected in the available literature (Coates and Dodd, 1994), but are important to understand the performance of a gravel nourishment under moderate and extreme storms.

References

- AMINTI P.L. (2005) – Propagazione a costa del clima meteomarinario e stima del trasporto solido litoraneo nell'intorno del porto di Viareggio. Report. Comune di Viareggio (LI). 57 pp.
- AMINTI P.L., PRANZINI E. (2001) – Indagine sperimentale per la ristrutturazione delle difese di Marina di Pisa. Studi Costieri, 3, 57-70.
- BUOYOCOZ G.J. (1928) - The hydrometer method for studying soils. Soil Science. Vol. 25, p. 365-366
- COATES T.T., DODD N. (1994) – The response of gravel beaches in the presence of control structures. Proc. Int. Conf. Coastal Engineering, Vol. 2, pp. 1880-1894.
- ESSINK K., VAN DALFSEN J.A. (1998) - Ecological risks of shoreface nourishment. Wadden Sea Newsletter.
- KAMPHUIS J.W. (2000) – Introduction to coastal engineering and management. Advanced series on ocean engineering, Vol. 16. World Scientific, 437 pp.
- Standard Test Method for Particle-Size Analysis of Soils ASTM International / 10-Nov-2002
- TANAKA H., TAKAHASHI G., MATSUTOMI H., IZUMI N. (2006) – Application of old maps for studying long-term shoreline changes. Proc. XXX Int. Conf. Coastal Engineering, Vol. 3.

**5. RAPPORT OF PHASE B:
REGISTRO ITALIANO DIGHE – P5
MEASURE 3.3
GESA**

Petaccia¹, A., Greco¹, A., Maistri¹, A., Sammarco², P., Camilletti³, S.

¹ Registro Italiano Dighe, ² Dip. Ingegneria Civile, Università degli studi di Roma "Tor Vergata", ³ Studio Pietrangeli, Roma

Analysis relative to the recovery of reservoir hydrological capacities by the removal of the sediments downstream and to the outlets characteristics; definition of the sediments quality for a possible reuse.

1. Introduction

The construction of a barrage along a stream deeply alters the balance between the inflow and the outflow of sediments, creating an area marked by low current speeds and by a high sediments interception capacity.

Therefore, a relevant part of the sediments carried by the streams that feed the reservoirs is accumulating in the same reservoirs, generating a number of issues related to different fields:

- economic issues
 - reduction of the dam effective life
 - quantitative and qualitative reduction of utilizations (hydroelectric, irrigation, etc.)
- hydraulic-environmental issues
 - reduction of the capacity of outflows regulation and floods lamination,
 - coastlines erosion, due to the modification of sediments balance and to the consequent reduction of solid supply to the coastlines,
 - lowering of the riverbed downstream of the dam with possibile localized erosions, and dangers for the stability of infrastructures such as bridges, embanking and intakes,
 - head reduction,
 - modifications of the bed upstream,
 - reduction of the influent's mouth slope and elevation of the free surface,
- energetic issues
 - reduction of the production capacity of the hydrostation eventually present (proportional to the product between the volume of the settled materials and the geodetic leap)
- ecological-environmental issues
 - sediments quality,
 - impact on flora and fauna,
 - water turbidity,
- geotechnical-structural issues
 - thrust of the solid materials accumulated against the upstream face and consequent increase of the stress on the dam and possibile localised erosions at the foot of the dam
 - increase of the seismic risk,
- management issues
 - operational management of the discharge outlets,
 - obstruction and efficiency loss of the bottom outlets and of the intakes,
 - abrasion of engineering structures (floodways, galleries) and electromechanical devices (turbines and floodgates),
 - criteria and feasibility of the possibile reuse of sedimented materials,
- naturalistic issues

- waters colour
- waters turbidity
- availability for recreational uses

The control of the sedimentation in the artificial reservoirs and the recovery of the reservoirs effective capacity gradually lost during the time, due to the filling phenomenon, are issues of great importance by virtue of the dimension reached by this phenomenon.

The problem is relevant in Europe and in the developed countries, where the possibility to realize new reservoirs is very low and therefore is vital to maximize the efficiency of the existing reservoirs, but it is not less relevant for the basins in planning and/or in realization where a modern management of the hydrological resource must take into account an exact prevision of the phenomenon entity and of the needed interventions of attenuation and/or control.

Moreover, the sedimentation control is a priority in the countries where the water is a limiting factor for the development.

The storage capacity represents today a resource economically definable almost "scarce" and therefore it requires an attentive management policy.

Moreover, the settled sediments may have an intrinsic economic value, if not polluted or, eventually, correctly treated, because these sediments can be used in different areas, among which the interventions of beach nourishment. In summary, it can be stated that, especially in the countries with developed economies, the cost to recover a cubic metre of "filled with sediments" reservoir can be compared with the cost of the same cubic metre "made" using a new dam.

Therefore, it is necessary an integrated management of the life cycle of the sediments as well as of the water in a perspective of a sustainable long term use: from the idea, widespread up to now, of reservoirs with a finite effective life, typically of the order of 100 years, it is necessary to move to a concept of reservoirs management which should extend their life, finally making the storage capacity and the consequent benefits really renewable.

2. Objectives and intervention strategies

The control of reservoir sedimentation can be carried out in every phase of the life of the studied reservoir:

- Planning/design phase
 - Phenomenon entity estimation.
 - Definition of the techniques to control the quantity of material flowing into the reservoir.
 - Definition of management procedures and manoeuvres of outlets to limit the deposition phenomenon allowing the downstream release of the flowing sediments.
 - Identification of the structures necessary to manage the sediments.
 - Preparation of a reservoir management plan, which includes the management of the sediments as well as the hydrological resource.
- Operation phase
 - Realization of water and sediments management procedures.
 - Control and adaptation of the directions identified in the planning phase.
 - Planning of interventions to restore the reservoir removing the settled sediments.
 - Functionality restoration and outlets adaptation.
 - Auxiliary works construction

Two intervention categories can be identified to control the filling phenomenon, to restore the storage capacity and to remove the settled sediments:

- “active” defense interventions
- “passive” defense interventions

The first category includes the interventions to control the process of erosion and the process of sediments transport to the reservoirs, and the interventions to reduce the phenomenon of sedimentation. We pursue methods that aim to remove the problem of reservoir sedimentation by limiting the quantity of sediments flowing into the reservoir and by limiting the mechanics of the deposition phenomenon.

The target of the second interventions category is the recovery of the effective capacity removing the settled material.

The choice of the method to be adopted depends mainly on the following factors:

- dimensions, function and geometry of the reservoir,
- knowledge of the deposit areas, of the quantity and quality, of the granulometry of the sediments on the bed,
- hydrological regime of the affluent stream,
- site accessibility
- normative, environmental and anthropic restrictions
- final destination, in other words reuse of the material not settled or restored,
- costs/benefits of the intervention.

The choice of the intervention to be carried out must necessarily considerate both the economics and managerial aspects related to the costs of the operation itself and to the interference with the uses, and the aspect related to the environmental impact of the used method.

2.1. Preliminary evaluations

In order to perform a preliminary evaluation of the most appropriate sediments management method for the studied reservoir two empirical indexes have been introduced (Basson, 1997):

- $K_W = V/W_D$ corresponding to the ratio between the reservoir capacity V (m^3) and the average liquid outflow entering in the reservoir per year W_D ($m^3/year$);
- $K_T = V/W_S$ corresponding to the ratio between the reservoir effective capacity V (m^3) and the average solid supply per year W_S ($m^3/year$).

Both the ratios have the dimensions of a time and represent respectively the theoretical time of filling and the theoretical time of sedimentation of the reservoir. They are theoretical times calculated assuming that the solid and liquid volumes getting out are null.

In the diagram in Figure 1 are reported the lines $W_S/W_D = cost$, in other words the lines characterized by a given average annual concentration of the water entering in the reservoir. Such ratio varies generally between 10^{-4} for not very erodible hydrographic basins and 10^{-2} for very erodible basins.

Instead the ratio V/W_D is used to classify the reservoirs as big ($K_W > 1$), small ($K_W < 0.01$) or medium ($0.01 < K_W < 1$). The big reservoirs present coefficient of interception of solid material (to be defined) close to 100%. The small reservoirs include mainly the gate-structures dam, characterized by a lower coefficient of interception of the transported material.

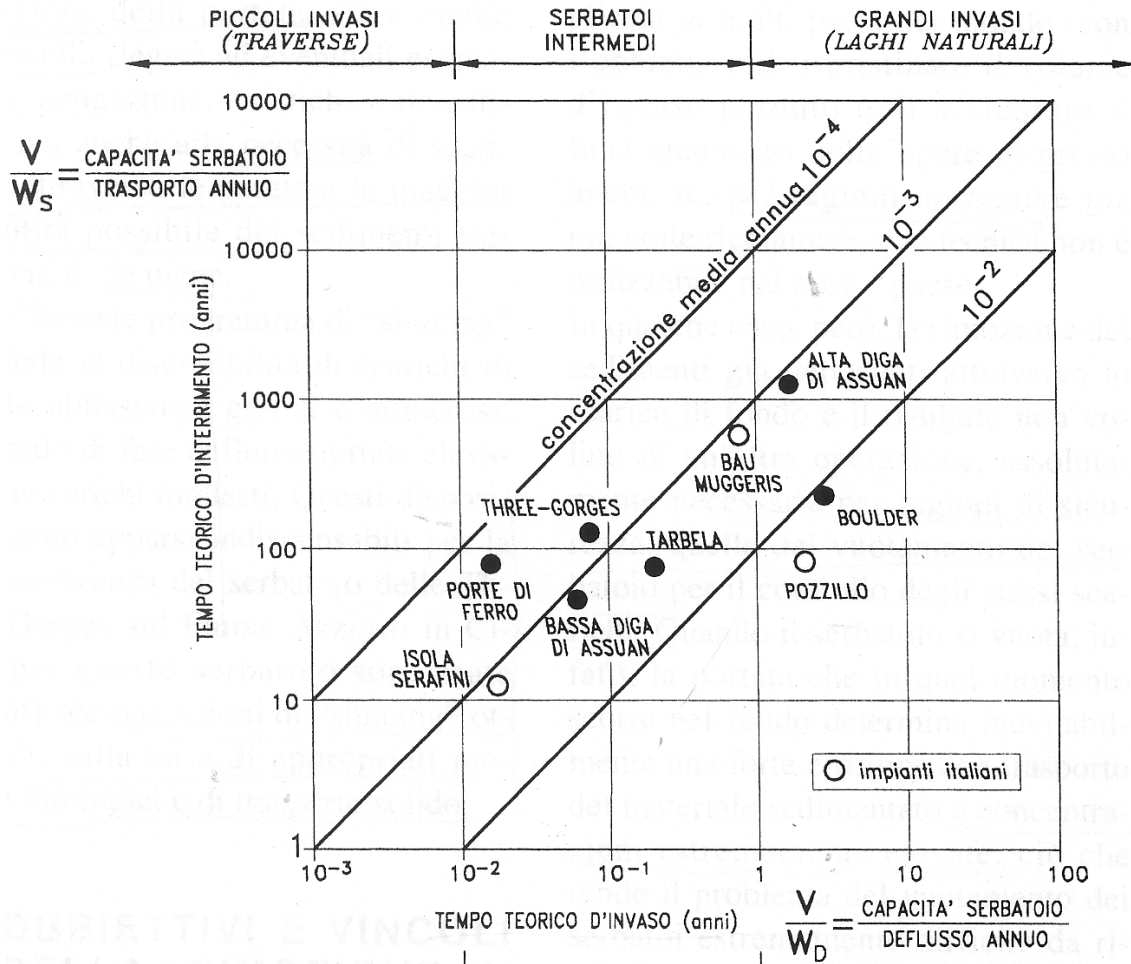


Figure 1. Reservoirs classification based on the V/W_s ratio (from Di Silvio, 1996).

The operational diagram of Basson & Rooseboom (1997) is further used to define the most effective management operational method for a given reservoir as a function of the reservoir hydrologic dimension and of the annual sediments supply (Figure 2).

Referring to the figure 2 (whose axes are the same of figure 2) three macro phases on the sedimentation control strategy are defined

- I = "storage operation"
- II = "regulation of water and sediment"
- III = "storage and sedimentation control alternating"

The procedure I, defined "storage operation", consists in keeping the reservoir always at the level of maximum storage, trapping on the bed almost all the entering sediments. This procedure can be applied only in reservoirs with moderate quantities of entering sediments and great storage capacity. Because of the lack of a water surplus to be released downstream, the only applicable solutions are the sediments removal with density currents and the mechanical dredging.

The strategy II of water and sediments regulation includes the operations of sediments evacuation by means of the expulsion from the bottom outlets. In the storages with $K_T < 30$ the effective volume annually lost because of the sediments accumulation exceeds 2%. The availability of exceeding hydrological resource is the most important parameter to define the applicability of the techniques to release the

sediments from the bottom outlets. We believe (Basson 1997) that it is not possible to perform releases if $K_w > 0.2$, while for $K_w < 0.03$ the method of expulsion from the bottom outlets is the most appropriate.

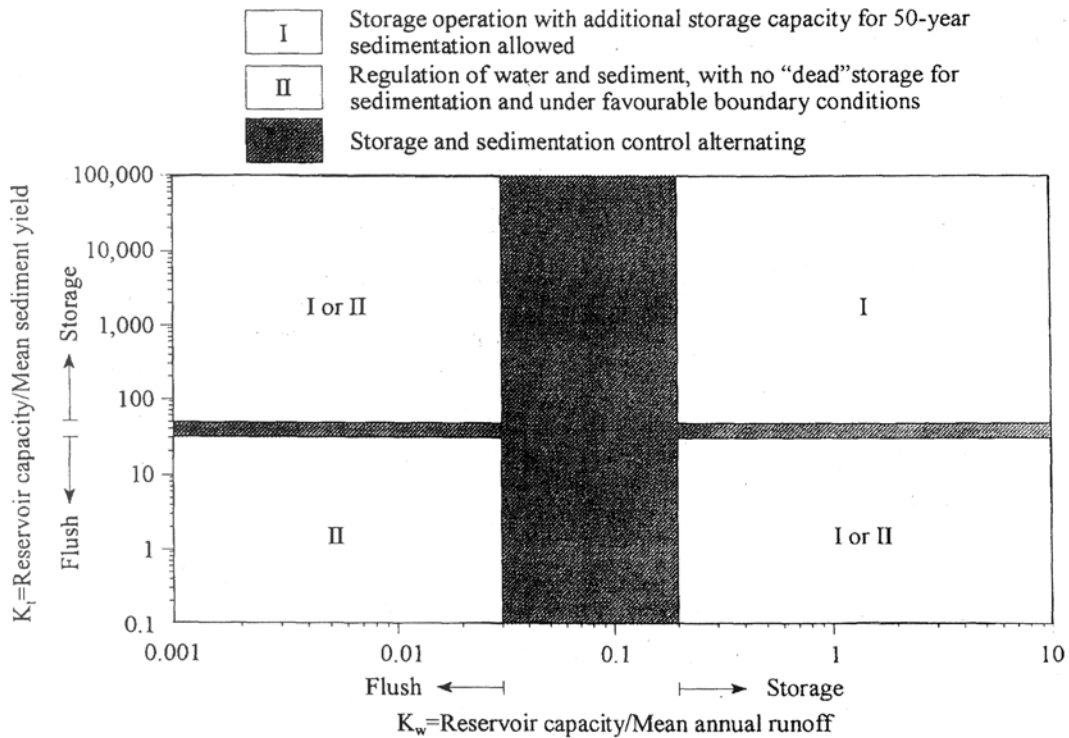


Figure 2. Basson and Rooseboom operational diagram

The following figure 3 represents grafically the values taken by the two indexes for 177 dams in the world. The lines represent the areas with the greater number of reservoirs.

The values of $K_w > 0.2$ indicate that it is not available a water surplus to be released downstream during the dam draining: in these cases the sediments evacuation by means of density currents represents the only possible strategy, if there are in the reservoir the conditions propitious to the establishment of these currents.

On the contrary, for the reservoirs located on the left down area the techniques of release by the outlets represent the best method of sediments management.

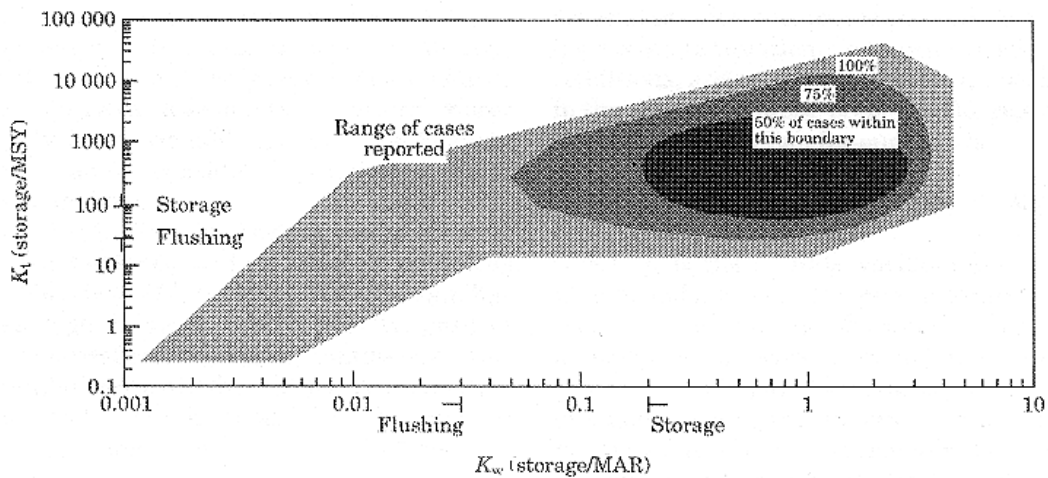


Figure 3. Value taken by the index K_w and K_T for 177 reservoirs in the world.

2.2. “Active” defense

The main active defense techniques applicable to the reservoirs in order to reduce the sedimentation are the following:

- Sediment Routing
 - Sluicing
 - By-Passing
- Venting
- Flushing

The differences between the procedures lie in the type of sediments management: with the sediment routing we manage the route followed by the sediments from a hydraulic and geometric point of view, with the venting and the flushing the management is more connected to the outlets manoeuvres.

2.2.1. Sediment routing

The “sediment routing” techniques, in other words the techniques to manage the route of sediments, include all the methods used to manipulate the reservoir hydraulic and/or geometry in order to let the sediments pass internally or around the reservoir and the intakes by minimizing the deposition.

These techniques try to identify the inflow part that transports the greatest quantity of sediments and to manage it differently compared with the “clean” water in order to prevent, minimize and concentrate the sedimentation.

Although some routing procedures count with the reservoir draw-off, they are different from the flushing techniques because the routing focuses on minimizing the deposition in the reservoir and on the balance between sedimentation and erosion during the flood, while the flushing aim to remove the materials already settled.

From an environmental point of view the sediment routing is the best technique of sediments management, because, as already reported, it respects the temporal distribution of the stream solid transport and it involves less accentuated concentration peaks; moreover, we succeed to drain both coarse sediments and fine material limiting the effects of the dam on the morphology of the river downstream.

Moreover, the sediment routing concentrates the deposition in reservoir areas where the interference with the uses is minimal or where the removal of the settled material is easy.

The routing procedures can reduce the frequency, the costs and the environmental impacts related to the dredging and flushing techniques, and they can extend the effective life of the reservoir for which it is not possible the sediments removal.

The efficiency of these operations can exceed 100% in case of erosion of the settled material. To obtain a sediments balance for a given granulometric class, the periods of crossover of reservoirs must be studied in order that they produce tangential stresses on the bed able to transport the material for the reservoir whole length and in order that the duration of the drainage is enough to allow the drainage of the entire quantity of entering sediments.

The passage from a conventional reservoir management to a management with sediment routing techniques involves an alteration of the sediments deposition scheme in the reservoir: the deposition longitudinal profile changes both in the geometry and in the distribution according to the granulometry because also the coarsest material is transported in areas closer to the dam and the delta deposits may be mobilized and moved downstream of the reservoir queue.

However, not in all sites these procedures may be implemented with low cost and they require the use of real-time hydrological estimations. In addition to this, we must consider that it is necessary to release downstream a remarkable quantity of water

to transport the sediments. As a consequence the sediment routing is applicable to small reservoirs where the water discharged during the turbid floods exceeds the reservoir storage capacity, making the water available to the sediments release without interfere with the uses; finally, we must consider that the sediment routing does not allow the removal of the material already settled and the passage of the coarsest material.

It is possible to separate the sediment routing techniques in two classes:

- Sluicing (also known as Sediment Pass-Through)
 - Seasonal draw-off
 - Draw-off during the floods
- By-Passing
 - On-line accumulation
 - Out-line accumulation
 - Underground accumulation

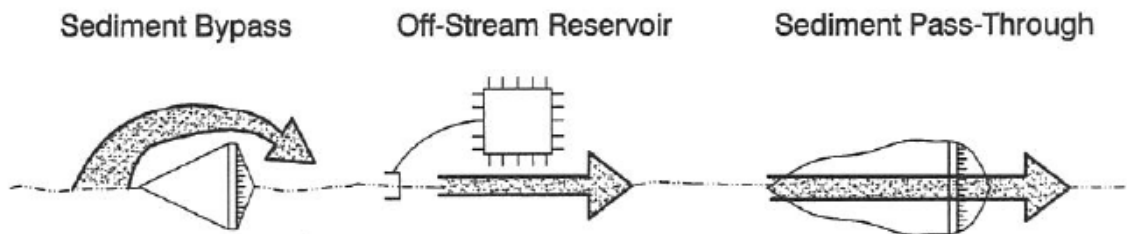


Figure 4: Sediment routing techniques classification (from Morris et al. 1997)

2.2.1.1. Sluicing

The most common and used sediment routing procedure is the sluicing, that consists in “discharge turbid water and store clean water” and can be realized by means of operations of seasonal draw-off or during the floods to maximize the reservoir crossover speed and to drain the sediments downstream through the bottom outlets.

Sluicing techniques can be differentiated on the base of the hydraulic control method.

The seasonal draw-off counts with extended periods (weeks or months) where the reservoir is kept in a low water level to reduce the hydraulic residence time and the coefficient of sediment interception. The efficiency of sediments release is determined by the capacity the current has to transport the sediments on the entire length of the reservoir. This operation is appropriate only for reservoirs with an water level naturally low for long periods in the year and for reservoirs whose uses present a marked seasonal character.

With the procedures of draw-off during the floods, the reservoir is emptied for reduced periods limited to the flood events: in this way we try to discharge the biggest part of the entering sediments reducing the sediment interception coefficient, obtaining on one side the reduction of the reservoir filling phenomenon and on the other side the reduction of morphological alterations of the downstream bed due to the imbalance on the sediments assessment.

Two techniques of the draw-off hydraulic control during the floods are used. In very small reservoirs from a hydrologic point of view, the operations are controlled by means of a default control curve. For bigger reservoirs instead the water level is reduced before the floods arriving on the base of the estimated flood hydrograph: the outlets are opened before the flood beginning and kept opened until the flood peak occurrence, after which the outlets are closed and we start to store water.

This technique supposes that the rising limb of the flood wave has a turbidity bigger than the decreasing limb and requires a real-time knowledge of the flood hydrograph to manage the manoeuvres efficiently.

The essential sluicing requirement is the presence of an runoff excess to be discharged downstream during the raining periods: it is applicable only to reservoirs hydrologically small and without multi-year regulation characteristics.

Favorable conditions to the sluicing application come to fruition in reservoirs with prolonged morphology, narrow and not much deep, with bottom outlets close to the bed level, flowed by streams with solid transport mainly in suspension and with a well known hydrologic regime, located in arid or semi-arid areas.

The operation cost is closely related to the value of the water released and wasted from the point of view of uses.

Sluicing benefits reside in the low costs and in the fact that the manoeuvres are focused in some periods of the year, even quite short in case of draw-off during the floods; moreover, the impact on the downstream ecosystem is limited because the concentrations of the discharged currents are of the same order of magnitude that the concentrations during the floods. However, it is not possible to remove the deposits already created.

2.2.1.2. By-Passing

The sediment by-pass consists in the avoidance of the reservoir by the solid material, with opportune topographic conditions that allow the construction of a canal or of a gallery of by-pass with remarkable capacity and acceptable costs, and in the hypothesis that the basin hydrologic regime gives a remarkable surplus of liquid outflow compared with the reservoir capacity.

The sediments by-pass can be used if, for example, the dam is located downstream of a river curve, where it is possible to build a canal that passes through the curve and returns the water downstream of the embankment.

The waters deviation is realised by means of a flood check dam located in the reservoir initial part, in the areas with little depth; the floods control sluices generally are kept closed, allowing the entrance in the reservoir to the affluent discharges, and they are opened during the floods in order that the discharges result deviated into the by-pass canal (figure 5).

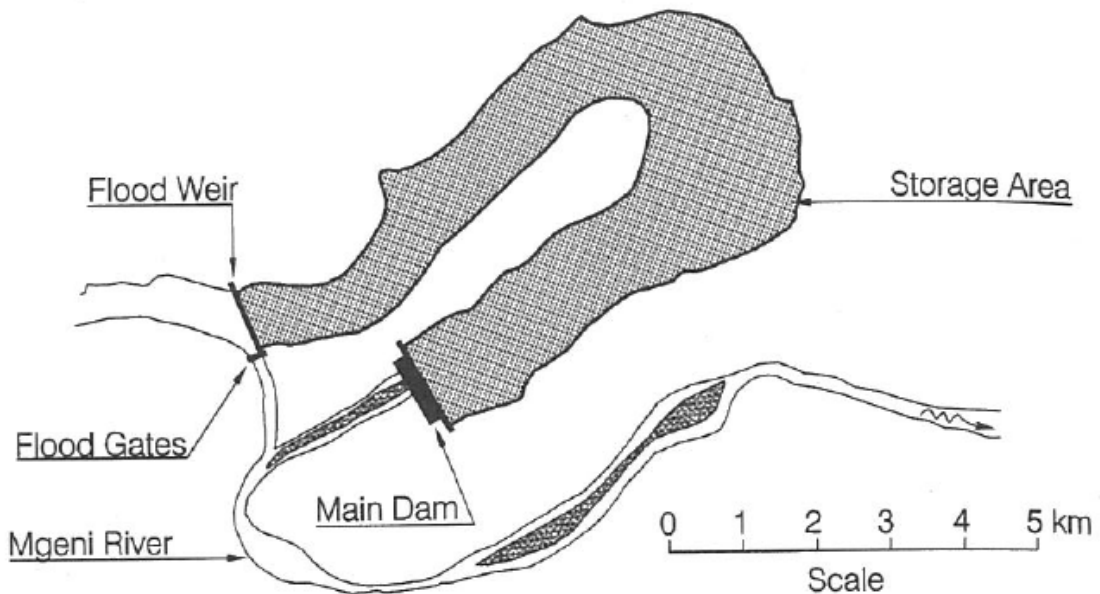


Figure 5. Configuration of the “sediment by-pass” of Nagle reservoir in South Africa (from Annandale, 1987).

A different by-pass technique consists in building the dam out of the main stream, and it is flowed deviating the water with low sediments concentration.

Different methods to reduce the sediments inflow in a reservoir placed offline have been identified: *i)* the turbid discharges can be partially or totally excluded from the reservoir limiting the hydraulic capacity of the intakes or controlling the catchment sluices selectively, *ii)* the catchment structures can be designed to exclude the coarse materials and *iii)* the deviation barrage can be controlled like a sediments interceptor for the deviated waters, and the retained sediments are removed later by means of flushing procedures.

Finally, we can use underground reservoirs, created in deposits of coarse material, in whose cavities the water is stored, building an interception dam. The water is extracted by means of a pipe that passes through the dam base and extends upstream through the permeable deposits.

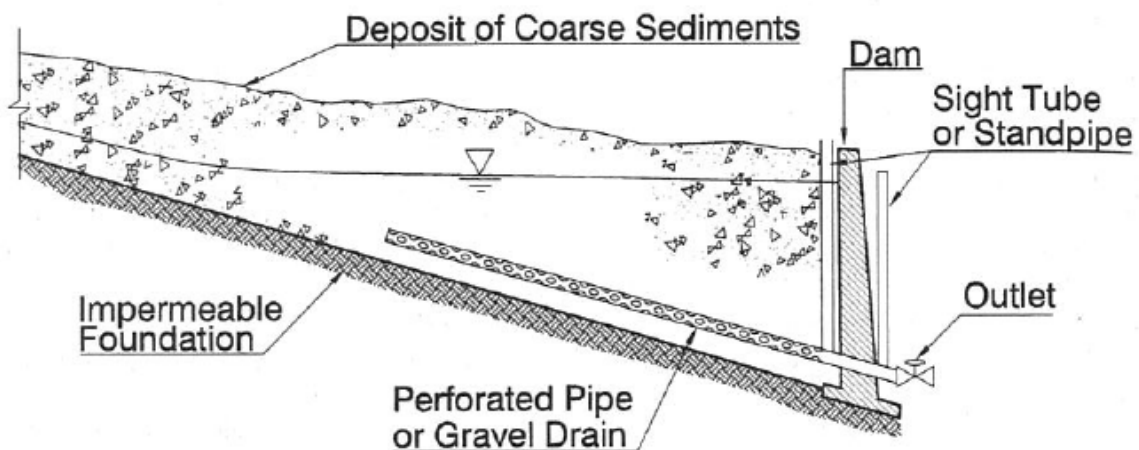


Figure 6. Configuration of the sediment routing by means of an interception dam and an underground reservoir (from Morris et al., 1997).

The main advantages resulting from the adoption of such a scheme consist in the almost total exclusion of the sedimentation problem, in the improvement of the water quality consequent to the filtration in a porous medium, and in the exclusion of loss by evaporation.

The necessary requirements for the achievement consist in the presence of a river with essentially bed load solid transport and made of coarse material located on an impermeable foundation.

However, up to now, the use of this configuration is limited.

2.2.1.3. Venting

A different active defence technique exploits the principle of the stratified motion related to the density differences.

Due to the remarkable density, the turbid currents can dip under the reservoir surface and flow along the reservoir bed toward the outlets, keeping their concentration almost unchanged. The density currents reaching the barrage can be eliminated through the bottom outlets reducing the sediments accumulation without reducing the water level in the reservoir and with a consequent lower waste of the hydrological resource, being a technique applicable also to big-sized reservoirs.

These density currents move quite slowly, with velocities between 0.1 m/s and 0.3 m/s, according to the density difference between the densest fluid and the above water, and they are alimented only during the inflow: as a consequence if the turbid discharge duration is lower than the time required by the current to reach the dam, the current dissipates on the bed; if instead the current succeed in reaching the dam it accumulates creating a submerged muddy lake, that can be eliminated opening the

bottom outlets. If the current is not discharged, or if it is discharged slowly, the muddy lake takes a horizontal profile upstream. The sedimentation in the muddy lake causes the increase of sediments concentration and of density with the depth; as a consequence, the following turbid inflows distribute over the fluid with greater density: the affluent density current changes from “underflow” into “interflow”.

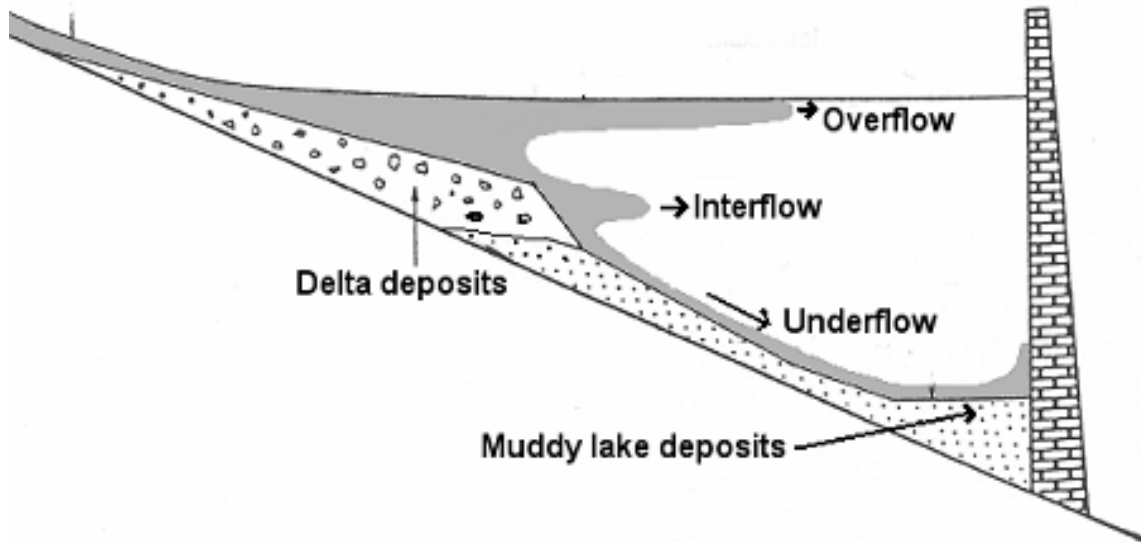


Figure 7: overflow, interflow and underflow

The area where the affluent turbid water dips under the clean water is called point (or line) of immersion. In the narrow reservoirs the submerged flow creates a line that follows the reservoir width with turbid water upstream and clean water downstream.

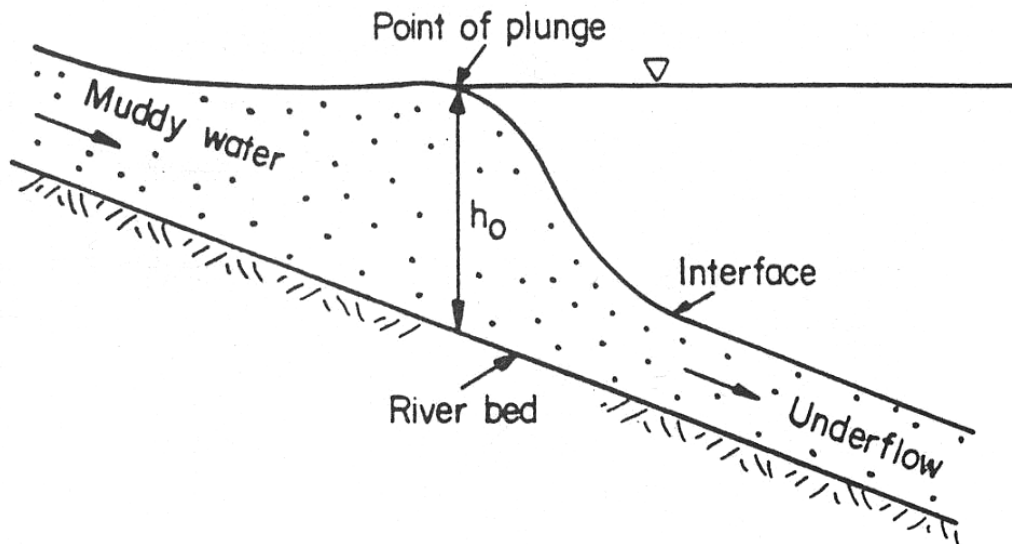


Figure 8: Identification of the immersion point

Having a motion controlled essentially by the gravity, density currents concentrate in the deepest area of the transversal section following the submerged thalweg and they produce two types of deposits: the deposits along the thalweg, due to the sedimentation, that develop from the immersion point and that are produced both by the currents that reach the dam and by the currents that dissipate along the route, and the horizontal deposits of fine material that extend upstream from the dam, produced only by the currents that reach the dam and create the muddy lake.

These deposits change the reservoir geometry and reduce the current capacity to reach the dam on equal terms with the entering current: the deposits along the thalweg fill the stream original canal producing a wide and flat bed profile that detract from the density currents the necessary bed slope; it reduces the thickness, increases the current size, increasing the friction both on the bed and at the interface and causing an increase of clean water transport at the interface; the deposits corresponding to the muddy lake replace the original bed slope with a sub-horizontal profile: in this way the gravitational force that guides the current is reduced.

A periodic reservoir flushing is an effective way to keep a canal along the thalweg, combating both the mentioned processes and maintaining the reservoir conductive geometry.

Instead, the delta deposits at the reservoir entrance facilitate the density currents, because they reduce the distance from the dam immersion point and at the same time they increase the bed slope.

The efficacy of venting operations depends on the convenient localization of the bottom outlets and on the timing they are opened to release the current, discharging a runoff according to the affluent turbid current. In some reservoirs it is possible to release downstream approximately half of the entire quantity of affluent sediments during a flood.

However, in several reservoirs it is not possible to carry out venting operations, and moreover the efficiency of these procedures is decreasing during the time because of the sedimentation along the thalweg. Finally, the density currents may obstruct the bottom outlets because of the sedimentation in correspondence to the dam: this problem is accentuated especially in the reservoirs located in mountain areas.

The density currents flow during the inflow of turbid water in the reservoir; then, when the inflow ends, the part of current along the reservoir stops and begins leaving sediments.

The duration of the downstream release is proportional to the duration of the inflow for a given length: for short distances the release time may be also bigger than the inflow time, and increasing the distance the current must cover, the drainage is supported for an always smaller fraction of the inflow period, because an increasing part of the current is retained in the reservoir.

As a first approximation we can assert that the maximum quantity of dischargeable turbid current is equal to the difference between the total affluent volume and the volume of the current retained along the reservoir: then, the venting efficiency increases as the reservoir length decreases.

Sometimes, it is possible to reach venting efficiencies bigger than 100 per cent, related to the transport of eroded additional sediments in deposits located between the downstream measuring station and the immersion point, and to the release of not consolidated sediments present in a muddy lake produced by a previous event.

In fact, the venting efficiency is strongly influenced by the timing the outlets are opened and by their distribution in the dam: it is then very important to know the moment when the current reaches the dam to plan the opening and the closing of the outlets. The motion of turbid current can be measured with in-situ instrumentation, like turbidimeters, or on the base of previous measurements, and on the consideration that the velocity of a current in a given reservoir increases as the affluent discharge increases.

The biggest quantity of suspended sediment can be discharged when the outlets capacity is close to the runoff of the turbid current that reaches the dam.

In conclusion, the conditions that promote the density currents venting may be resumed in this way: high bed slopes, small-sized basin, remarkable turbidity of the affluent current, duration of the flood event bigger than the time the current needs to pass through the reservoir, big-sized bottom outlets located close to the bed level, affluent sediments with essentially fine granulometry.

The main obstacles reside in the fact that only fine sediments can reach the dam and that the venting operation is, on the whole, not much manageable.

Moreover, we believe that only 10 per cent of the sediments affluent to the reservoir per year may be removed by means of density currents.

2.2.2. Flushing

The flushing (also known as hydraulic drain) consists in the reservoir draw-off by means of the opening of the bottom outlets in order to create a regime of river motion in the reservoir, digging a canal through the deposits and releasing later downstream the eroded sediments through the discharge outlets. Unlike the sediment routing, that try to prevent the deposition during the floods, the flushing uses the draw-off to erode and to discharge the sediments already settled. However, the sediments affluent to the reservoir during the flushing operations are released directly downstream as well as in the sluicing, and the flushing results a hybrid technique between the active interventions, limiting the deposition, and the passive interventions, removing the deposits.

With the flushing, the temporal distribution of sediments release moves away considerably from the inflows, even if it is carried out during a flood because a high quantity of sediments is discharged in a short period of time causing extremely high concentrations. On the contrary, the routing keeps the natural periodicity of sediments transport along the river.

We discern two flushing techniques:

- empty-free flow flushing that consists in the reservoir draw-off until the level of discharge with river regime in the reservoir;
- pressure flushing that requires a less important draw-off but is also less effective and, because of this, less used.

Usually the flushing is also classified on the base of the season in which it is carried out: generally it is more effective if performed during the rainy season because with bigger discharges the current erosive force increases.

The flushing has been successfully applied to several reservoirs with a wide range of sizes but all with a small hydrologic size, in other words with a capacity/inflow ratio typically lower than 0.3. In this way, the reservoir can be quickly filled after the draw-off. It has been used also in bigger reservoirs partially buried.

The flushing procedure is normally composed of three steps: draw-off, erosion and filling.

The water level droop to begin the flushing can be separated in two phases: the preliminary draw-off that takes the reservoir to the minimum operative level giving the water to the uses and that can last days or weeks; and the final draw-off that consists in the rapid reservoir draining under the minimum operative level using the bottom outlets and that occurs in a few hours.

During the draw-off the sediments in the highest part of the reservoir are removed and transported downstream where they settle again; the eroded sediments can generate a density current.

In the initial phase of the drain, in correspondence to a still high water level, the deposits erosion is concentrated in a limited area of the bed close to the discharge outlets, where a recall cone is able to occur.

Reducing further on the level, the recall cone augments and a retrogressive erosion starts: the current excavates a canal in the deposits proceeding from the barrage upstream.

When the water level reaches the level of the bottom outlets, in the reservoir a river regime is settled with high velocities that allow the beginning of a progressive erosion, starting from the reservoir queue area downstream.

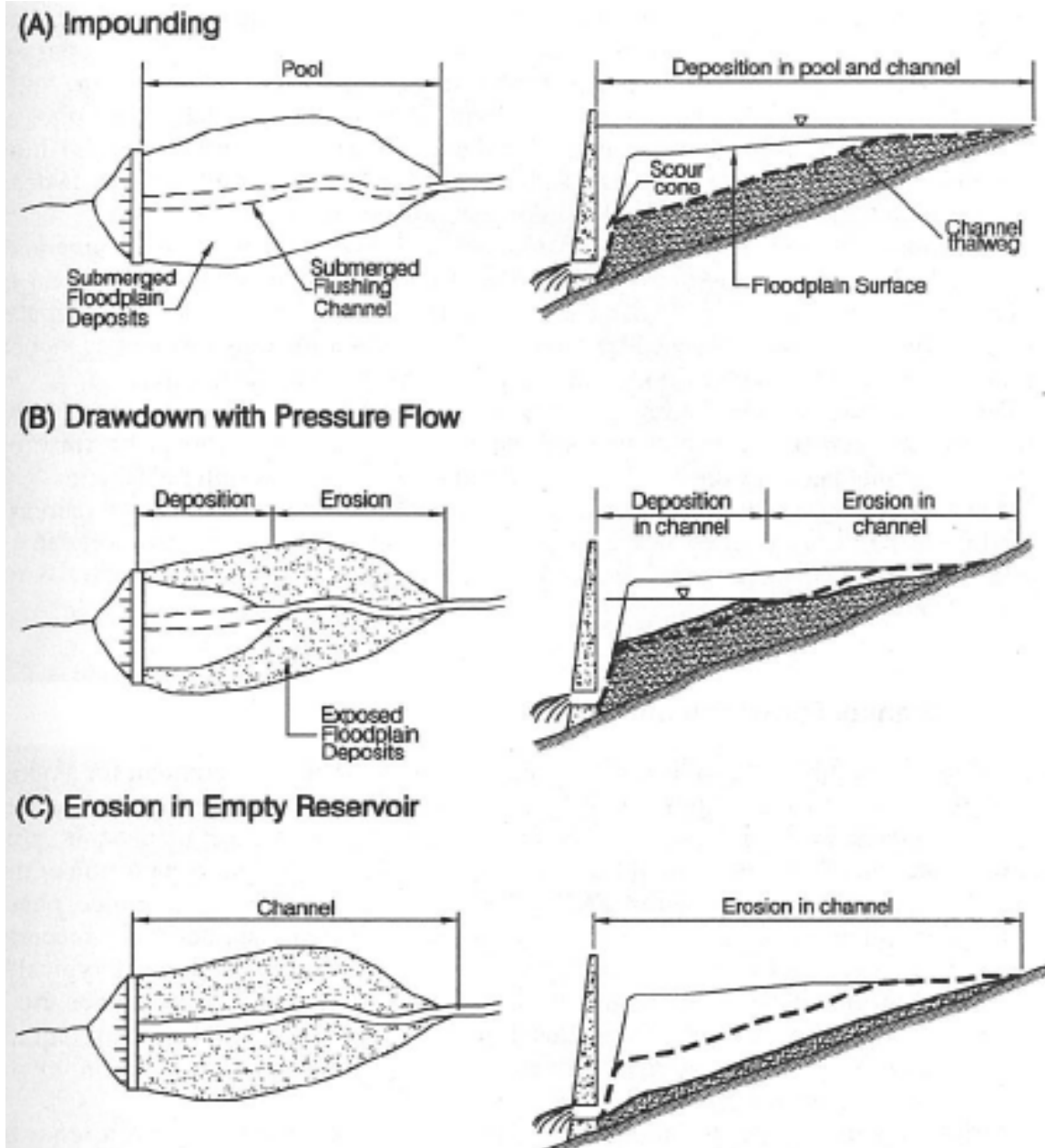


Figure 9. Plan and profile along the thalweg that show the sediments redistribution in the reservoir further to flushing operations (from Morris et al., 1997)

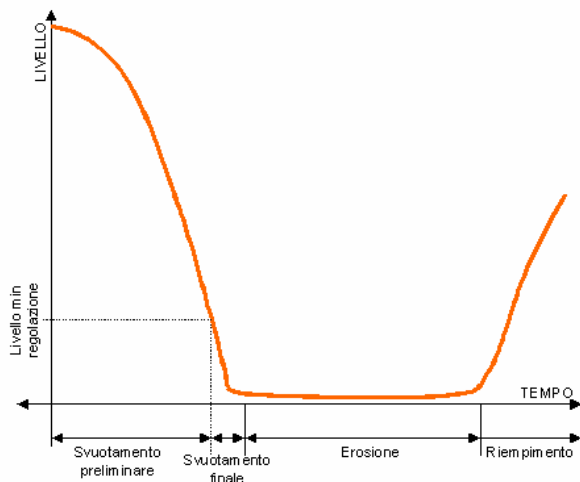


Figure 10. Level – time diagram during a drain (from Tremolada)

The erosion may continue for a few days or for weeks depending on the site, requiring longer flushing periods in the presence of remarkable sediments quantities or insufficient discharges available for the flushing.

The filling phase completes the flushing procedure and starts with closing the bottom outlets.

The flushing erodes a canal in the deposits of fine material located along the thalweg while the deposits located on the sides are not influenced, then as the reservoir age increases, the lateral deposits increase their depth while the central canal, that usually follow the ancient stream previous to the reservoir, is maintained by means of repeated flushing.

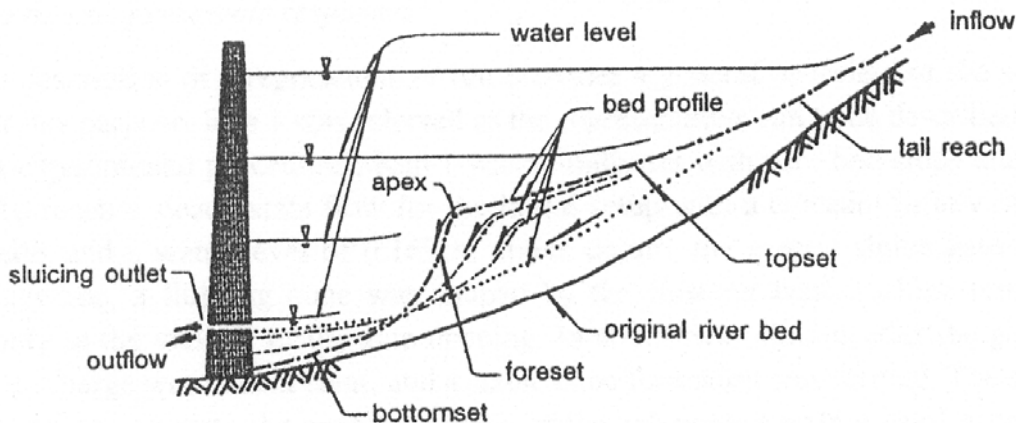


Figure 11. Deposits erosion as a function of the drop of the reservoir level.

The flushing efficiency is defined as the ratio between the volume of eroded deposit and the water volume using during the flushing and it depends on:

- Hydraulic conditions:
 - the low reservoir levels represent the most effective condition for the sediments drain;
 - the release discharges must be at least double compared with the annual average discharge;
 - the released volumes must be at least equal to 10% of the annual inflow volume;
 - the bottom outlets must be placed at the lowest level, close to the reservoir bed;
 - the discharge outlets must have an appropriate capacity, that passes at least twice the annual average discharge.
- Available water quantity:
 - the released water quantity must be enough to transport downstream the sediments;
 - the hydrologic regime must guarantee the reservoir filling after the draw-off procedure.
- Mobility of accumulated sediments:
 - coarse sediments are more difficult to be removed than the fine material;
 - it is very problematic to mobilize the blinding sediments once consolidated.
- Reservoir shape:
 - the most indicated are the narrow and extended reservoirs, with ripid banks and a high bed slope.

Anyhow, the flushing efficiency results very low, especially if the bottom outlets are not used.

However a high efficiency is not synonym of an effective sediments management: the flushing efficiency for the coarse material removal is always lower than the efficiency related to fine material, therefore if a reservoir is managed to maximize the efficiency, it accumulates continuously coarse sediments.

Moreover, high efficiencies produce high concentrations of sediments downstream, unacceptable for environmental reasons and for reasons related to the use.

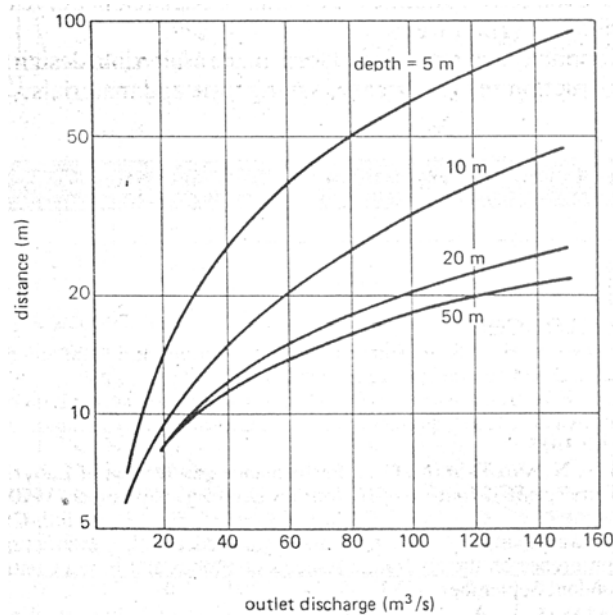


Figure 12. Limit distance where the effects of sediments erosion are felt (from Paul et al., 1988)

The flushing limitations are essentially two: in the first place it is necessary to empty the reservoir with a remarkable hydrological resource waste, this aspect limits the flushing application to reservoirs hydrologically small and without multi-year regulation; in the second place the flushing releases the sediments downstream of the dam with concentrations bigger than the natural concentrations. During the first phases, that may endure from a few hours until several days depending on the reservoir sizes, in correspondence to the dam can occur very high concentrations, typically bigger than 100 g/L, able to reach 1000 g/L.

These concentrations can generate unacceptable impacts downstream, like, for example, the obstruction of the irrigation canals and of the heat exchangers for the industrial cooling systems, and they are not appropriate for hydroelectric use; the presence of muddy deposits and of a high turbidity compromises strongly the recreational uses and the environmental risk is also remarkable: the combination of high sediments concentrations and of anoxic conditions may kill the living organisms in the river.

Moreover, the sediments released by a reservoir upstream can fill a reservoir eventually located downstream if they are not managed jointly.

Finally, the flushing periods do not coincide necessarily with the floods periods, as a consequence a significant quantity of bed material can be retained in the reservoir during the reservoir periods: these delta deposits of coarse material may be a problem in sites where the fine sediments accumulation is controlled by flushing operations.

2.3. Passive defense

The passive defense strategies consist in the hydraulic or mechanic removal of sediments by dry excavation or by means of dredges.

These techniques are usually separated in two principal classes:

- Empty reservoir excavation
- Full reservoir removal
 - Mechanic dredging

- Hydraulic dredging
- Gravity hydrosuction (with/without pumping)

The choice of removal method depends on the sediments volume, on the granulometry and on the deposits geometry, on the available discharges and/or on the reuse possibilities, on the water levels and on environmental criteria. All these factors influence both the feasibility and the costs related to the different excavation methods.

Generally, all the excavation methods involve high costs because of the big volumes of materials involved, and because of the difficulty to find sites appropriate to dump the material within economically acceptable distances. However, once the sediments settled on the reservoir, the removal by excavation or dredging is frequently the only available management possibility and the most effective technique that allows an out-bed sediment management.

A dredging intervention must be evaluated referring to 4 basic elements: the material to be removed, in other words the dredging site, the equipment to remove and to lift the sediments, the equipment to transport the dredged material and the material final destination.

2.3.1. Dry excavation

The dry excavation is performed using the traditional mechanic equipments for the ground handling. Movement of the soil

The main restriction that limits the use of this technique stays in the fact that the reservoir must be emptied: we can count with the dry excavation in reservoirs located in areas with arid climates that are naturally empty in some periods of the year or that may be emptied for extended periods.

The dry excavation is usually more expensive than the hydraulic dredging, but the cheapness of the two solutions depends on the characteristics of the site, because the dry excavation eliminates the necessity to dry the dredged muds and reduces the volumes of removed sediments compared to the hydraulic dredging.

2.3.2. Mechanic dredging

The reservoirs dredging techniques count with three phases: the excavation, the transport and the deposit.

The mechanic dredges excavate the submerged sediments by means of a bucket or of a dredge generally located on a barge or on floating sheers fixed by means of anchors or of anchor piles.

The sediments are dredged from the bed and raised by the bucket, hunged to the uplift rope of an excavating or installed on a rigid arm, located on barges (floating provided of cargo hold and watertight) and settled on the reservoir banks from where they can be transported to the final destination, dump or reuse place.

The mechanic dredges give a product with a lower water content compared with the hydraulic dredges, but they have a lower production capacity (approximately 50-100 m³/h), and they are a valuable alternative in reservoirs where the gravel predominates, or in the case of sediments with a high degree of compactness and with "trovanti" included in the deposits.

2.3.3. Hydraulic dredging

The hydraulic dredge with a rotating head at the end of the pumping line is the most used type of dredge. The removed muds are raised and pumped in a pipe that transports the sediments from the dredging place to the dump. It is a convenient removal method because it allows to transport a wide range of materials, from the fine materials to the coarse sand. Coarser materials can be hydraulically dredged but with higher costs related to the high velocities required to maintain the material in suspension.



Figure 13. Mechanic dredge

The advantages of this system are the high productive capacity that reaches 400 m³/h, and in the possibility to operate in the reservoirs without interfere with the normal reservoir operations.

However, the hydraulic dredges produce big volumes of fine sediments, because of the water presence, and a subsequent drying up is necessary, and they have an excavation depth limitation related to the fact that the pump efficiency decreases if the depth increases: as a general rule the maximum production capacity of a dredge that excavates at 15 m is half of the capacity it would have excavating at 3 m. The efficiency is also influenced by the depth, the texture and the heterogeneity of the material to be removed, further by the linearity of the pipe used to transport the sediments and by the geodetic height difference between the basin and the deposit area.

The dredging techniques, both hydraulic and mechanic, are the most expensive methods to recover the effective capacity with costs that fluctuate between 10 and 30 € per m³, even using easily available equipment, and they are used only in small basins or in the area of delta deposit.

2.3.4. Gravity hydrosuction

The gravity hydrosuction, known as S.E.P.S., Sediment Evacuation Pipeline System, uses siphon dredges, different from the hydraulic dredges because of the absence of the pump and because the discharge pipe is submerged.

The system does not require energy contribution from the exterior, because the mud is forced in a pipe by the hydraulic height difference between the extreme sections of the pipe: the water level on the reservoir and the discharge point, that should be as low as possible.

The siphon dredges may have a flat termination (with a shovel shape) or they can be equipped with a mechanic milling cutter to remove more easily the sediments breaking them up.

The pipe upstream end is located on a floating barge that allows the movement along the reservoir.

The volume of inhaled material depends on the available water load, on the granulometry of the sediments to be removed and on the siphon characteristics like the pipe length and diameter.

In the following figure are presented the graphs of the IHC, Dutch manufacturer of suction and reclamation dredges, that refer the hourly productive capacity of dredges with pipe diameters of 250 and 400 mm depending on the sediment nature (A fine sand, B medium-sized sand, C coarse sand, D coarse sand/gravel, E gravel).

The mixture movement in the pipe happens like heterogeneous flow with the coarsest material on the bed and the fine material in suspension, and the concentration of the sediments released downstream is about 10 %.

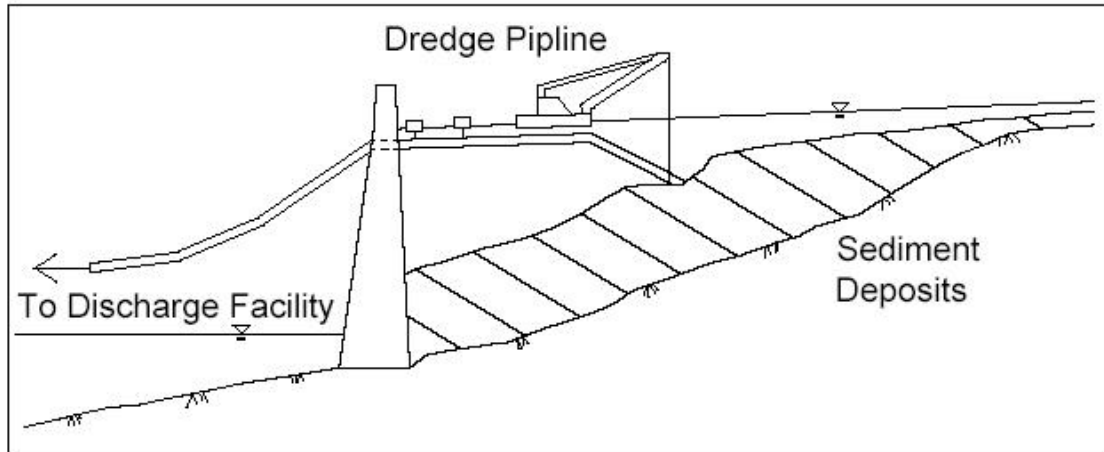


Figure 14. Gravity hydrosuction functioning scheme



Figure 15. Entrance of the pipe with shovel shape

On the base of the available hydraulic charge it is possible to calculate the maximum length of the pipe to be used, as a function of the material to be removed.

In case that planning evaluations may suggest the use of a longer pipe, it is possible to count with the presence of a pumping station, that makes the system more flexible against a costs increase.

The hydrosuction system has several advantages like the low cost, the reduced energy use, an easy and manageable system, the subtraction to the uses of water volumes definitely less than the volumes released during operations that use the bottom outlets, the possibility to reuse the recovered sediments, the possibility to control the sediments quantities released downstream and the re-establishment of the sediments natural balance in the bed downstream.

The hydrosuction dredging, that allows to reach a productivity of 200-250 m³/h, is effective and competitive from the economic point of view, especially in case of remarkable volumes to be removed.

The main obstacles to the gravity hydrosuction consist in the fact that, because of the low hydraulic height difference available, the sediments may be transferred only in areas close to the dam, whose maximum distance depends on the dam height, on the pipe diameter and on the diameter of the dredged material; moreover, the system is effective to remove fine material, not cohesive, considerably thick and not exceedingly compact. Finally, these dredges discharge in the river downstream of the dam: it is necessary to verify the discharge outlets compatibility from an environmental and ecological point of view and in case that the sediments concentration in the discharged

current is higher than the limits imposed by the laws in force, a mixture treatment must be used.

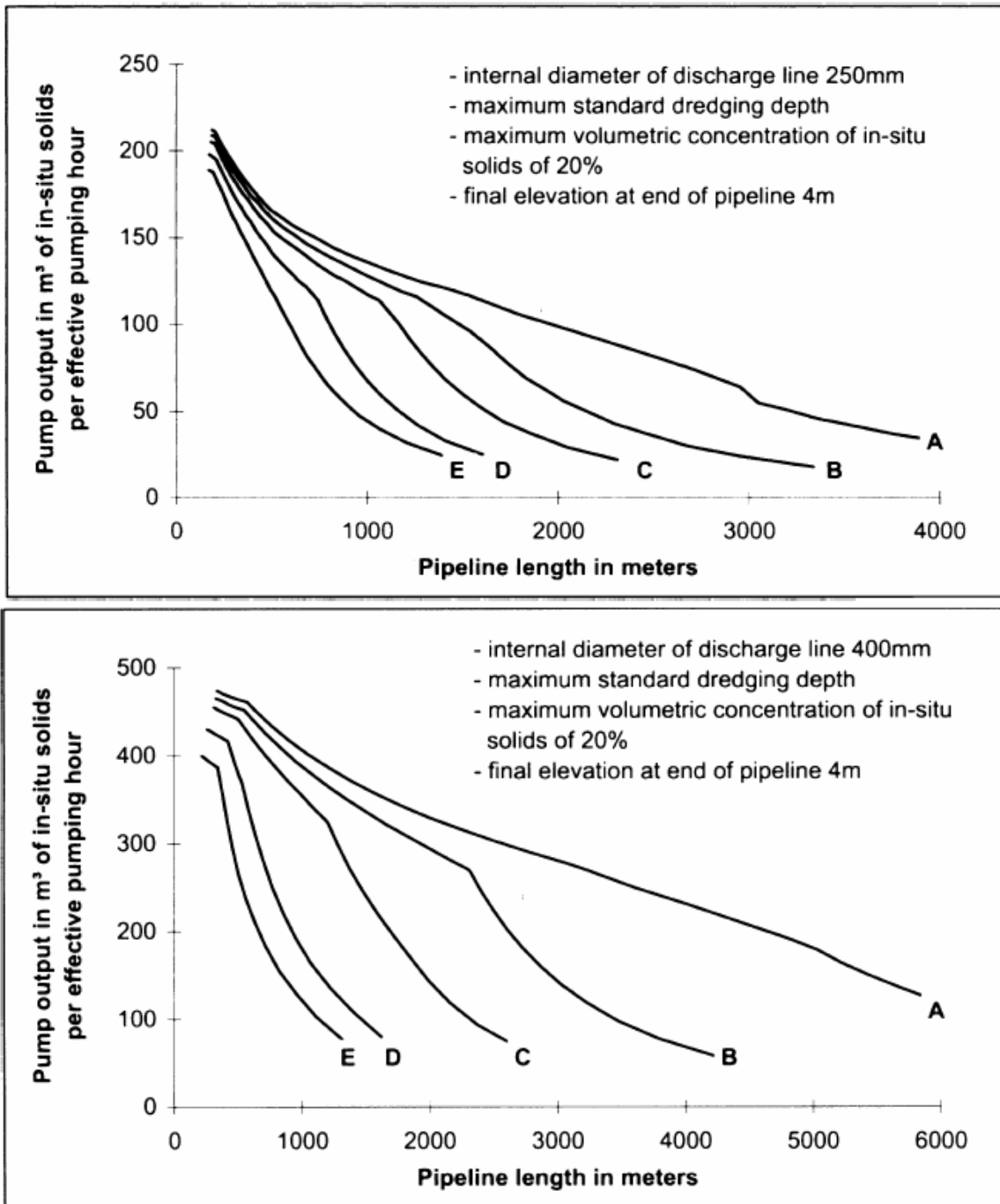


Figure 16. IHC graphs for suction dredges

3. Sediments reuse

The removal methods that allow an active management of the removed sediments are the mechanic removal and the hydrosuction. Where these methods are used it is necessary to count with a final destination of the sediments, after the appropriate analysis and the possible treatment. Generally, to dump the removed material is a waste because the sediments are of very high quality, already granulometrically well mixed in the reservoir, especially if the water level remains high for long periods, and appropriate for a reuse in several sectors.

D (mm)	DATI SPERIMENTALI (DATI GEOLIDRO)		PREVISIONI TEORICHE	
	$\Delta h/L$ (m/km)	Q_{Smed} (m ³ /h)	$\Delta h/L$ (m/km)	Q_{Smed} (m ³ /h)
500	40	350	40	300
600	32	450	-	-
700	27	550	27.9	500
800	24	700	-	-

Table 1. Experimental data of the hydrosuction system patented by Geolidro

The reuse of the sediments resulting from the operation of reservoirs rehabilitation allows to add to the economic benefits resulting from the effective capacity recovery, the benefits resulting from the use of the material.

A first possible reuse of removed sediments consist in the controlled discharge downstream of the dam to restore the balance in the sediments assessment along the stream: however the feasibility of this operation is related to the availability of remarkable overflow discharges with which it is possible to dilute the outbound mixture respecting the normative and environmental constraints without apposite waste of hydrological resource.

In the industrial sector the sediments can be used in the Portland cement production, replacing, partially or totally, the clayey part.

A different possible reuse consists in the employment of clayey and loamy sediments as agricultural soil to create beds made by impermeable material and mixtures of soils for cultures, to be used in areas where the natural soil, very permeable, requires remarkable water volumes for the irrigation.

Another possibility of reuse is the mashing-in of the removed sediments in mixtures containing amendments called "manufactured soil", useable as soils for several purposes like cover for dumps, soil for gardens, substrate for garden-center uses or for the pits renaturization.

In the construction sector the coarse material can be reused as inert.

Finally, the sediments removed from reservoirs economically "close" to the river mouth can be used for the beach nourishment.

Every use postulates a series of verifications of compatibility, between these, the verifications relative to the granulometry, to the physical-chemical and mineralogical characteristics and to the microbiology and the bacteriology.

References

- BASSON G.R. (1997) – Hydraulic Measures to deal with reservoir sedimentation: flood flushing, sluicing and density current venting, Proceedings of the 3rd International Conference on River Flood Hydraulics, University of Stellenbosch, South Africa.
- BASSON G.R. (1998) - Prediction of Sediment Induced Density Current Formation in Reservoirs.
- BASSON G.R., BECK J.S. (2002) - Control of the impacts of a dam on the downstream river morphology through flood flushing and the release of artificial floods, Proceedings of International Workshop on Ecological, sociological and economic implications of sediment management in reservoirs, Paestum, Italy 8-10 April 2002.



- BIANCHINI A. (2000) - Rimozione dei materiali sedimentati dagli invasi artificiali. Convegno: "Piccole dighe e bacini di accumulo", Torino 26 ottobre 2000.
- DI SILVIO G. (1996) - Interrimento e riabilitazione degli invasi artificiali. L'Acqua 6, 49-54
- MOLINO B. (1998) -Interrimento e riabilitazione degli invasi artificiali mediante rimozione intubata dei sedimenti: il caso dell'invaso di Camastra (Pz)
- MOLINO B., VITA M. (2004) - Il processo di interrimento degli invasi: genesi, effetti ed interventi per la tutela dell'ambiente Autorità Interregionale di Bacino della Basilicata Collana Editoriale di Studi e Ricerche n. 4.
- MORRIS G., FAN J. (1997) – Reservoir Sedimentation Handbook, McGraw-Hill.
- PALMIERI A., SHAH F., DINAR A. (2001) - Economics of reservoir sedimentation and sustainable management of dams Journal of Environmental Management, 61, 149-163.
- PALMIERI A. (2002) - Strategic alternatives for the sustainable management of reservoirs. Proceedings of International Workshop on Ecological, sociological and economic implications of sediment management in reservoirs, Paestum, Italy 8-10 April, 2002
- PALMIERI A., SHAH F., ANNANDALE G.W., DINAR A. (2003) - Reservoir Conservation Volume I: The RESCON Approach Economic and engineering evaluation of alternative strategies for managing sedimentation in storage reservoirs.
- PAUL T.C., DHILLON G.S.(1988) - Sluice dimensioning for desilting reservoirs International Water Power and Dam Construction, pp. 40-44.
- TREMOLADA L., Manutenzione straordinaria degli invasi di regolazione per l'eliminazione dell'interrimento.
- US ARMY CORPS of ENGINEERS (1997) Hydrologic Engineering Requirements for Reservoirs Publication Number: EM 1110-2-1420, 148 pp.
- US ARMY CORPS of ENGINEERS (1995) Engineering and Design - Sedimentation Investigations of Rivers and Reservoirs Publication Number: EM 1110-2-4000, 268 pp
- US BUREAU of RECLAMATION (1987) – Design of Small Dams, 860 pp
- VANONI V.A.(1975) – Sedimentation Engineering, ASCE, 418 pp

**6. RAPPORT OF PHASE B:
LABORATORY OF MARINE GÉO-ENVIRONMENTAL STUDY, LEGEM - P6
MEASURE 3.3
GESA**

PART 1. Physical modeling in the lab: Tests of offshore nourishment scenarios on beach profiles in similitude with the nature

The feasibility of off-shore nourishment techniques is not plainly demonstrated. The success of nourishment closely depends on the wave climate, the type of near-beach environment, of the beach profile and above all the proper dynamics of the beach profile. Beach nourishment relies therefore on the precise knowledge of the cross-shore sand transport. Engineering rules of art in this field are mostly based on the equilibrium beach profile concept (Dean, 1991). The dynamics are apprehended in terms of departures from these equilibria.

Numerical hydrodynamic models coupled with sediment transport modules can be used to predict nourishment time evolution. Erosion sequences are usually well and reliably reproduced since erosion is dominated by the undertow dynamics under strong wave climates. Scenarios that involve sediment transport towards the shore are difficult to capture numerically. However it is the on-shore directed sediment fluxes that will contribute to beach nourishment and berm accretion. These on-shore fluxes are related to very complex interactions between bed forms and the boundary layer dynamics driven by waves with asymmetries (vertical acceleration on the wave front; Drake & Calantoni, 2001) and skewness. Moreover a correct prediction of transient beach profile ensures that the sediment fluxes are correctly evaluated.

It can be stated that erosion scenarios have been successfully modeled since the 80's (Kriebel & Dean, 1985; Gunaydin & Kabdasli, 2003) while scenarios involving on-shore sediment transport are still under development and validation (Hoefel & Elgar, 2003). The quantitative description of complex equilibrium profiles have received little attention and remains highly empirical (Plant et al., 2001; Ribas, 2004).

For all these reasons experimental studies at laboratory scale are a precious alternatives but less used (Dette et al., 2002). The Laboratoire des Ecoulements Géophysiques et Industriels (LEGI) has developed in the last years physical modeling of beach cross-shore dynamics in the 36m long flume. This flume is equipped with piston type wave maker for irregular waves (Hasselmann et al., 1993; Dean & Dalrymple, 1984). Our research actions will focus on the comprehension of the dynamics of micro-tidal beaches of Mediterranean type, on the hydrodynamic phenomenon responsible for these dynamics and laboratory flume tests of schematics off-shore nourishment scenarios. Physical modeling should be able to address such issues as long as the hydrodynamics and the sediment transport are correctly down-scaled.

Our study aims at understanding the interactions between waves and long term beach morphology evolutions. Literature on experimental studies concerning this topic is very scarce essentially because experiments are lengthy. Typically one requires running experiment during 50h to obtain quasi-equilibrium beach profiles (Kamalinezhad et al., 2004). Note that experiment duration also depends on how "far" the initial profile is from the target one. According to the classification by Wright & Short (1984), the relevant non-dimensional number that delineates different types of beach profiles is the Dean number:

$$\Omega = \frac{H_{1/3}}{T_p w_c}$$

where $H_{1/3}$ is the significant wave height, T_p peak period of the incident wave spectrum et w_c the sediment fall velocity. This Dean number is a sort of Rouse number

that measures the ratio between the mixing of sediment induced by waves and the settling due to the fall velocity w_c . The Dean number hereafter will be evaluated for the incident waves at the depth of closure. In the experiment this depth is close to the wave maker.

Two beach profiles will be said similar if they are related to the same Dean number. Experiments by Kamalinezhad (2004a,b), show that the range of Dean numbers easily obtained in the flume is $\Omega < 5$. In the classification of Wright & Short (1984) this corresponds to intermediate beach profiles which exhibit a terrace and a doubly-convex profile (Black et al. 2002). In these profiles the upper part close to the shoreline is very close to an equilibrium Dean (1991) profile:

$$h(x) = A(d)x^{2/3}$$

where h is the water depth, x the horizontal coordinate pointing seaward and A a constant which depends on d the sediment grain diameter.

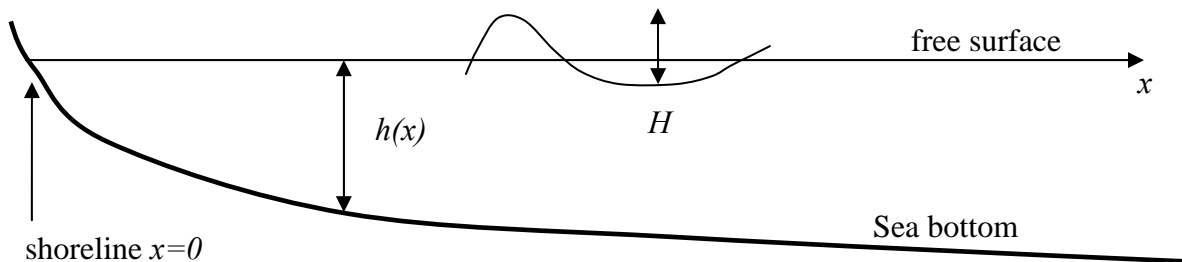


Figure 1. Schematic & notations. The wave height is H and the wave propagates on-shore in waters of depth $h(x)$.

In order to precisely relate our experiments to the nature let us analyze the Lido beach in Sète. We will base our discussion on the BT166700 beach profile (LITEAU I report; Certain, 2004):

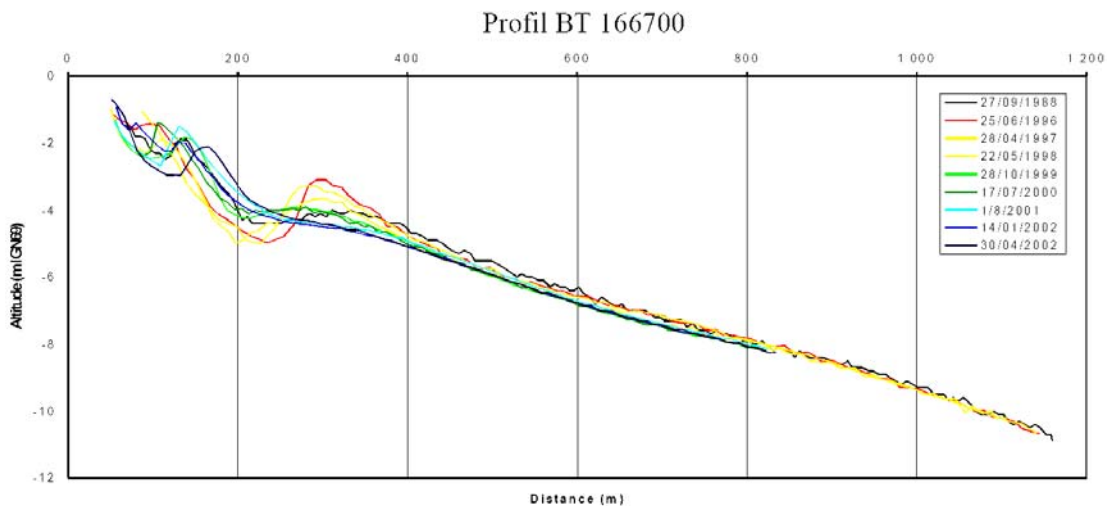


Figure 2. BT166700 beach profile & 18 years evolutions. The shoreline is located at (0,0).

On the time scale of the year, the closure depth can be evaluated as -5m which locates it at 400 m from the shoreline. A geometrical downscaling of 1/10 will enable to reproduce such beach profile in our flume. The required length is roughly 40m and the water depth at the wave-maker of roughly 50cm. The waves generated in the flume should also be similar to those in the natural environment. This is obtained with a choice of wave periods (time scales) that give identical Froude numbers in the flume and in nature and leading to smaller laboratory wave periods. The wave Froude number is defined as:

$$F = \frac{A \omega_p}{\sqrt{gh}} \quad A = \frac{H}{2 \sinh(kh)}$$

where H is the wave height, ω_p the angular peak frequency of the wave ($T_p=2\pi/\omega_p$), h the water depth at rest and k the wave number of the incident wave.

In the LITEAU I framework different wave forcing scenarios were defined and used by the numerical modelers. These are given in Table 1. With respect to our goal in the present work we will only retain those scenarios that are prone to produce berm accretion: falling storm (Certain & Barousseau, 2006). However we will also explore summer prototype waves representing very mild wave climates. All wave scenarios are given in Table 1.

		SETE	LAB
1. exceptional storm	H	4 m	0.4 m
	T_p	10 s	3.03 s
	F	0.37	0.19
2. standard Storm (TC)	H	2.5 m	0.25 m
	T_p	7s	2.12 s
	F	0.21	0.21
3. falling storm (TT)	H	1m	0.1 m
	T_p	6.5 s	1.97 s
	F	0.08	0.08
4. summer weak climate (E)	H	0.6	0.06 m
	T_p	6.5 s	1.97 s
	F	0.05	0.05

Table 1. Nature-lab similitude with geometric scales of 1/10, a closure depth of 5m in nature and of 50cm in the lab close to the wave-maker.

H is the wave height, T_p the peak period and F the Froude number

In this table all the Froude numbers are calculated at the closure depth. In the shoaling part of the profile the wave will amplify and become steeper (as the wave length decreases). The Froude number also increases as the wave propagate on-shore and in all cases reaches an ultimate value of approximately 0.38 at the breaking point.

Taking into account the fact that the scale of the model is 1/10 our experimental device cannot reproduce scenarios involving the 2 strongest storms. Indeed such waves will break just at the wave-maker. This would lead to unrealistic wave propagation. Nonetheless such scenarios would be possible if a stronger geometric reduction (1/40 for instance) was adopted. However it should be recalled that our aim is to reproduce beach reconstruction processes and off-shore nourishment which occur mainly for wave climates 3 & 4.

Sediment grain size of cell 24 which contains the beach profile profil BT166700 described above have the main following characteristics. The berm zone is composed of grains of median diameter d_{50} of 0.3mm, an internal zone comprising the inner bar where $d_{50}=0.2$ mm and an off shore zone starting at the external bar with a grain size

$d_{50}=0.15\text{mm}$. Such grain size distribution along with wave forcing scenarios allows comparing non-dimensional numbers related to sediment transport processes between the nature and the lab.

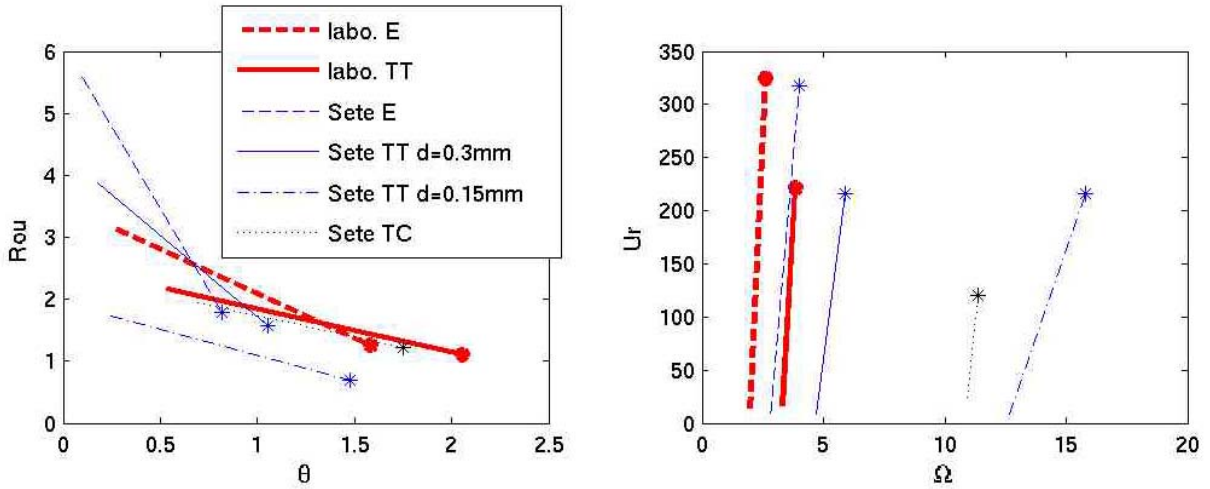


Figure 3. Non-dimensional numbers in nature and on the model. Rou is the Rouse number, θ is the Shields number, Ur is the Ursell number and Ω the Dean number (the values of the parameters used to compute such numbers are those of Tab. 1). The marker (*) indicates values at the breaking point.

There are 4 main non-dimensional numbers. The Rouse number,

$$Rou = \frac{w_c}{u'}$$

where u' is an estimate of the intensity of the turbulent fluctuations. Implementing the Rouse similitude ensures that suspensions generated by wave breaking are similar in the lab and in the nature (same exponential vertical decrease). Notice in Fig. 3 that our experiments are similar to the nature for falling storm and summer climates. The Shields number is,

$$\theta = \frac{1}{2} f_w \frac{(A\omega)^2}{g(s-1)d_{50}}$$

where f_w is the friction coefficient which depends on the grain size and the Reynolds number, s is the density ratio between the sediment and the water. In the present analysis the Shields number measures how the sediment is set in motion and transported by the waves in the shoaling zone. It also indicates if bed forms are to develop. Once more our experiments are in similitude as seen on Fig. 3. The Ursell number is purely a hydrodynamic non-dimensional number, which writes,

$$Ur = \frac{gHT_p^2}{h^2}$$

It measures the ratio of nonlinearities to dispersive effects. There is nothing surprising to note on Fig. 3 that the range of values for this number is the same in the lab and in the nature. Indeed this number only contains hydrodynamic information and therefore is redundant with the Froude number.

Concerning the Dean number Fig. 3 shows contrasting behavior. Estimations of this number for grain size 0.15mm are very different from those of the lab. This probably indicates that the long term dynamics of the outer part (seaward of the external bar) of the beach profile will not be correctly reproduced. However for grain size 0.3mm and for

the « falling storm » and “weak summer climate” the Ω are in the correct range. It is reasonable to expect that the motion of the grain size fraction 0.2-0.3 mm is respectfully downscaled in the experiments. More specifically off-shore nourishment using this fraction of grain size can be tested.

As pointed out in the introduction nourishment dynamics are closely linked to how the the beach profiles naturally evolve. In order to gain understanding in the proper morphodynamic of the beach we will undertake specific lab experiments. We will therefore apply various wave climates to the beach profile during tens of hours and measure bottom profiles evolutions, wave characteristics and infragravity motions.

It is well known that wave breaking transfers part of the high frequency energy to motions of low frequencies (Guza & Short, 1982). This process is the so-called « surf beat » (Munk, 1949) that seems to play a part not well understood in beach morphodynamics (Symonds & Bowen, 1984, Janssen *et al.*, 2003). Infragravity wave amplitude are generally small with a peak period very large typically 30s in the lab and 100s in nature. These have been identified to be generated by 2 complementary mechanisms:

- As waves break the bound long waves (set down) are released (Longuet-Higgins & Stewart, 1962)
- Waves come in wave packets that produce break point and set-up oscillations at the envelope frequencies that in turn acts as a piston at wave group frequencies (Symonds *et al.*, 1982).

In both instances, the long infragravity waves released in the surf zone reflect at the shoreline on the beach and interfere with the incident infragravity waves propagating generating the “surf beat” which length scales are of the order as the distance between the shoreline and the bar crest. This suggests that these long waves are associated with bar formations. However the quantitative verification of this suggestion has been disappointing (Dally, 1987).

On the other hand orbital motions associated to the surf beat are maximum at the shoreline. Even though small, symmetric and unable to set sediment in motion they actively modulate the transport of sediment stirred by the high frequency waves. Moreover they can be a source to second order effects such as streaming. There is evidence that a suspended load can be moved from antinodes towards the nodes of the surf beat. Consequently it has been suggested (Shi & Larson, 1984 ; Bowen 1980) that these infragravity waves play an important role in the beachface shaping. The characteristics of these waves are being documented (Michallet *et al.*, 2007) and their influence in terms of morphology will be investigated in the present project. More specifically we will investigate how transient profiles (with bars) influence the intensity and the structure of the infragravity waves.

References

- BALDOCK T.E., & HUNTLEY D.A., (2002). Long wave forcing by the breaking of random gravity waves on a beach, *Proc. R. Soc. Lond.*, A 458, 2177-2201.
- BALDOCK T.E., O'HARE T.J. & HUNTLEY D.A., (2004). Long wave forcing on a barred beach, *J. Fluid Mech.*, 503, 321-343.
- BLACK, KP, GORMAN, RM, AND BRYAN , KR, (2002) Bars formed by horizontal diffusion of suspended sediment. *Coastal Engineering*, 47, 53-75
- BOWEN AJ, (1980), Simple models of nearshore sedimentation; beach profiles and longshore bars. “*The coastline of Canada*”, Ed. SB McCann, Geological Survey of Canada, Paper 80-10, pp 1-11.
- CERTAIN, R., (2004). Etude de faisabilité pour l'utilisation des barres sédimentaires d'avant-côte dans la lutte contre l'érosion côtière. *Rapport de projet LITEAU, Ministère de l'Ecologie et du Développement Durable.*



- CERTAIN R. & BARUSSEAU J.-P. (2006) - Conceptual modelling of straight sand bars morphodynamics for a microtidal beach (Gulf of Lions, France), *ICCE'06*, San Diego, USA.
- DALLY W.R. (1984) Longshore bar formation – Surf beat or undertow? *Coastal Sediment '87*, 71-86
- DEAN, R. G., (1991). Equilibrium beach profiles: characteristics and applications. *J. Coastal Res.* 7(1), 53-84.
- DEAN R.G. & DALRYMPLE R.A., (1984), *Water Wave Mechanics for Engineers and Scientists*, World Scientific.
- DETTE H.H., M. LARSON, J. MURPHY, J. NEWE, K. PETERS, A. RENIERS, H. STEETZEL (2002) Application of prototype flume tests for beach nourishment. *Coastal Engineering* 47, 137–177.
- DRAKE TG & CALANTONI J (2001) Discrete particle model for sheet flow sediment transport in the nearshore, *J. Geophys. Res.*, 106(15), 19859-19868
- GUNAYDIN, K., KABDASLI, M. S., (2003). Characteristics of coastal erosion geometry under regular and irregular waves. *Ocean Engng.* 30 1579-1593.
- HASSELMAN, K., BARNETT, T.P., BOUWS, E. (1993). Measurements of wind-wave growth and swell decay during the Joint North Sea Wave Project (JONSWAP). *Deutsches Hydrographisches Institut, Hamburg, Reihe A (8)*, 12, 95 pp.
- HOEFEL F. & S. ELGAR (2003) Wave-induced sediment transport and sand migration, *Science*, 299, 1885-1887
- JANSSEN, T.T., BATTJES, J.A. & VAN DONGEREN A.R., (2003). Observation of long waves induced by short wave group. *J. Geophys. Res.* 108, 3252-3264.
- KAMALINEZHAD, M., (2004). Plages en équilibre morphologique et hydrodynamique associée, *Thèse INPG Grenoble*.
- KAMALINEZHAD, M., MICHALLET, H. & BARTHELEMY, E. (2004) Equilibre morphologique de barres de déferlement : expériences. *8^{èmes} Journées Nationales Génie Côtier - Génie Civil*, Compiègne,.
- KRIEBEL D.L. & DEAN R.G. (1985) – Numerical simulation of time-dependent beach and dune erosion. *Coastal Engineering* 9:33, 221-245.
- LONGUET-HIGGINS M.S. & STEWART R.W., (1962), Radiation stress and mass transport in gravity waves, with application to 'surf-beats', *J. Fluid Mech.*, 13, 481-504.
- MICHALLET H., GRASSO F. & BARTHELEMY E. (2007) Long waves and beach evolution profiles. *J. Coastal Res.*, 2007. to be published.
- MUNK, W. H., (1949), Surf beats, *Trans. Am. Geophys. Union* 30, 849-854.
- PLANT N.G., RUESSINK B.G. & WIJNBERG K.M. (2001) Morphological properties derived from a simple cross-shore sediment transport model, *J. Geophys. Res.*, 106(C1), 945-958.
- RIBAS PRATS, F. (2004). *On the growth of nearshore sand bars as instability processes of equilibrium beach states*. PhD, Departamento de Física Aplicada, UPC
- SHI N.C. & LARSON L.H. (1984) – Reverse transport induced by amplitude modulated waves, *Marine Geology*, 54, pp181-200
- SYMONDS, G. & BOWEN A.J., (1984), Interaction of nearshore bars with incoming wave groups, *J. Geophys. Res.*, 89, 1953-1959.
- SYMONDS, G., HUNTLEY D.A. & BOWEN A.J., (1982), Two dimensional surf beat: long wave generation by a time-varying break point, *J. Geophys. Res.*, 87(C1), 492-498.
- WRIGHT L.D & SHORT A.D (1984) Morphodynamic variability of surf zones and beaches: a synthesis. *Marine Geology* 56, 93-118.

PART 2. Morphodynamic modelling

As shoreface nourishment is an increasingly recognized solution for self-beach protection, efficient nourishment methodologies have to be established for various kinds of natural conditions. Due to their predictive character, numerical models may provide a valuable contribution to the design process (Hamm *et al.*, 2002 and Capobianco *et al.*, 2002). Various modelling strategies have been tested for beach nourishment assessment purposes. To our knowledge, numerical models are used to be validated for an in-situ shoreface nourishment. For example, three successive shoreface nourishments were performed on the Egmond site (The Netherlands) between 1999 and 2000 with a continuous monitoring (van Duin *et al.*, 2004). Several numerical models, 2DV, 2DH and 3D (Van Rijn *et al.*, 2003; van Duin *et al.*, 2004; Grunnet *et al.*, 2004; Grunnet and Ruessink, 2005; Grunnet *et al.*, 2005) have been used to model the nourished beach behavior during that period. The results shows that these process-based models were not yet suitable for detailed modelling of the beach profile evolution after nourishment in particular close to the shoreline. Van Rijn *et al.* (2003) showed that process-based models providing accurate results for hydrodynamics do not always yield good results for morphodynamics either at storm or seasonal time scales. Hamm *et al.* (2002) pointed out that the description of swash zone as well as the wave-related sediment transport are important for self-beach protection purposes.

The goal of this study is to use a numerical model to estimate the efficiency and the durability of a nourishment plan on sandy beaches. In order to answer these questions, proper evaluation criteria have to be defined. The criteria definition which is part of an engineering practise, is also a goal of this work.

Four numerical models are used. They require in-situ data as the natural beach profile and the incoming waves characteristics. From the initial bathymetry, several shoreface nourishments are built as for example, the nourishment of the littoral bars or the troughs and/or the creation of an additional offshore bar in an outermost position. As most of the shore erosion occurs during storm events, the study is focussed on the typical storm time scale according to the observations of Van Rijn *et al.* (2003), of the order of one day.

The main approach will be to perform several simulation strategies based on the above considerations. A validation of these results with the in-situ data will also be done and would induce a comparison between several numerical approaches and parameterizations.

From an initial beach profile, several types of shoreface nourishment are investigated, as for example nourishment of huge volume of sand on the bars or in the troughs, or creation of a new offshore bar. The simulation time scale is the 24 hours storm. Four profiles were selected for this study: profiles BT204935 for Petit-Travers site, BT128050 for Valras-Vendres, BT185590 and BT194555 for Frontignan-Maguelone. Several waves conditions based on statistical observations were selected

	Hs,o (m)	Ts (s)
Exceptional storm ES	4	10
Classical storm CS	2,5	7
Waning storm conditions WS	1	6,5

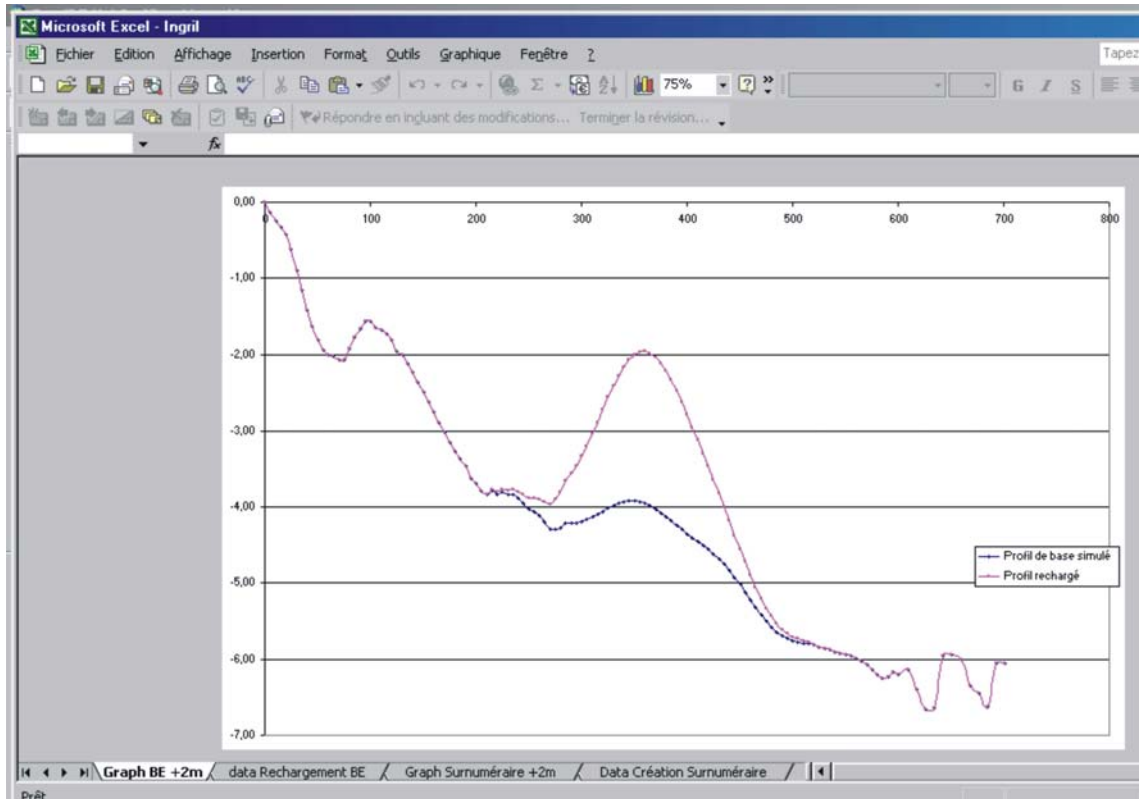


Figure 4. Example of bar nourishment for Ingril. In bleu the natural profile; in pink the nourished one.

TELEMAC and the multi 1-DH model (LEGI)

The sedimentary evolution is modeling under the action of the oblique incident waves and is coupling with different numerical tools dedicated to the other process involved in the nearshore zone. We can mention the following modules:

- Module of wave with hold in account of the energy dissipation by surge (hyperbolic equation of extended Berkhoff), (LNHE, Artemis, 2002). The Artemis code (Agitation and Refraction with Telemac2d on a Mild Slope) solves Berkhoff equation taken from Navier-Stokes equations with some other hypothesis (little camber of the surface wave, little slope...). Main results are, for every node of the mesh, the height, the phase and the incidence of the waves. Artemis can take into account the reflection and the refraction of waves on an obstacle, the bottom friction and the breakers. One of the difficulties due to Artemis is that a fine mesh must be used to have good results when Telemac2d do not need such a fine mesh.

- Module that calculates currents induced means by the surge of the waves, from the concept of radiation constraints gotten according to the module of waves, (LNHE, Telemac2d, 2002). Telemac2d is designed to simulate the free surface flow of water in coastal areas or in rivers. This code solves Barré Saint-Venant equations taken from Navier-Stokes equations vertically averaged. Then, main results are, for every node of the mesh, the water depth and the velocity averaged over the depth. Telemac2d is able to represent the following physical phenomena: propagation of long periodic waves, including non-linear effects, wetting and drying of intertidal zone, bed friction, turbulence...

- Sedimentary module integrating the combined actions of the waves and the current of waves (2D or 3D) on the transport of sediment, (LNHE, Sisyphe, 2002),

The Sisyphe code solves the bottom evolution equation which expresses the conservation of matter using directly a current field result file given by Telemac2d. Four of the most currently empirical or semi-empirical formulas are already integrated in Sisyphe (Peter-Meyer, Einstein-Brown, Engelund-Hansen and Bijker formulas). We integrate two other ones which seem more appropriate to coastal sediment transport (Bailard, 1981 and Dibajnia-Watanabe, 1992). Main results are, for every node of the mesh, the bottom evolution and the solid transport.

ARTEMIS

The ARTEMIS code (Agitation and Refraction with TELEMAC on a Mild Slope) solves Berkhoff equation taken from Navier-Stokes equations with some other hypothesis (little camber of the surface wave, little slope...). Main results are, for every node of the mesh, the height, the phase and the incidence of the waves. ARTEMIS can take into account the reflection and the refraction of waves on an obstacle, the bottom friction and the breakers.

One of the difficulties due to ARTEMIS is that a fine mesh must be used to have good results when TELEMAC2D do not need such a fine mesh. That implies a very long computing time for TELEMAC2D (computing time for TELEMAC2D is already a lot longer than ARTEMIS or SISYPHE ones).

The coupling of each of these modules rests on a methodology to adapt according to the maritime condition type reigning on the studied area: for example actualisation of the surge calculation all $\frac{1}{2}S$ hours in the case of a sea where the middle level varies with the tide; actualisation of funds for the calculation of currents, etc... Developed of such methodologies and these will be applied in the present project. The TELEMAC system possesses two modules of surge:

ARTEMIS: solves the equation of Berkhoff with integration of dissipation processes by surge and rubbing on the bottom (Artemis, 2002).

$$\nabla(C.C_g.\nabla\phi)+\omega^2\frac{C_g}{C}\phi=0$$

where $C = \frac{\omega}{k}$: phase velocity

$$C_g = \frac{1}{2} \left[1 + \frac{2kh}{sh(2kh)} \right] . C : \text{group velocity}$$

To take in account the energy dissipation du to the breaking and the stress at the sea bottom we use a supplementary term

$$\nabla(C.C_g.\nabla\phi)+\omega^2\frac{C_g}{C}(k^2+ik\mu)\phi=0$$

with $\mu = \frac{W}{(CC_g)^{1/2}}$ dissipation coefficient

where W is the dissipation function

We also can use a second model to compute the wave with a different approach, this code is COWADIS: model of stationary spectral surge also taking in account phenomena of dissipation (Cowadis, 2002).

TELEMAC2D

TELEMAC2D is designed to simulate the free surface flow of water in coastal areas or in rivers. This code solves Barré Saint-Venant equations taken from Navier-Stokes equations vertically averaged. Then, main results are, for every node of the

mesh, the water depth and the velocity averaged over the depth. TELEMAC2D is able to represent the following physical phenomena:

- Propagation of long periodic waves, including non-linear effects,
- wetting and drying of intertidal zone,
- Bed friction,
- Turbulence...

The 2D and 3D modules are:

-TELEMAC-2D: equations of Saint-Venant coming with hold in account of forçage terms by the surge (constraints of radiation)

-TELEMAC-3D: equations of Navier-Stokes with hypothesis of hydrostatic distribution of the pressure on the vertical, also integrating terms of forçage by the surge and the induced 3D effect by the surge (effect of roller, Svendsen, 1984).

One of the difficulties due to the TELEMAC2D code is the optimisation of the mesh with respect to time step. Indeed, fine meshes need a little time step to avoid too much iteration.

The TELEMAC2D solve the following equation: the Barré Saint-Venant equations and the tracer equation:

$$\frac{\partial h}{\partial t} + \vec{u} \cdot \text{grad}(h) + h \cdot \text{div}(\vec{u}) = q$$

$$\frac{\partial u}{\partial t} + \vec{u} \cdot \text{grad}(u) + g \frac{\partial h}{\partial x} - \text{div}(v \text{grad}(u)) = S_x - g \frac{\partial Z_f}{\partial x}$$

$$\frac{\partial v}{\partial t} + \vec{v} \cdot \text{grad}(v) + g \frac{\partial h}{\partial y} - \text{div}(v \text{grad}(v)) = S_y - g \frac{\partial Z_f}{\partial y}$$

$$\frac{\partial T}{\partial t} + \vec{u} \cdot \text{grad}(T) - \text{div}(v_T \text{grad}(T)) = S_T$$

with :	h	(m)	:	sea level,
	u,v	(m/s)	:	velocity component,
	T	(-)	:	passive tracer,
	g	(m/s ²)	:	gravity,
	v, v _T	(m ² /s)	:	velocity and tracer diffusion coefficient,
	Z _f	(m)	:	sea bed level,
	q	(m/s)	:	flux,
	S _x , S _y	(m/s ²)	:	source term,

The S_x and S_y terms include a lot of parameter coming from the different term as we can see in the following equation:

$$S_i = f \cdot u_i + \frac{1}{\rho} \left(\frac{\partial \tau_{ii}}{\partial x_i} + \frac{\partial \tau_{ij}}{\partial x_j} \right) + \frac{1}{\rho \cdot h} [\tau_{ik}(x_i, x_j, Z_f + h) - \tau_{ik}(x_i, x_j, Z_f)] + C_{Hi}$$

\nearrow
Coriolis

\nwarrow
Diffusion, turbulence

\uparrow
Wind

\nearrow
Shear stress sea bottom

\nwarrow
Wave

SISYPHE

The SISYPHE code solves the bottom evolution equation which expresses the conservation of matter using directly a current field result file given by TELEMAC2D :

$$\frac{\partial Z_f}{\partial t} + \text{div} \vec{Q}_s = 0 \quad (1)$$

where : Z_f is the bottom level,

\vec{Q}_s is the sediment discharge per unit width (porosity is taken into account)

Four of the most currently empirical or semi-empirical formulas are already integrated in SISYPHE (Peter-Meyer, Einstein-Brown, Engelund-Hansen and Bijker formulas). We integrate two other ones which seem more appropriate to coastal sediment transport (Bailard, 1981 and Dibajnia-Watanabe, 1992 & 1995). Main results are, for every node of the mesh, the bottom evolution and the solid transport. Moreover, SISYPHE can take into account the slope effect (formulation of Koch and Flokstra, 1981) and offer a method for long-term simulation.

MULT1DH

A hydrodynamic simplified model (called Multi1DH) use the following assumptions: a random wave approach, in a 1DH (cross-shore) direction. An offshore wave model (shoaling + bottom friction + wave asymmetry) is used with the break point estimation. The waves in the surf zone are modeled with the classic model of Svendsen (1984) with an undertow model (roller effect, Svendsen, 1984, Dally et al. 1984). The long shore current model is the Longuet-Higgins's model (1970).

MODHYS (IMFT)

The nourishment strategy is estimated by a 2DV process-based beach profile model. A detailed description of the model used here and the corresponding validation tests are introduced in Spielmann *et al.* (2004). Given the incoming wave characteristics, the wave height along the profile is estimated and the vertical distribution of the mean horizontal velocity and mean sediment concentration are computed at each cross-shore location. The total sediment flux and the time evolution of the bottom profile are then estimated.

The wave submodel is based on a phase-averaged description. The estimation of random waves characteristics along the profile is performed using either linear or first order cnoidal wave theory. In the surf zone, the wave energy dissipation rate is parameterized by the classical Battjes and Janssen (1978) approach which allows to take into account the randomness of waves. The transition zone effects are included through the breaking roller description (Stive and De Vriend, 1994; Nairn *et al.*, 1990).

The current submodel includes the description of the mean water level (Svendsen, 1984a) and of the vertical profile of the mean horizontal velocity to estimate the undertow. The numerical approach is based on the conservation of x -momentum component using a flow discharge condition based on the depth-integrated mass balance taking into account the roller mass flux and a zero bottom shear stress condition at the bottom (Spielmann *et al.*, 2004). It needs also a parametrization of the mean turbulent viscosity including turbulence production by both wave-induced bottom friction and wave breaking using the roller characteristics (Stive and De Vriend, 1987). It is taken uniform along the depth (Spielmann *et al.*, 2004).

The sediment transport submodel calculates the total mean sediment flux as the sum of both the bedload flux induced by the wave bottom shear stress asymmetry and the undertow-driven suspended flux. The bedload flux is estimated from the Bailard and Inman (1981) formula using the first-order cnoidal theory for bottom velocity estimation. The suspended flux is explicitly computed from the vertical profiles of the mean velocity and the mean suspended sediment concentration. The latter is the solution of the equilibrium between turbulent diffusion and gravity-driven sediment settling with a no-mass flux condition at the sea surface. The turbulent diffusivity is parameterized by the same model as turbulent viscosity taking into account the vertical variation for the wave contribution (Spielmann *et al.*, 2004). The seabed sediment concentration is imposed. A new parameterization (Spielmann *et al.*, 2004) based on the surface shear stress induced by the breaking roller (Deigaard and Fredsoe, 1989) was shown to give accurate results.

The bed evolution submodel computes the new sea bottom using the sediment mass conservation from the total sediment flux. The numerical resolution is based on the method proposed by Rakha *et al.* (1997) with a diffusion coefficient.

The process-based model used here cannot estimate the emerged beach evolution as the swash zone processes are not taken into account. Thus relevant criteria for beach protection have to be defined based on the model results and related to the expectations of a nourishment project. These criteria can be sorted into (1) « design criteria » used to estimate the relevance of the nourishment strategy and (2) « diagnostic criteria » used to perform a detailed analysis of the system behavior. First, the studied beach profile is outlined into typical zones Z_i as the offshore area, the bar area, the trough area and the near-beach area. Before introducing the criteria themselves, some integrated variables over each zone should be defined:

- the volume of sediment deposit in the concerned zone during a nourishment phase:

$$V_{Z_i} = \frac{1}{L_{Z_i}} \int_{Z_i} (z_b^{PX-Y}(x, t=0) - z_b^{P_n}(x, t=0)) dx$$

where: L_{Z_i} is the length of the zone Z_i ,

$z_b^{PX-Y}(x, t=0)$ the initial bottom position for the $PX-Y$ profile

$z_b^{P_n}(x, t=0)$ the initial bottom position for the natural beach profile P_n .

- the volume of sediment moved by the flow in the zone Z_i between $t=0$ and t :

$$V_{Z_i}^P(t) = \frac{1}{L_{Z_i}} \int_{Z_i} (z_b^P(x, t) - z_b^P(x, t=0)) dx$$

with: $z_b^P(x, t)$ the bottom position for the P profile.

“Design criteria” are defined with respect to three following goals:

1. Cost of the nourishment operation: it is based on the assumption that this cost is related to the volume of displaced sand.
 - a. The cost of the nourishment project is estimated with the total volume of sediment moved during the nourishment operation:

$$V_{P,1} = \int_P |z_b^{PX-Y}(x, t=0) - z_b^{P_n}(x, t=0)| dx$$

- b. If combined dredging/nourishment operations are performed along the profile, the total excess/deficit of sediment can be estimated with :

$$V_{P,2} = \int_P \left(z_b^{PX-Y}(x, t=0) - z_b^{P_n}(x, t=0) \right) dx.$$

If $V_{P,2}$ is positive, there is a global lack of sand; if $V_{P,2}$ is negative, there is a global excess of sand in the dredging and/or nourishment operation.

2. Efficiency of the beach protection. Several criteria are used for this purpose:

- Total wave energy dissipation criterion, $|E_{it} - E_0|/E_0$, where E_{it} is the wave energy in the inner trough and E_0 the offshore wave energy. This criterion estimates the remaining wave energy close to the beach which is related to the amount of energy available for sand displacement and thus erosion. The value of this criterion should be as low as possible since this energy will contribute to beach erosion.
- Mean water level increase criterion, $\bar{\eta}(x_b) - \bar{\eta}_0$, where $\bar{\eta}(x_b)$ is the mean water level near the beach and $\bar{\eta}_0$ the offshore mean water level (Longuet-Higgins, 1953). Indeed, this criterion gives information on the position where the wave-induced erosion processes will take place on the emerged beach.
- Cross-shore migration of the inner bar after 1 hour, Δx_{ib} . This criterion allows to quantify the impact of the nourishment on the motion of the inner bar *i.e.* the stability of the submerged beach.
- Ratio of the sediment volumes moved by the flow for the profile $PX - Y$ and for the natural profile P_n , $V_{Z_i}^{PX-Y}(t)/V_{Z_i}^{P_n}(t)$. This criterion compares the volume of eroded sand over the zone Z_i before and after the nourishment operation. The impact of the nourishment plan on a given zone is thus estimated.

3. Durability of the nourishment operation. The durability is related to the erosion rate of the nourished zones which should be as low as possible:

- Ratio of the sediment volume eroded by the flow during a given time period and of the volume of sand nourishment in the zone Z_i , $V_{Z_i}^{PX-Y}(t)/V_{Z_i}^{P_n}(t)$. This criterion allows to know how fast the sand added during the nourishment phase is removed by the flow and thus if the nourishment scenario is relevant with respect to durability.
- $V_{Z_i}^{PX-Y}(t)/V_{Z_i}^{P_n}(t)$ (see before) estimated over the nourished zone.

Diagnostic criteria are introduced to analyse the system behavior. Wave and roller dissipation rates are important criteria as they give informations on how the wave energy is dissipated along the beach profile and on the quantity of wave energy which arrives at the shore. The bottom concentration parameterization used in the present study is a function of the roller dissipation rate $D_r(x)$ so that $D_r(x)$ plays a key role in the cross-shore distribution of the suspended sediment flux (Spielmann *et al.*, 2004).

The diagnostic criteria used here are for a two-barred beach profile for example:



1. Maximum of the roller dissipation rate over the outer bar, D_r^{ob} . This criterion estimates the intensity of wave attenuation over the outer bar.
2. Maximum of the roller dissipation rate over the inner bar, D_r^{ib} . This criterion estimates the intensity of wave attenuation over the inner bar.
3. Ratio between the two local maxima of $D_r(x)$, D_r^{ib} / D_r^{ob} . This criterion evaluates the relative effects of both bars on total wave dissipation.

S-BEACH 2D model (CEREGE)

SBEACH is a model developed by the Coastal Engineering Research Center of the U.S. Army's Corps of Engineers specifically for examining the performance of beach systems subject to onshore/offshore sand movements under wave action. SBEACH give information on the berm and the dune erosion during storms. The model can be used to simulate artificial nourishment.

The primary application of the SBEACH model is to predict cross-shore beach morphology, on a scale of feet or meters, resulting from storm events on a time scale of hours or days. A fundamental assumption made by the authors of SBEACH is that within the short time frame of a storm event the primary transport mode is normal to the shore, and thus longshore transport is assumed to maintain continuity. Continuity infers that whatever sediment enters a particular profile from the up-drift direction, the same amount exits the profile in the down-drift direction.

Sediment transport equations used by SBEACH, for the most part, are based heavily on empirical data derived from wave tank tests. The majority of transport in SBEACH is assumed to occur within the surf zone and is assumed to be driven mainly by the dissipation of energy from breaking waves.

SBEACH works on 3 steps:

1. wave transformation from the offshore to the swash zone
2. sediment transport distribution (based on empirical equations)
3. profile changes based on the sediment mass conservation equation

The authors of SBEACH used relationships between wave and profile parameters observed in large wave tank experiments (CE and CRIEPI data sets) to develop transport rate equations for four distinct transport zones.

Principal zone of cross-shore wave propagation and sand transport

In order to simulate the wave propagation and the sediment transport, SBEACH analyses the profile into 4 zones (Figure 1):

Zone I: From the seaward depth of effective sand transport to the break point (prebreaking zone).

Zone II: From the break point to plunge point (breaker transition zone). The distance between the beginning and the end of the breaking point (l_p) is based on Galvin [1969].

$$\frac{l_p}{H_b} = 4.0 - 9.25 \tan \beta \quad \text{equation 1}$$

Zone III: From the plunge point to the point of wave reformation or to the swash zone (broken wave zone).

Zone IV: From the shoreward boundary of the surf zone to the shoreward limit of runup (swash zone).

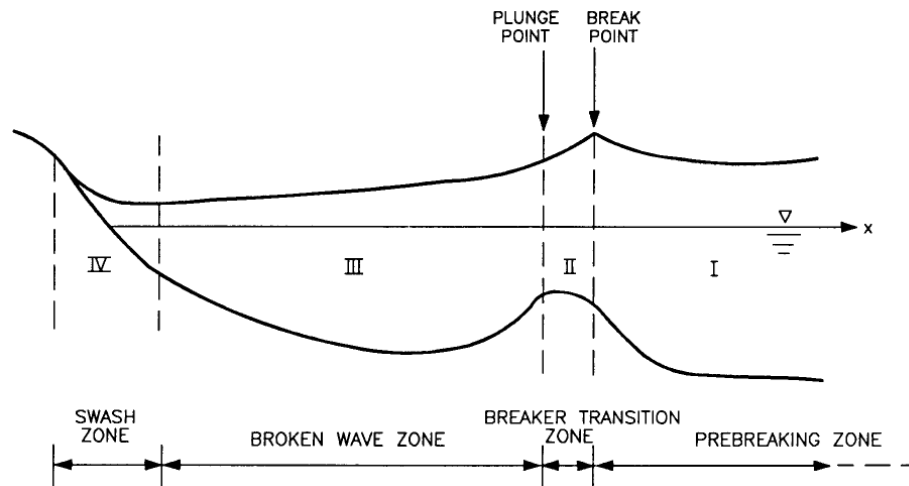


Figure 1. Definition sketch for four principal zones of cross-shore sand transport

Wave propagation

On **Zone I**, the wave propagation is based on the linear theory:

$$\left(\frac{H}{H_0}\right)^2 = \frac{\sqrt{gh}}{2C_g \sqrt{hk_0}} \quad \text{equation 2}$$

The **Zone I to Zone II** boundary is defined by the breaking criterion:

$$\frac{H_b}{h_b} = 1.14 \left(\frac{\tan \beta}{\sqrt{(H_0/L_0)}} \right)^{0.21} \quad \text{equation 3}$$

Such as the ratio H/h is smaller than equation 3, SBEACH does not consider that the wave are breaking.

On **zone III and IV**, trough the surf zone, the wave reformation is calculated by:

$$\frac{dF}{dx} = -\frac{\kappa}{h} (F - F_s) \quad \text{equation 4}$$

In this equation, the cross-shore coordinate x has its origin at the break point and is directed positive shoreward.

The assumption behind equation 4 is that the energy dissipation per unit plan beach area is proportional to the difference between the existing energy flux and a stable energy flux below which a wave will not decay. By using linear wave theory, the energy flux in shallow water is

$$F = \frac{1}{8} \rho g H^2 \sqrt{gh} \quad \text{equation 5}$$

The solution of equation 4 applying linear wave theory, is given by:

$$H = \left[\frac{1}{\sqrt{h}} \left(H_b^2 \sqrt{h_b} e^{-\kappa \int_0^x \frac{dx}{h}} + e^{-\kappa \int_0^x \frac{dx}{h}} \kappa^{-2} \int_0^x h \sqrt{h} e^{-\kappa \int_0^x \frac{dx}{h}} dx \right) \right]^{\frac{1}{2}} \quad \text{equation 6}$$

Transport rate equations

The transport rate, q , in **Zone I** is given by :

$$q = q_b e^{-\lambda(x-x_b)} \quad \text{equation 7}$$

with $\lambda =$ spatial decay coefficient $0.40 \left(\frac{D}{H_b} \right)^{0.47}$ equation 8

On **Zone II**, the transport rate is calculated with the same equation than on **Zone I** but with a smaller decay coefficient (0,2 in spite of 0,4).

Trought the **Zone III**, the transport rate is proportional to the wave dissipation and the autors of SBEACH adopt the assumption that the profile morphology run to the equilibrium profile defined by Dean [1977]. The rate of transport, q , is calculated by :

$$q = \begin{cases} K \left(D - D_{eq} + \frac{\varepsilon}{K} \frac{dh}{dx} \right) \text{ pour } D > D_{eq} - \frac{\varepsilon}{K} \frac{dh}{dx} \\ 0 \text{ pour } D < D_{eq} - \frac{\varepsilon}{K} \frac{dh}{dx} \end{cases} \quad \text{equation 9}$$

The **zone IV** is very complex because of the poorly knowledges of the processes, specially when SBEACH were developped during the end of the 80's. Consequently, it was not possible to derive a relationship connecting the net transport rate on the foreshore to local wave properties and other factors. Thus, the profile changes is based on an avalanching concept.

Profile changes

Changes in the beach profile are calculated at each time-step from the distribution of the cross-shore transport rate and the equation of mass conservation of sand. The equation of mass conservation is written as

$$\frac{\partial q}{\partial x} = \frac{\partial h}{\partial t}$$

equation 10

In calculation of the wave height distribution across shore at a specific time-step, the beach profile from the previous time-step is used, and the transport rates are calculated explicitly. The mass conservation is written in difference form as :

$$\frac{h_i^{k+1} - h_i^k}{\Delta t} = \frac{1}{2} \left[\frac{q_{i+1}^{k+1} - q_i^{k+1}}{\Delta x} + \frac{q_{i+1}^k - q_i^k}{\Delta x} \right]$$

equation 11

where k denotes the time level and i the cell number over which the discretization is carried out.

Data input

To simulate profile erosion with SBEACH model, we need to import specifics files:

- a morphologic profile (dune to offshore)
- time series of waves conditions (H, T, direction)
- time series of wind conditions (velocity and direction)
- time series of sea level conditions (height)

Several tests realized by CERC and CEREGE on a microtidal double barred profile, evidenced that SBEACH is very sensitive to the the wave and the sea level conditions.

FIELD MEASURE OF SEDIMENT

Methodologies and techniques used for the future seismic acquisition made to determine sand stock availability region

DISTART

LEGEM= methodologies and techniques used for the future seismic acquisition made to determinate sand stock availability in region LR.

Investigation of the sediment availability will be done at a large scale on the Hérault littoral and at more dense sites by high and very high seismic survey. Indeed, it seems necessary to control the sand stock of the shoreface to arrive to a better management of the littoral zone. The small volumes are generally associated to beach erosion and high sandy volume to beaches without any erosion problem. The work will be realised on the whole inner shelf with seismic profiles separated by some km and at high frequency on particular sites of several hundred of linear meters with a boomer. The goal is to quantificate the sandy volumes under the substrat.

1. Research strategies

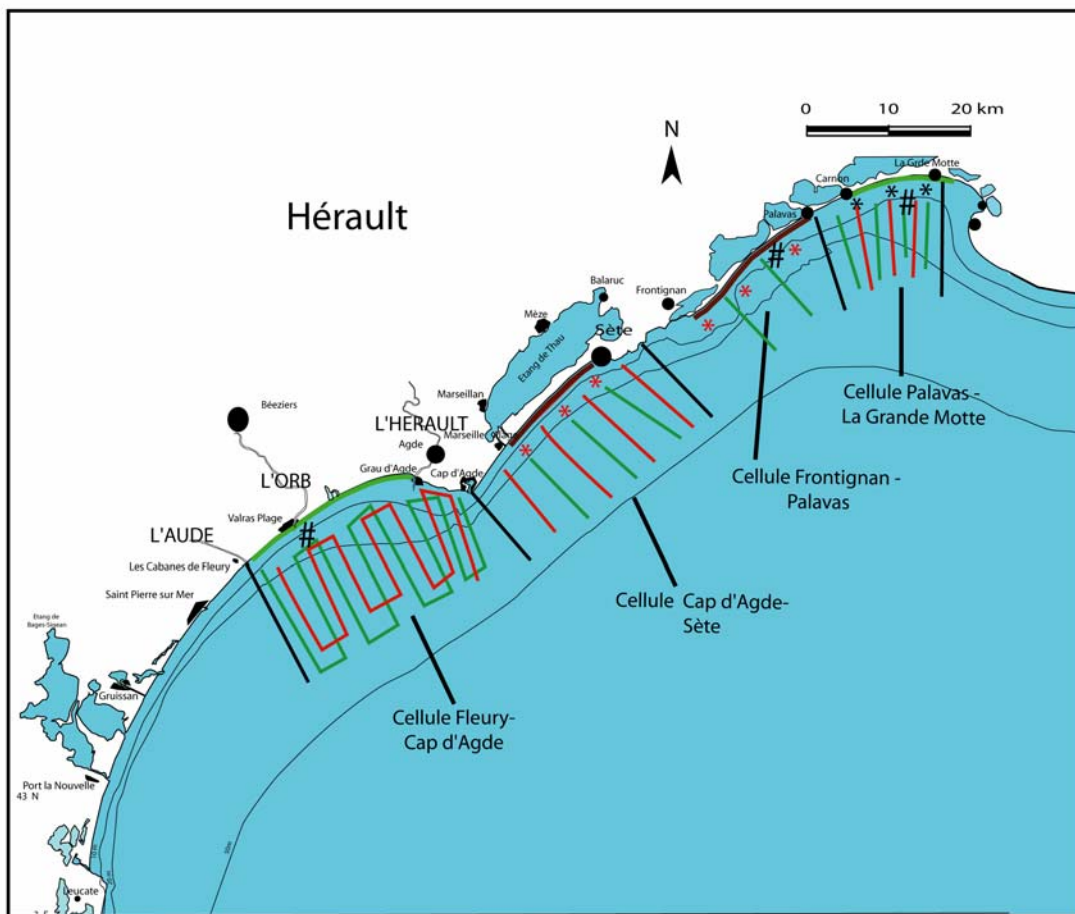
The quantification of sand stocks of the shoreface, associated to beach morphodynamics and sediment transport, constitute now an essential step to a better management of the shoreline. The sedimentary budgets made only with bathymetric profiles are not sufficient for a good analyse of beach vulnerability. This investigation can be made by using geophysical technics.

Large HR seismic investigation on the Hérault littoral

The aim is to obtain for the Hérault littoral the depth of the geological substrat and a map of the sedimentary layers above. The propection will be made from 30m depth to shallow water. The general scheme of the geological layers obtain for the inner shelf will be used to analyse the more dense seismic propection and superficial sedimentary unit obtain on several nearshore sites (1.2).

VH Resolution and high density seismic on littoral sites (Carnon-La Grande-Motte, Hérault)

The goal is to obtain a high density profiles and cores on littoral sites to have a precise estimation of sandy volumes and realise a quasi 3D image of the layers. This work is going to complete this strategy made on others sites before. The propection is made on a zone in strong erosion with a poorly littoral drift.



Etude ciblée du prisme sableux par boîtes

- * boîte sismique littorale déjà prospectée
- * boîte sismique littorale à prospecter

Imagerie à maille large de l'ensemble du prisme sédimentaire

- prospection sismique HR
- Base de données HR

Modélisation numérique de rechargement d'avant-côte

- # Zone sur laquelle vont s'effectuer les simulations

Figure 5. Sedimentary cells and study sites on the Hérault littoral

Technics and methodologies

Technics used for VH Resolution and high density seismic

The main purpose is to obtain information on the various sedimentary units of the prism and particularly on the Upper Sand Unit (USU). In the target cell Carnon-La grande Motte, three sectors were prospected by very high resolution seismics: Grand-Travers in the supposed transport zone, Carnon in the sedimentary source zone, and Carnon in the sink zone. We chose to limit the investigation at a small number of sectors, called "boxes", 500 m-long and extended offshore until the closure depth. This allows a rather dense grid of crossshore and longshore profiles and a finer analysis inside each box, leading to a good description of the sedimentary bodies and a satisfying assessment of the sand reservoirs.

The seismic device used for the study is a boomer IKB – Seistec (Simpkin & Davis, 1993). It is characterized by a line-in-cone receiver located close to the boomer plate (70 cm). Its frequency band is 1-10 kHz. During the surveys carried out on a small open boat (5 m), a SIG Energos power supply was used on board with a power of 100 J and a shooting rate of 2 shots/s. The seismic data were recorded with a Delph system, and position was determined by a differential GPS directly connected to the Delph. Post-survey seismic data processing with Delph software included frequency band pass filtering, automatic gain correction (usually TVG), trace stacking, swell filtering if necessary. The IKB-Seistec boomer is particularly well adapted to very shallow water surveys (Simpkin & Davis, 1993) and, with a vertical resolution of some decimetres, to the study of superficial sediments and present-day evolutions. It has already been used successfully to prospect the upper shoreface off the Gulf of Lions (Tessier et al., 2000; Certain et al., 2004). In complement, lithological data were collected in each box using a 2 m percussion sampler (LEGEM and CG34, 2003) and hand samples by divers.

Acquisition des données sur le terrain pour la sismique à maille large

The seismic method and the way to work on the data are the same but the system used is strong and penetrates deeper in the sediment. The ECHOES 1500 used Janus-Helmholtz transducteurs with a band 300-3000 Hz that can penetrate 30 ms of sedimentary layers.



Figure 9. Boat used for HR prospectation.



Figure 10. Transducteur Echoes 1500

**7. RAPPORT OF PHASE B:
DEMOCRITUS UNIVERSITY OF THRACE-SCHOOL OF ENGINEERING - P7
MEASURE 3.3
GESA**

Kotsovinos N., Koutitas C., Hrissanthou V., Angelidis P., Andredaki M., Georgoulas A., Samaras A. & Valsamidis A..

During Phase B the research team of the region East-Macedonia Thrace, worked along three particular projects:

- 1) To elaborate on the appropriate methodologies in order to calculate the reduction of the sediment yield at the mouth of (big) rivers due to construction of dams.
- 2) To model the turbidity currents generated during floods at the rivers mouth, and examine in particular the importance of the turbidity currents of river Nestos and Evros in the overall morphodynamics of the continental shelf.
- 3) To apply appropriate software programs (CEDAS) for the simulation of morphodynamic modelling and shoreline changes in the vicinity of coastal structures, like ports.

Part 1. Reduction of the sediment yield at the mouth of (big) rivers due to construction of dams.

Description of the adopted methodology to calculate the sediment yield

The main physical processes are: runoff resulting from rainfall, soil erosion due to rainfall and runoff, inflow of soil erosion products into streams, and sediment transport in streams. The quantification of the above chain of physical processes leads to the computation of sediment yield at the basin outlet. Particular emphasis is given to the soil erosion models. The problem of sediment yield at the mouth of big rivers has attracted the interest of many investigators. There are numerous models for soil erosion (see Hrissanthou 2005). These models are based upon

- a) Empirical concepts
- b) **Causal or fundamental concepts**
- c) The concept of unit sediment graph
- d) Stochastic concepts.

The methodology that has been adopted belongs to the class of models of fundamental concepts. It is called RUNERSET model and is based on the papers of Hrissanthou (2002; 2005).

This model estimates the monthly sediment yield and consists of three submodels:

- a rainfall-runoff sub-model,
- a surface erosion submodel (Schmidt, 1992) and
- a stream sediment transport submodel (Yang and Stall, 1976).

In RUNERSET model, the calculations are performed on a monthly time basis for each sub basin. The required input data for the rainfall-runoff submodel for each sub basin are summarized as follows: rainfall amount, temperature, sunlight hours per day, relative humidity, wind velocity, altitude, latitude, land use, and hydrological soil group. The additional input data for the erosion submodel, with reference to the rainfall-runoff submodel, are: soil slope gradient, sub-basin area, soil cover factor, main stream length of the sub-basins, grain diameter, sediment and water density, roughness coefficient and critical erosion velocity of the soil surface. The corresponding additional input data for the stream sediment transport submodel, with reference to the foregoing submodels,

concern the main stream of each sub-basin: baseflow, bottom slope, bottom width, bed roughness, diameter of suspended particles, grain diameter of bed material, and kinematic viscosity of water. Finally, the physiographic characteristics of the basins are calculated on digitized topographic and geological maps by using AUTOCAD. The results of each simulation are added in order to estimate the total mean annual yield, for the entire hydrological basin.

At this phase of the research, we applied RUNERSET model, for a only a part of the basin of Nestos river, the basin of "Platanovrysi".

Subsequently, we present in detail the three components of the RUNERSET model.

1.1 Rainfall-runoff submodel

A simplified water balance model is used for the computation of the runoff, h_o (mm), in a sub-basin. As is well known, a part of the rainfall water can be stored in the root zone of the soil. If S_{max} (mm) is the maximum available soil moisture and S_n (mm) the available soil moisture for the time increment, n , the difference ($S_{max} - S_n$) represents the soil moisture deficit for the time increment considered. It is obvious that the available soil moisture, S (mm), increases through the rainfall, N (mm), and decreases through the potential evapotranspiration, E_p (mm), the deep percolation, IN (mm) and the runoff, h_o (mm). The water balance equation is written as:

$$S_n' = S_{n-1} + N_n - E_{pn}$$

The runoff, h_{on} (mm), and the deep percolation, IN_n (mm), for the time step n can be evaluated as follows:

If $S_n' < 0$ then $S_n = 0$, $h_{on} = 0$ and $IN_n = 0$

If $0 \leq S_n' \leq S_{max}$ then $S_n = S_n'$, $h_{on} = 0$ and $IN_n = 0$

If $S_n' > S_{max}$ then $S_n = S_{max}$, $h_{on} = k(S_n' - S_{max})$ and $IN_n = k'(S_n' - S_{max})$ where $k' = 1 - k$

The maximum available soil moisture, S_{max} , is estimated by the following relationship of the US Soil Conservation Service (SCS, 1972):

$$S_{max} = 25.4[(1000/CN) - 10]$$

where CN is the curve number depending on the soil cover, the hydrological soil group and the antecedent soil moisture conditions ($0 < CN < 100$).

The potential evapotranspiration, E_p (mm), is estimated by the radiation method improved by Doorenbos & Pruitt (1977).

1.2 Surface erosion submodel

According to Schmidt (1992), the erosive impact of droplets and overland flow is proportional to the momentum flux contained in the droplets and the flow, respectively. The momentum flux exerted by the falling droplets, φ_r (kg m s^{-2}), is given by:

$$\varphi_r = Cr\rho Au_r \sin a \quad (1)$$

where: C : soil cover factor
 r : rainfall intensity (m s^{-1})
 ρ : water density (kg m^{-3})
 A : considered area (m^2)
 u_r : mean fall velocity of the droplets (m s^{-1})

a : slope gradient ($^{\circ}$)

According to Equation (5), the “active” factors of the rainfall erosion process are r and u_r , while the “passive” factors are C , A and a . The fall velocity of the droplets, u_r , is a function of the rainfall intensity, r , according to:

$$u_r = 4.5r^{0.12} \quad (2)$$

The momentum flux exerted by the overland flow, φ_f (kg m s^{-2}), is given by:

$$\varphi_f = q\rho bu \quad (3)$$

where: q : runoff rate per unit width ($\text{m}^3 \text{s}^{-1} \text{m}^{-1}$)
 b : width of the considered area (m)
 u : mean flow velocity (m s^{-1})

The mean flow velocity u can be obtained from the well-known Manning formula.

The available sediment discharge, q_{rf} ($\text{kg m}^{-1} \text{s}^{-1}$), due to rainfall and runoff, in the soil area considered, is given by:

$$q_{rf} = (1.7E - 1.7)10^{-4} \quad (4)$$

where:

$$E = (\varphi_r + \varphi_f) / \varphi_{cr} \quad E > 1 \quad (5)$$

The critical momentum flux, φ_{cr} (kg m s^{-2}), which designates the soil erodibility, can be calculated from:

$$\varphi_{cr} = q_{cr}\rho bu \quad (6)$$

where: q_{cr} : runoff rate per unit width at initial erosion ($\text{m}^3 \text{s}^{-1} \text{m}^{-1}$)

Equation (5) suggests the concept of a critical situation characterizing the initiation of sediment motion on the soil surface. However, this concept is mostly encountered in stream bed load formulas.

The sediment supply to a stream is estimated by means of a comparison between the available sediment in the corresponding basin area and the sediment transport capacity by overland flow. The sediment transport capacity by overland flow, q_t ($\text{kg s}^{-1} \text{m}^{-1}$), is computed as follows:

$$q_t = c_{\max}\rho_s q \quad (7)$$

where: c_{\max} : concentration of suspended particles at transport capacity ($\text{m}^3 \text{m}^{-3}$)
 ρ_s : sediment density (kg m^{-3})

According to Equation (7), the sediment transport capacity by overland flow consists only of suspended load. On the other hand, Yalin (1963) assumed that the mechanism of sediment transport by a shallow flow, e.g. by the overland flow, is similar to the mechanism of bed load transport in channels.

The concentration, c_{\max} , is calculated by:

$$c_{\max} = \frac{1}{x} \frac{\varphi_r + \varphi_f}{\rho_s A w^2} \quad (8)$$

where: x : factor depending on the soil slope gradient
 w : terminal fall velocity of sediment particles (m s^{-1})

Equation (8) is obtained from the equilibrium condition between the vertical component of the total momentum flux ($\varphi_r + \varphi_f$) and the critical momentum flux of the suspended particles. If the critical momentum flux is exceeded, the particles do not remain in suspension. The equilibrium condition is valid when the sediment transport capacity is achieved.

1.3 Sediment transport submodel

The sediment yield at the outlet of a stream can be computed by the concept of sediment transport capacity by streamflow using the following relationships (Yang & Stall, 1976):

$$\log c_t = 5.435 - 0.286 \log \frac{wD_{50}}{\nu} - 0.457 \log \frac{u_*}{w} + \left(1.799 - 0.409 \log \frac{wD_{50}}{\nu} - 0.314 \log \frac{u_*}{w} \right) \log \left(\frac{ui}{w} - \frac{u_{cr}i}{w} \right) \quad (9)$$

$$\frac{u_{cr}}{w} = \frac{2.5}{\log(u_*D_{50}/\nu) - 0.06} + 0.66 \quad \text{if } 1.2 < u_*D_{50}/\nu < 70 \quad (10)$$

$$\frac{u_{cr}}{w} = 2.05 \quad \text{if } u_*D_{50}/\nu \geq 70 \quad (11)$$

where: c_t : total sediment concentration by weight (ppm)
 D_{50} : median particle diameter (m)
 i : energy slope
 u : mean flow velocity (m s^{-1})
 u_{cr} : critical mean flow velocity (m s^{-1})
 u_* : shear velocity (m s^{-1})
 w : terminal fall velocity of sediment particles (m s^{-1})
 ν : kinematic viscosity of the water ($\text{m}^2 \text{s}^{-1}$)

Equation (9) was determined from the concept of unit stream power (rate of potential energy expenditure per unit weight of water, symbolized with the product, ui) and dimensional analysis. The variable, u_{cr} , in Equation (9) suggests that a critical situation is considered at the beginning of sediment particle motion, as in most sediment transport equations.

The sediment yield at the outlet of a stream can be estimated by means of a comparison between the available sediment in the stream and the sediment transport capacity by streamflow.

1.4 Preliminary estimation of mean annual sediment yield at the outlet of Nestos River basin, before and after the construction of the dams.

1.4.1 Introduction

The construction of dams along a river creates accumulation of sediments upstream, decreasing considerably the quantity of sediments that reaches the outlet of river basin, and disturbing the balance of sediment transport from the river to the sea. The perturbation of this balance has as main consequence the erosion of coastal region that is located at the river's outlet to the sea.

Nestos River has a total length of 234 km, 94 km of which are in the Bulgarian territory, where the river is called Mesta, while 140 km are in the Greek territory. The river basin has a total area of 5761 km^2 , from which 2280 km^2 belong to Greece and

3481 km² belong to Bulgaria. The mean altitude of the Bulgarian part of the basin is 1318 m.

Nestos River springs from the Bulgarian territory between the mountains Rila (altitude 2716 m) and Rodopi. Its outlet is in the North Aegean Sea, forming a delta of 2 km width. Nestos River also constitutes the natural border between Macedonia and Thrace (Greece).

In the Greek as well as in the Bulgarian part, a number of dams (reservoirs) that serve various aims, have been constructed. In the Bulgarian part, Dospat dam has been constructed in 1967. The reservoir of Dospat dam has a storage capacity of 443 million cubic meters. In the Greek territory, Thisavros dam and Platanovrysi dam have been constructed in 1995. The storage capacity of their reservoirs is 565 and 63 million cubic meters, respectively. Beyond their basic aim, however, these dams retain a quantity of sediments that were transported to the estuaries before their construction. Thus, the balance of sediment transport has been disturbed involving erosion in the coastal region in the east and the west part of the delta, as well as in the adjacent shorelines. In Figure 1, the entire basin of Nestos River and the location of these three dams are illustrated.



Figure 1. Nestos River basin and the location of dams

1.4.2 Sediment yield before the construction of the dams

The mean annual sediment yield of Nestos River basin up to Thisavros place, before the construction of the dams, has been estimated by the consulting office which designed the construction of the dam (Design Office of Public Electrical Company of Greece) equal to one million tonnes per year. The Paraskevopoulos Consulting office which was responsible for the report on the Environmental Consequences of the Thisavros Dam, reports a rough estimation of the Sediment yield up to Thisavros place, equal to 10 million tonnes per year. In the Bulgarian part, there exist measurements of suspended sediment yield at the basin of Mesta-Kula (area 1511 km²) with a measured suspended load 202 t/km²-an. This value, applied to the whole Bulgarian basin gives suspended load about 0.87 million tonnes per year. Apparently there is a dispute about the proper value for the sediment yield before the

construction of the Thisavros dam. RUNERSET model will be used at the subsequent phase of this research in order to estimate more accurately the sediment yield.

At this phase of the research, a preliminary study has been made using an empirical model (MONERIS model) for the basin up to Thisavros Dam in the Bulgarian part , mainly due to difficulties in gathering the necessary data of this transboundary river. MONERIS empirical model (Behrendt et al., 1999) is applied preliminary to estimate the overland flow and the surface erosion in the Bulgarian part. The model is based on flow data and on a Geographic Information System (GIS), which includes digital maps. The annual sediment yield (SED) at the outlet of the hydrological basin at Thisavros is estimated by the Moneris model using the following empirical equation:

$$SED = BA * SDR \quad (12)$$

where: BA: soil loss (t/a)
SDR: sediment transport ratio (%)

The sediment transport ratio is calculated by the following equation:

$$SDR = 0.012 * (SL - 0.25)^{0.3} * A_{ACKER}^{1.5} \quad (13)$$

where: A_{ACKER}: arable land area (ha)
SL: slope (%)

The basin up to Thisavros Dam was divided into 11 natural sub-basins for more precise calculations using the Moneris model.

The annual sediment yield (SED) at the outlet of the hydrological basin from Thisavros up to the river mouth (Platanovrysi dam basin and basin between Platanovrysi dam and Toxotes) has been accomplished using RUNERSET model. The Platanovrysi basin was divided into 9 natural sub-basins for more precise calculations, see Figure 2, and 20 sub basins for the basin between Platanovrysi dam and Toxotes outlet.

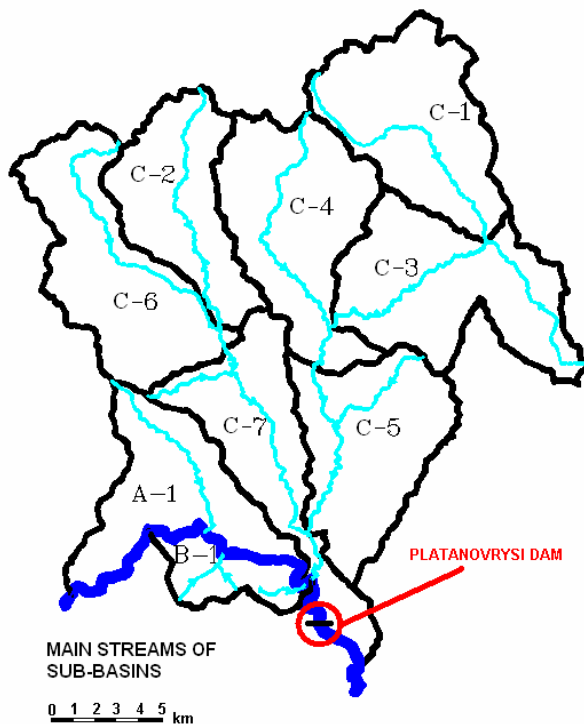


Figure 2. The division of Platanovrysi basin in nine sub basins in order to calculate the sediment yield using RUNERSET model.

In Table 1, we present the preliminary estimations regarding the sediment yield before the construction of dams. The mean annual sediment yield was calculated, considering three successive basins. The results of each simulation were added in order to estimate the total mean annual yield, for the entire hydrological basin. We estimate that the mean annual sediment yield of Nestos River basin at the mouth is about 2.400.000 t/year.

Basin	Number of sub-basins	Model	Basin area [km ²]	Mean annual sediment yield [t/year]
Thisavros dam basin	11	EMPIRICAL MODEL	4315.50	1 800 000
Platanovrysi dam basin	9	RUNERSET	405.01	300 000
Basin between Platanpvrysi dam and Toxotes	20	RUNERSET	840.00	300 000
Total	-	-	5560.51	2 400 000

Table 1. Mean annual sediment yield before the construction of the dams

1.4.3 Sediment yield after the construction of the dams

Sediment yield at the outlet of Nestos River basin (Toxotes), after the construction of the dams, originates mainly from soil erosion and bed erosion in the basin part downstream of Platanovrysi dam. However, it has to be taken into account that sediment yield originating from Thisavros dam basin is accumulated in Thisavros Reservoir, while sediment yield originating from Platanovrysi dam basin is accumulated in Platanovrysi Reservoir.

The mean annual sediment yield at the outlet of Nestos River basin (Toxotes), close to the river mouth, after the construction of the dams, is given in Table 2. We estimate that the mean annual sediment yield of Nestos River basin at the mouth after the construction of dams is about 300.000 t/year, i.e. a severe reduction .

Basin	Number of sub-basins	Model	Basin area [km ²]	Mean annual sediment yield [t/year]
Basin between Platanpvrysi dam and Toxotes	20	RUNERSET	840.00	300 000

Table 2. Mean annual sediment yield after the construction of the dams

1.4.4 Remarks and conclusions

According to the results of the present work, it becomes obvious that the mean annual sediment yield that reaches the outlet of the Nestos River basin has been decreased by about 2.100.000 t/year, after the construction of the dams. It is therefore obvious, that the balance of sediment transport from Nestos River to its coastal region has been disturbed considerably.

1.4.5 Future work planning

In the next phase of this project, RUNERSET model will be calibrated using data from the Mesta –M.Koula sub-basins of the Bulgarian part of Nestos River basin, for which water discharge and sediment yield data are available.

Subsequently RUNERSET model will be applied to the entire Bulgarian part of Nestos River basin and to Greek part of the basin up to the Thisavros dam for more accurate estimations .

Part 2. Modeling the turbidity currents generated during floods at the rivers mouth

2.1. Overview

When the density of sediment-laden river water exceeds that of the lake or ocean into which it discharges, the river plunges to the bottom of the receiving water body and continues to flow as a hyperpycnal flow. These particle-laden underflows, also known as turbidity currents, can travel remarkable distances and profoundly influence the seabed morphology from shoreline to abyss by depositing, eroding, and dispersing large quantities of sediment particles Kassem et al (2001), Khan et al (2005).

2.2. Aim

The main aim of the current work is to reveal the dynamics, the flow structure and the corresponding erosional and depositional characteristics of hyperpycnal flows (Turbidity currents) that are usually formed during an extreme flood event at the river mouths of the major rivers in the Region of East=Macedonia-Thrace , with considerable water and sediment discharge values (Nestos river, Evros river) .

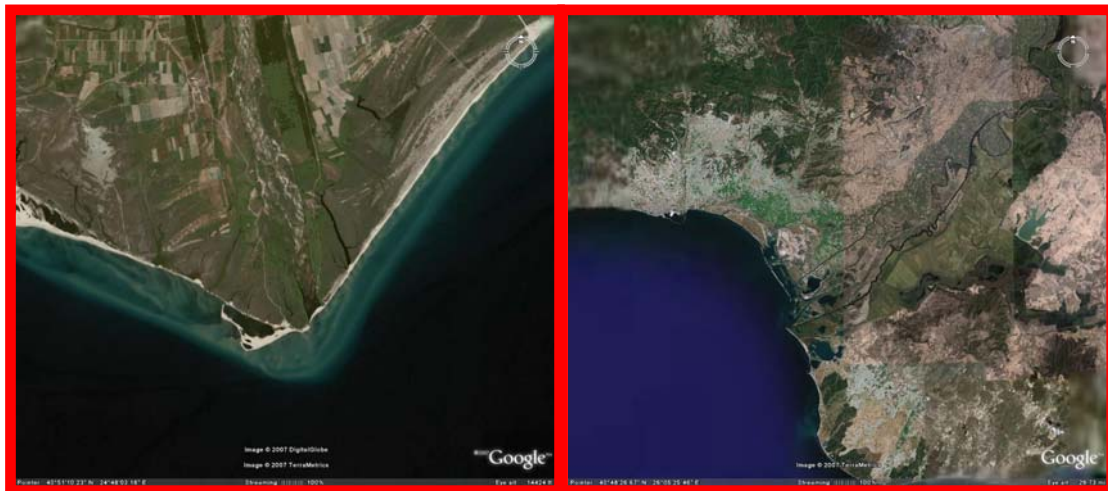


Figure 3: Nestos (left) & Evros (right) River Deltas

2.3 Applied Methodology

Solution of Reynolds-averaged Navier-Stokes equations along with sediment-conservation equations for individual grain-size classes treated as species. Closure of the turbulence stress terms is obtained by using the k-e model (where k is the turbulent kinetic energy and e is the turbulence dissipation rate), modified for the buoyancy effect, Imran (2004) , Kassem (2001) .

- The model treats the turbidity current and the ambient flow as a mixture of species, water being the dominant species and the suspended sediment representing the rest .

- A robust CFD (Computational Fluid Dynamics) solver (FLUENT) is used for the computations, FLUENT Incorporated (2000).
- Comparison of the model with existing laboratory experimental results for verification purposes.
- Application of the model in field scale for Evros and Nestos rivers in order a) to investigate the contribution of their flood turbidity currents in the general morphodynamics of the region, b) to explore sediment transport, erosion and deposition in the “neighbor” of the rivers delta, c) to explain the surficial bottom sediments which are distributed along zones almost parallel to the coastline.

Part 3. Methodology for the simulation of morphodynamic modelling and shoreline changes in the vicinity of coastal structures (Ports).

3.1 Introduction

There are a few software packages that have been developed for the simulation of morphodynamic modeling. The two most successful and popular software packages are the Mike21 (developed by the Danish Hydraulic Institute) and the CEDAS (Coastal Engineering Design and Analysis System). CEDAS 4.03 is a commercial, comprehensive collection of coastal engineering design and analysis software, developed by or for the U.S. Army Engineer Waterways Experiment Station with Veri-Tech Inc. Its contents range from simple technologies, to sophisticated models for multi-dimensional hydrodynamics, wave propagation, near shore hydrodynamics and beach processes, inlet technology, and harbour oscillation. The powerful tools in this package are complemented by pre- and post-processing routines, multi-dimensional graphical tools for results visualization and animation, grid generation software, and access to extensive wave/wind/bathymetric data resources. The Region of East Macedonia-Thrace adopted the CEDAS 4.03 software for the simulation of coastal morphodynamics and for simulation of shoreline changes in the vicinity of coastal structures. The Near shore Evolution Modelling System of CEDAS (NEMOS) is a set of codes that operates as a system to simulate the long-term evolution in response to imposed wave conditions, coastal structures, and other engineering activity (e.g., beach nourishment). Basically, in our modeling, we use the following key codes of CEDAS 4.03:

- **STWAVE** (**ST**eady **WAVE**) is a 2-D finite-difference representation of a simplified form of the spectral balance equation to simulate near-coast, time-independent spectral wave energy propagation (see USACE, 1999). The model assumes:
 - a) Mild bottom slope and negligible wave reflection,
 - b) Spatially homogeneous offshore wave conditions,
 - c) Steady-state waves, currents, and winds,
 - d) Linear refraction and shoaling,
 - e) Depth-uniform currents and
 - f) Negligible bottom friction,
 - g) Only wave energy directed into the computational grid is significant, i.e., wave energy not directed into the grid is neglected, and
 - h) Wave conditions vary slowly enough that the variation of waves at a given point over time may be neglected relative to the time required for waves to pass across the computational grid.
- **GENESIS** (**GENE**ralized Model for **SI**mulating **S**horeline Change) is a model for calculating shoreline change caused primarily by wave action and can be applied to a diverse variety of situations involving almost arbitrary numbers, locations, and

combinations of groins, jetties, detached breakwaters, seawalls, and beach fills (see USACE, 1989). The system is based on one-line theory, whereby it is assumed the beach profile remains unchanged permitting beach change to be described uniquely in terms of the shoreline position. The program can be applied to a diverse variety of situations involving almost arbitrary numbers, locations, and combinations of groins, jetties, detached breakwaters, seawalls, and beach fills. Other features included in the system are wave shoaling, refraction, and diffraction; sand passing through and around groins, and sources and sinks of sand.

- **SBEACH** (**S**torm-induced **BEA**ch **CH**ange) simulates cross-shore beach, berm, and dune erosion produced by discrete storm events, describing the combined effect/action of waves, winds and water level changes.
- **GRIDGEN** is a code to create uniform grids at arbitrary orientations from random bathymetry/topography data. This code permits construction of both the wave model and **GENESIS** grids.

3.2. Methodology of applying CEDAS in Pilot Study Areas

The object of this research project is the prediction of shoreline change in Thrace due to the wave action which causes sediment transport along the beach, in combination with the problem of changing the sediment yield due to the construction of large dams or coastal structures.

In order to explore the CEDAS software capabilities and familiarize with the various models' Graphic User Interfaces (G.U.I.), a pilot application was made for two pilot cases a) the river Nestos Delta b) the Alexandroupolis area and the Port's construction impact on coastal morphology. Most of NEMOS auxiliary codes were applied (GRIDGEN, WWL, WSAV, SPECGEN), as well as the key codes STWAVE and GENESIS, resulting in maps that represent the wave climate and the shoreline change respectively for the study area.

3.3. Field discretization--Input of points to GRIDGEN

The initial field discretization (Figure 4) is confined between the sites of Alexandroupolis Port and Nestos River estuary, yet it will extend in the next phase to comprise the coastal area to the east as well, up to Evros River estuary.

Initially, we digitized Thracian Sea, from the Delta of Evros River to the Delta of Nestos River, by using the bathymetry of maps at scale 1:50000. We collected the coordinates of 2750 points in an arbitrary Cartesian system, which are referring both to the beach and to the ocean.

The digitization took place with the help of Autocad. The coordinates of these points were transferred to the GRIDGEN (sub-program of CEDAS), where the grid of the area was created (grid cell dimension: 25mx25m.). In addition, as **input structures' characteristics/data** we use the Port of Alexandroupolis and particularly, the external breakwaters which stop the transfer of sediments. These data are accurate and they were collected from the Organization of the Port of Alexandroupolis.

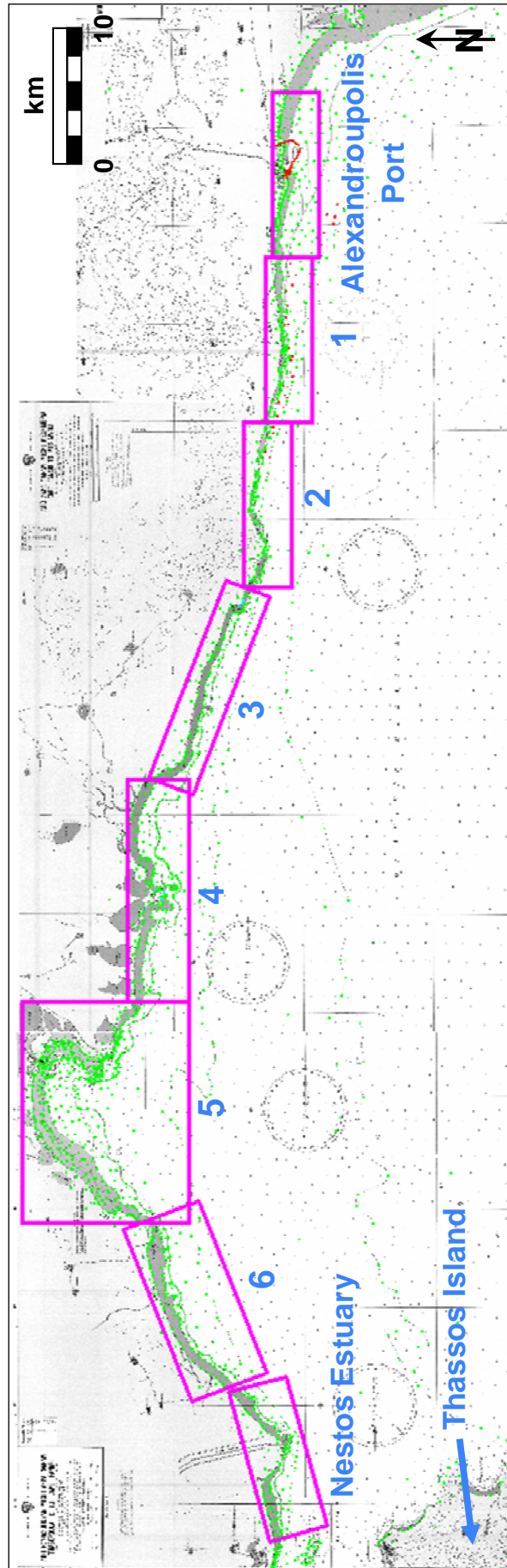


Figure 4. Spatial discretization of the East Macedonia and Thrace coastal region from Alexandroupolis Port to Nestos estuary Area for grid **generation**. Digitization of the studied area by using AUTOCAD.

3.4. Input of wave data

At the present phase of the research, we are using some preliminary wave data, mainly to develop the methodology that we will follow in phase C. These wave data will be used for running the wave model STWAVE of CEDAS and they are presented in a time series form which provides the wave parameters of height, period and direction every 6hr for one year. The complete set of wave data in the near shore that will be used at Phase C will be provided by Beachmed-e-sub program 2.2 (Nausicaa).

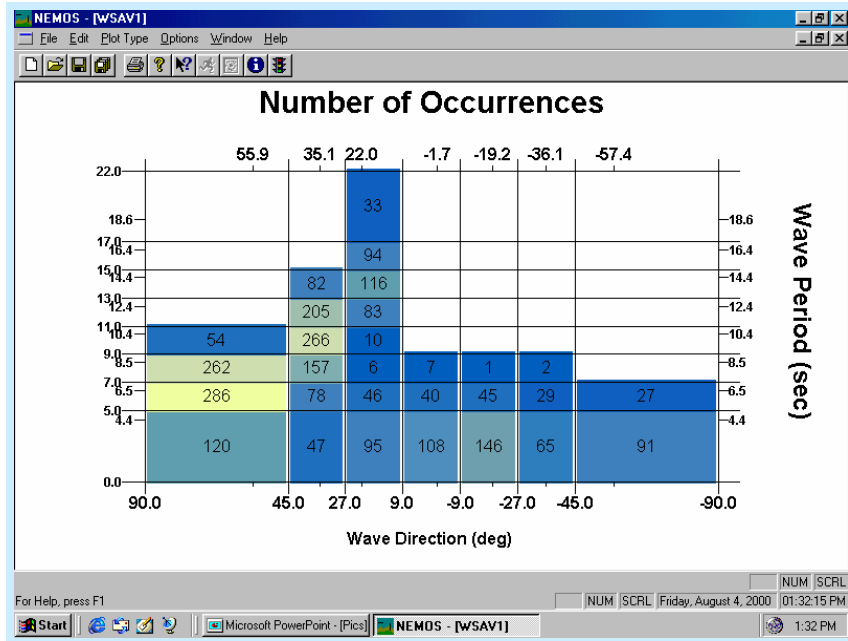


Figure 5. Bands of waves

The selection of bands chosen resulted in 29 cases to run with the wave model, its case representative of the possible periods and direction that may cause sediment transport.

These cases are used for the creation of the wave spectra:

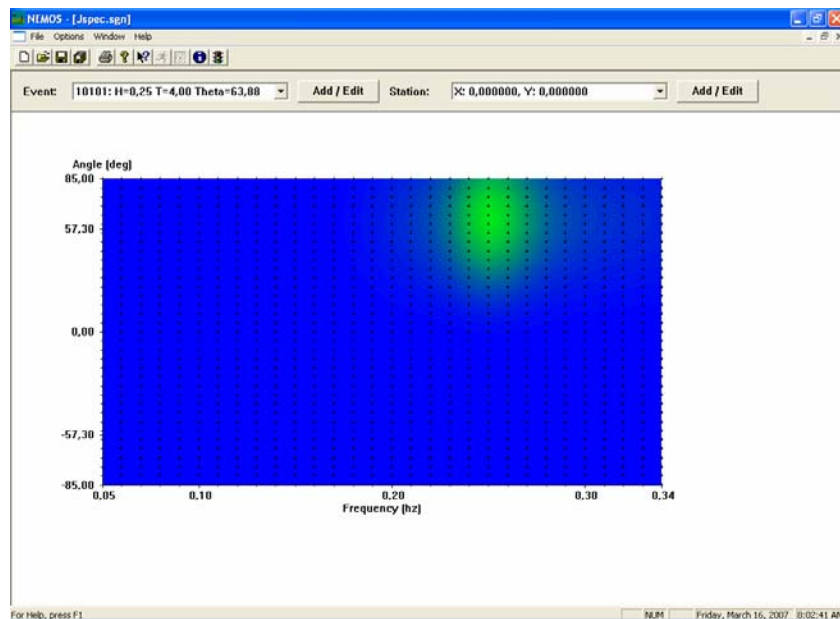


Figure 6. Graphical depiction of the wave spectra.

3.5. STWAVE simulation results for two pilot studies

Figure 7 presents the results of the wave model (STWAVE) simulation of the wave movement toward beach in the coast of Alexandroupolis port. Figure 8 presents the results of the wave model (STWAVE) simulation for the Nestos River Delta.

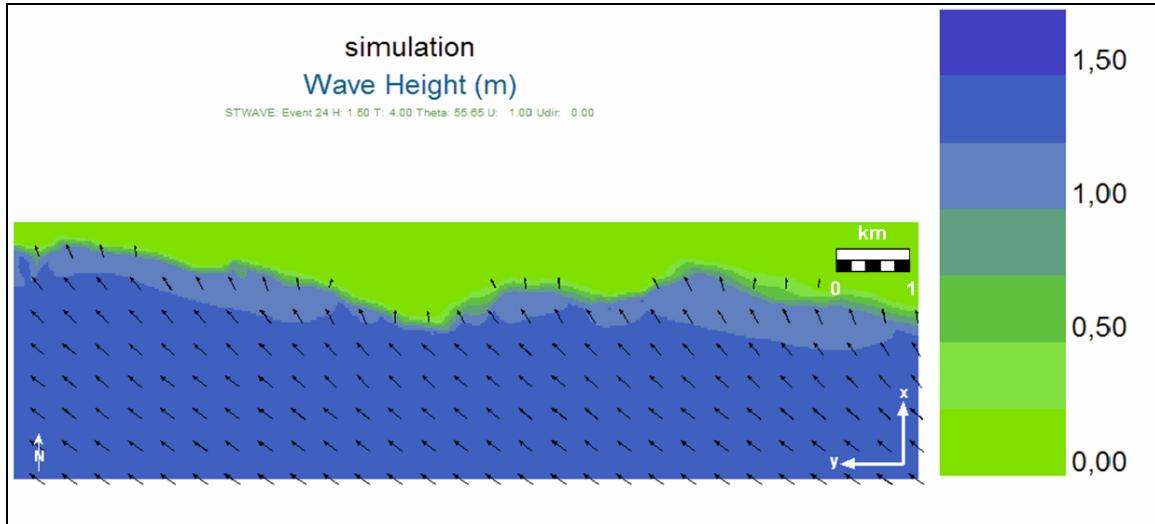


Figure 7: Alexandroupolis (Evros) port pilot study .Wave height contours and wave direction vectors for simulated event characteristics: $H=1.50\text{m}$ / $T=4.0\text{sec}$ / $\text{Theta}=55.65\text{deg}$. Wave movement toward beach. The vectors indicate the direction change of the waves due to the phenomenon of refraction.

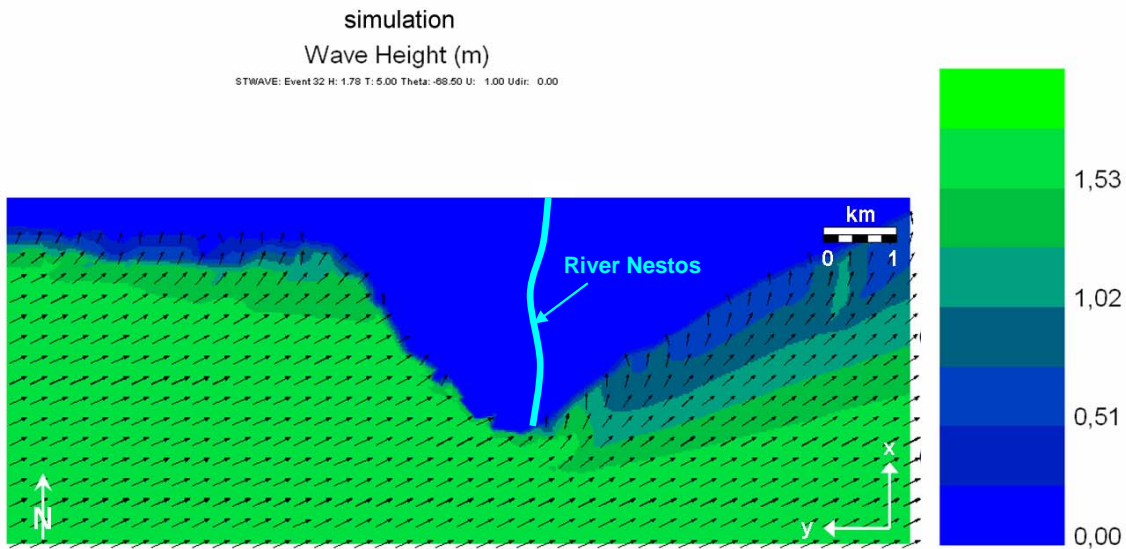


Figure 8: **Nestos Delta Pilot study**. Wave height contours and wave direction vectors at the Nestos estuary site for simulated Event characteristics: $H=1.78\text{m}$ / $T=5.0\text{sec}$ / $\text{Theta}=-68.50\text{deg}$.

3.6. Use of GENESIS model for simulating shoreline change

Output data from the wave model STWAVE and GRIDGEN are used as input to GENESIS.

Figure 11 presents the result of the shoreline change model (GENESIS) application for the Alexandroupolis Port area. The simulated time period is 40 years and the calculated volumetric change is $+1.67 \times 10^6 \text{ m}^3$, with positive values in GENESIS indicating accretion. Figure 12 presents the shoreline change over a 40-year period for the Nestos estuary site. The simulated time period is 40 years and the calculated volumetric change is $-2.75 \times 10^4 \text{ m}^3$, with positive values in GENESIS indicating accretion and negative values indicating erosion. These are preliminary numerical runs. The emphasis was given to establish the methodology of using CEDAS –GENESIS to simulate the coastal evolution. At the next phase, the emphasis will be given to use improved wave data, boundary conditions (including the river sediment yield), improved basic data, numerical test to calibrate transport and longshore coefficients of the program on the basis of known past erosion/accretion data in the area of study

Start X1 (m)	Position Y1 (m)	End X2 (m)	Position Y2 (m)	Model X-Index	Model Length	Seaward Depth (m)	Permeability
3396,760	209,870	3060,220	1115,840	110	2027,071	10,000	0,00
3060,220	1115,840	3470,010	1668,100	114	2317,656	10,000	0,00
4752,990	1141,470	4668,420	1202,290	149	3548,368	10,000	0,00

Figure 9. Input of breakwaters.

Sand and beach data

Effective grain size: (mm)

Average berm height: (m)

Closure depth: (m)

Longshore sand transport calibration coefficients

K1:

K2:

Figure 10. Input of grain size, average berm height, closure depth and alongshore sand transport calibration coefficients K1, K2.

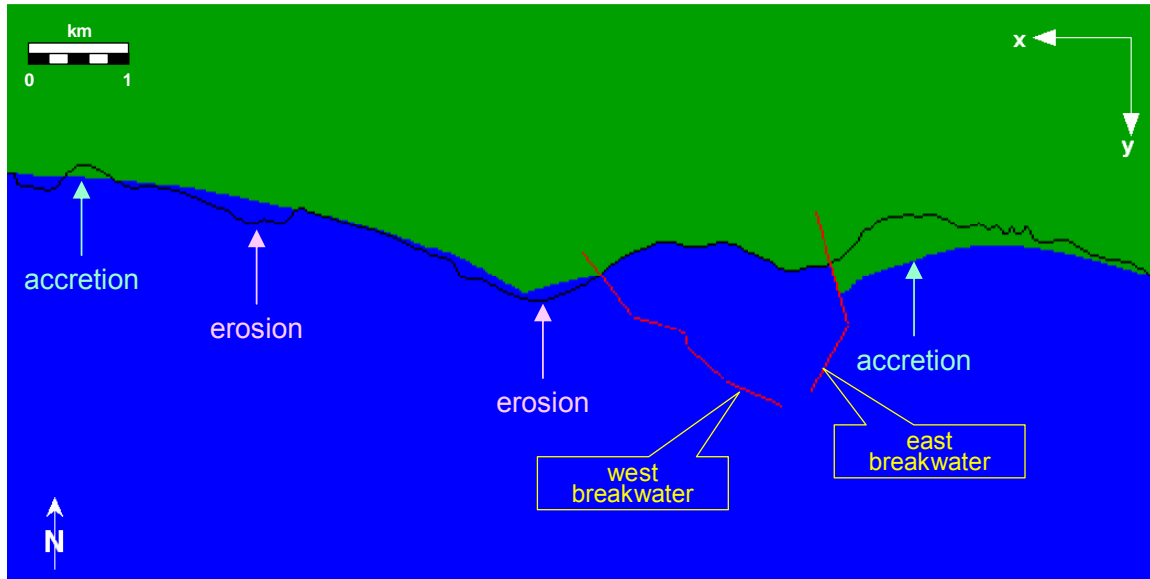


Figure 11. Shoreline change over a 40-year period in the vicinity of Port of Alexandroupolis (shoreline change model GENESIS)–The black line is the initial coastline and the green area is the situation after 40 years. The accretion of the beach on the eastern side of the Port and the corresponding erosion of the beach on the western side of the Port is obvious and is in agreement with the observations.

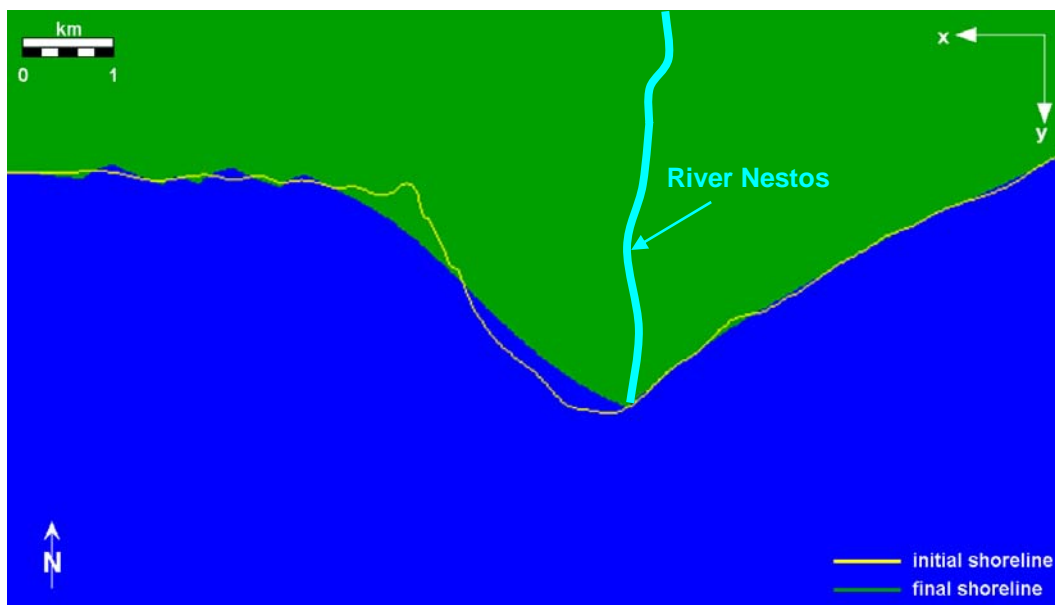


Figure 12. Shoreline change over a 40-year period for the Nestos estuary site. The simulated time period was 40 years and the calculated volumetric changes were $-2.75 \times 10^4 \text{ m}^3$, with positive values in GENESIS indicating accretion and negative values indicating erosion

References

- BEHRENDT H., HUBER P., KORNMILCH M., OPTITZ D., SCHMOLL O., SCHOLZ G. AND UEBE R., (1999), "Nutrient emissions into river basins of Germany", Institute of Freshwater Ecology and Inland Fisheries, Germany.
- DOORENBOS J. AND PRUITT W. O., (1977): "Crop water requirements", FAO, Irrigation and Drainage Paper 24 (revised), 156 p.



- FLUENT Incorporated (2000). FLUENT 5 User's Guide. Fluent Incorporated, Lebanon, NH, USA.
- HRISSANTHOU V., (2002), "Comparative application of two erosion models to a basin", *Hydrological Sciences Journal*, 47(2), pp. 279-292 .
- HRISSANTHOU V. (2005),: "Estimate of sediment yield in a basin without sediment data", *CATENA*, 64(2005), 2-3, pp. 333-347.
- HUGHES, S.A. (1984). *The TMA Spectrum Description and Applications*. TR-CERC-84-7, Coastal Engineering Research Center, USAE Waterways Experiment Station. Vicksburg, MS.
- IMRAN J., KASSEM A. AND KHAN S.M. (2004) "Three-dimensional modeling of density current. I. Flow in straight confined and unconfined channels". *Journal of Hydraulic Research* 42(6), 578-590.
- KASSEM A. AND IMRAN J. (2001). "Simulation of Turbid Underflows Generated by the Plunging of a River". *Geology* 29(7), 655–658.
- KASSEM A., IMRAN J. AND KHAN J.A. (2003). "Three-Dimensional Modeling of Negatively Buoyant Flow in Diverging Channels". *Journal of Hydraulic Engineering* , ASCE 2003, 937-947.
- KHAN S.M., IMRAN J. BRADFORD S. AND SYVITSKI J. (2005). "Numerical modeling of hyperpycnal plume". *Marine Geology* 222-223 (2005) 193-211.
- SCHMIDT J.,(1992), "Predicting the sediment yield from agricultural land using a new soil erosion model", *Proceedings 5th International Symposium on River Sedimentation*, Karlsruhe, pp. 1045-1051.
- SOIL CONVERSATION SERVICE (SCS), (1972) , "National Engineering Handbook", Section of Hydrology, Washington D.C.
- U.S. ARMY CORPS OF ENGINEERS (USACE, 1989). *GENESIS: Generalized model for simulating shoreline change*. Report 1 - Technical Reference. U.S. Army Corps of Engineers, Washington, D.C.
- U.S. ARMY CORPS OF ENGINEERS (USACE, 1999). *STWAVE: Steady-State Spectral Wave Model*. Report 1 - User's , Manual for STWAVE Version 2.0. U.S. Army Corps of Engineers, Washington, D.C
- YALIN, S., (1963), "An expression of bed-load transportation", *J. Hydraul. Div. ASCE* 89(3), 221–250.
- YANG C. T. AND STALL J. B., (1963) , "Applicability of unit stream power equation", *Journal of the Hydraulics Division, ASCE*, Vol. 102, No HY5, pp. 559-568.

**8. RAPPORT OF PHASE B:
FOUNDATION OF RESEARCH AND TECHNOLOGY-HELLAS,
INST. OF APPLIED MATHEMATICS – P8
MEASURE 3.3
GESA**

PART 1. Methodology analysis

Introduction

Shoreline change models are used to predict shoreline changes associated with coastal structures or storm effects over the long term. These models are based on the single line or multiple line theories, where the potential long shore and cross shore sediment transport components are calculated empirically for the open shore case. These models have the advantage of being very fast, and they can predict long-term shoreline changes very well after suitable calibration. However, they cannot accurately predict the impact of morphological changes in the vicinity of coastal structures that are due to short-term storms. An alternative approach involves the modeling of the whole suite of elementary processes responsible for the local morphological changes in a given area, Leont'yev, (1999). A typical coastal area model consists of several modules describing the wave field, the spatial distribution of wave-induced currents, the associated sediment transport fluxes, and finally the resulting spatial and temporal changes of the bed level. Such an approach is employed in the models developed by Delft Hydraulics, De Vriend et al. (1993), Roelvink et al. (1995), Danish Hydraulic Institute, Broker (1995), Broker et al. (1995), or HR Wallingford, Prince et al. (1995). The attempts to evaluate the short-term morphological impacts of coastal structures using these models are not yet numerous, but the results obtained are encouraging. Although these models can be used to predict medium-term morphological impacts on coastal structures, the long-term morphological impacts are still predicted solely by the shore-line models.

Many models exist for the evaluation of wave deformation in the coastal region but the most of them are based on the progressive wave assumption (period averaged refraction wave models) and employ elliptic or parabolic type differential equations which are in general difficult to numerically solve. Besides they are not valid for a compound wave field near coastal structures where the waves subject to the combined effects of shoaling, refraction, diffraction, reflection and breaking.

The evaluation of the wave field only is not sufficient for the design of coastal structures. The current pattern, the sediment transport and the bottom topography changes also play an important role in the design. Basic to the description of these currents is the incorporation of the wave breaking (into the wave model) and the formulation of the driving forces (radiation stress) from the wave model results.

In the present work the model ALS is presented. The wave submodel WAVE-L, based on the hyperbolic type mild slope equation, valid for a compound wave, after the incorporation of breaking and the evaluation of the radiation stress, drives the depth-averaged circulation and sediment transport submodel CIRC-L for the description of the nearshore currents and beach deformation. A new one-line model, 1L-L, with additional terms, is proposed in order to calculate shoreline position taking into account the cross-shore related seasonal shoreline variation.

WAVE SUBMODEL -WAVE-L-

The breaking and non breaking wave model is based on the hyperbolic type mild slope equation without using the progressive wave assumption. The model consists of the following pair of equations, Copeland (1985):

$$\begin{aligned} \frac{\partial \zeta_w}{\partial t} + \frac{c}{c_g} \nabla \frac{c_g}{c} \mathbf{Q}_w &= 0 \\ \frac{\partial \mathbf{U}_w}{\partial t} + \frac{c^2}{d} \nabla \zeta_w &= 0 \end{aligned} \quad (1)$$

where: ζ_w is the surface elevation,
 \mathbf{U}_w the mean velocity vector $\mathbf{U}_w = (U, V)$,
 d the depth,
 $\mathbf{Q}_w = U_w h_w = (Q_w, P_w)$,
 h_w the total depth ($h_w = d + \zeta_w$),
 c the celerity and
 c_g the group velocity.

The above equations, derived by Copeland (1985), are able to compute the combination of wave refraction, diffraction and reflection (total or partial).

The numerical model is adapted for engineering applications:

1. The input wave is introduced in a line inside the computational domain according to Larsen and Dancy (1983).
2. A sponge layer boundary condition is used to absorb the outgoing waves in the four sides of the domain Larsen and Dancy (1983).
3. Total reflection boundary condition (U_w or $V_w=0$) is incorporated automatically in the model. The existence of a vertical structure with 100% reflection coefficient is introduced from the depth file (depth $d=-1$).
4. Submerged structures are incorporated as in Karambas and Kriezi (1997).
5. Partial reflection is introduced from an artificial eddy viscosity file. The values of the eddy viscosity coefficient are estimated from the method developed by Karambas and Bowers (1996), using the values of the reflection coefficients proposed by Bruun⁴.
6. Floating structures are incorporated as in Koutandos et al. (2002).

The model is extended in the surf zone in order to include breaking effects providing the equations with a suitable dissipation mechanism by the introduction of a dispersion term in the right-hand side of momentum eqn (1):

$$v_h = \nabla^2 \mathbf{U}_w \quad (2)$$

where v_h is an horizontal eddy viscosity coefficient estimated from Battjes (1995):

$$v_h = 2d \left(\frac{D}{\rho} \right)^{1/3} \quad (3)$$

in which ρ is the water density and D is the energy dissipation given by Battjes and Janssen (1978) :

$$D = \frac{1}{4} Q_b f \rho g H_m^2 \quad (4)$$

with: f the mean frequency,
 H_m the maximum possible wave height and
 Q_b the probability that at a given point the wave height is associated with the a breaking or broken wave.

For a Rayleigh type probability distribution, Battjes and Janssen (1978):

$$\frac{1-Q_b}{\ln Q_b} = \left(\frac{H_{rms}}{H_m} \right)^2$$

in which: H_{rms} is the mean square wave height:
 $H_{rms}=2 \langle 2 \zeta_w^2 \rangle^{1/2}$ and
the brackets $\langle \rangle$ denote a time mean quantity.

WAVE-INDUCED CIRCULATION SUBMODEL -CIRC-L-

Radiation stress and wave-induced current submodel

Taking the horizontal axes x_1 and x_2 on the still water surface, and the z axis upward from the surface, the definition of the radiation stress S_{ij} component is:

$$S_{ij} = \langle \int_{-d}^{\zeta_w} (p \delta_{ij} + \rho u_i u_j) dz \rangle - 0.5 \rho g (d + \langle \zeta \rangle)^2 \delta_{ij} \quad (5)$$

where: δ_{ij} is the Kroneker's delta,
 $u_i(z)$ is the wave horizontal velocity component in direction x_i ,
 ζ is the mean sea level,
 p the pressure and
 $\langle \rangle$ denotes a time average.

The total pressure p is obtained from the vertical momentum equation:

$$p = \rho g (\zeta - z) - \rho u_3^2 + \frac{\partial}{\partial x_1} \int_z^0 \rho u_1 u_3 dz + \frac{\partial}{\partial x_2} \int_z^0 \rho u_2 u_3 dz + \frac{\partial}{\partial t} \int_z^{\zeta} \rho u_3 dz \quad (6)$$

where: u_3 is the z -velocity component.

Based on the above eqn (6) and after the substitution of u_i and p , from model results (eqn 1) using linear wave theory, Copeland (1985b) derived the expressions for S_{ij} without the assumption of progressive waves. Those expressions are used in the present model.

The radiation stresses are the driving forces of a 2D horizontal wave-induced current model:

$$\begin{aligned} \frac{\partial \zeta}{\partial t} + \frac{\partial(Uh)}{\partial x} + \frac{\partial(Vh)}{\partial y} &= 0 \\ \frac{\partial U}{\partial t} + U \frac{\partial U}{\partial x} + V \frac{\partial U}{\partial y} + g \frac{\partial \zeta}{\partial x} &= \\ -\frac{1}{\rho h} \left(\frac{\partial S_{xx}}{\partial x} + \frac{\partial S_{xy}}{\partial y} \right) + \frac{1}{h} \frac{\partial}{\partial x} \left(v_h h \frac{\partial U}{\partial x} \right) + \frac{1}{h} \frac{\partial}{\partial y} \left(v_h h \frac{\partial U}{\partial y} \right) - \frac{\tau_{bx}}{\rho h} \\ \frac{\partial V}{\partial t} + U \frac{\partial V}{\partial x} + V \frac{\partial V}{\partial y} + g \frac{\partial \zeta}{\partial y} &= \\ -\frac{1}{\rho h} \left(\frac{\partial S_{xy}}{\partial x} + \frac{\partial S_{yy}}{\partial y} \right) + \frac{1}{h} \frac{\partial}{\partial x} \left(v_h h \frac{\partial V}{\partial x} \right) + \frac{1}{h} \frac{\partial}{\partial y} \left(v_h h \frac{\partial V}{\partial y} \right) - \frac{\tau_{by}}{\rho h} \end{aligned} \quad (7)$$

where: h is the total depth $h=d+\zeta$, U, V are the current horizontal velocities
 τ_{bx} and τ_{by} are the bottom shear stresses.

In the current model the treatment of the bottom stress is critical (all longshore current models employing radiation stress solve for the mean current velocity through its role in the bottom friction term). The general expression for the time-average bottom shear stress in the current model is written:

$$\begin{aligned}\tau_{bx} &= \rho C_f \langle (U + u_b) \sqrt{(U + u_b)^2 + (V + v_b)^2} \rangle \\ \tau_{by} &= \rho C_f \langle (V + v_b) \sqrt{(U + u_b)^2 + (V + v_b)^2} \rangle\end{aligned}\quad (8)$$

where: C_f is the friction coefficient which depends on the bottom roughness and on the orbital amplitude at the bed, Karambas (1998),
 u_b and v_b are the wave velocities at the bottom.

Inside surf zone the existence of the undertow current that is directed offshore on the bottom cannot be predicted by a depth averaged model. However, representing the cross-shore flow is essential for a realistic description of the sediment transport processes. The present model calculates local vertical distribution of the horizontal velocity using the analytical expression for the cross-shore flow below wave trough level proposed by Stive and Wind (1986):

$$v_u = \frac{1}{2} \left[\left(\xi - 1 \right)^2 - \frac{1}{3} \right] \frac{h - \zeta_t}{\rho v_\tau} \frac{dR}{dy} + \left(\xi - \frac{1}{2} \right) \frac{(h - \zeta_t) \tau_s}{\tilde{n} v_\tau} - \frac{M \cos \Theta}{h - \zeta_t} \quad (9)$$

where: v_u is the undertow velocity in the y (shore-normal) direction,
 $\xi = z/(h - \zeta_t)$, ζ_t is the wave trough level, $dR/dy = 0.14 \rho g d h / dy$,
 τ_s is the shear stress at the wave trough level,
 M is the wave mass flux above trough level,
 Θ is the direction of the wave propagation
 v_τ the eddy viscosity coefficient given by equation (1).

The value of the coefficient in eqn (3) is now taken equal to 0.03 (instead of 2). The direction of the wave propagation Θ is given by:

$$\Theta = \arctan \left[\left(\langle Q_w^2 \rangle / \langle P_w^2 \rangle \right)^{1/2} \right] \quad (10)$$

SEDIMENT TRANSPORT MODEL -SED-L-

Sediment transport submodel

Sediment transport in the surf zone

The prediction of the sediment transport is based on the energetics approach, in which the submerged weight transport rates, i_{xt} in the x direction and i_{yt} in the y direction, are given by Karambas (1998):

$$\begin{aligned}i_{xt} &= \left\langle \left[\frac{\varepsilon_b}{\tan \phi} \left(\frac{u_o}{u_{ot}} + \frac{d_x}{\tan \phi} \right) \omega_b + \varepsilon_s \frac{u_{ot}}{w} \left(\frac{u_o}{u_{ot}} + \varepsilon_s d_x \frac{u_{ot}}{w} \right) \omega_t \right] \right\rangle \\ i_{yt} &= \left\langle \left[\frac{\varepsilon_b}{\tan \phi} \left(\frac{v_o}{u_{ot}} + \frac{d_y}{\tan \phi} \right) \omega_b + \varepsilon_s \frac{u_{ot}}{w} \left(\frac{v_o}{u_{ot}} + \varepsilon_s d_y \frac{u_{ot}}{w} \right) \omega_t \right] \right\rangle\end{aligned}\quad (11)$$

where: w is the sediment fall velocity,
 ϕ is the angle of internal friction,
 ε_b and ε_s are the bed and suspended load efficiency factors respectively ($\varepsilon_b=0.13$, $\varepsilon_s=0.01$),
 $u_{ot}=\sqrt{u_o^2 + v_o^2}$ (u_o , v_o are the total flow velocities at the bottom),
 d_x and d_y are the bottom slopes $\omega_b = C_f \rho u_{ot}^3$,
 ω_t is the total rate of energy dissipation given by Leont'yev¹⁵:

$$\omega_t = \omega_b + D e^{3/2(1-h/H)} \quad (12)$$

in which: H is the wave height ($H=H_{rms}$),
 D is the mean rate of breaking wave energy dissipation per unit area given by eqn (4).

In eqn (12) the first term express the power expenditures due to bed friction while the second due to excess turbulence penetrating into bottom layer from breaking waves.

The above method had been applied using a non linear dispersive wave model based on the Boussinesq equations (Karambas et al. (1995), Karambas (1998). A Boussinesq model automatically includes the existence of the mean wave-induced current and consequently there is no need to separate the bottom velocities into a mean and a oscillatory part. However, since the present model is a linear one, the total flow velocity at the bottom is considered as a sum of the steady U , V , v_u and the oscillatory u_b , v_b components which include two harmonics:

$$\begin{aligned} u_o &= U + u_{bm} \cos(\omega t) + u_{b2m} \cos(2\omega t) \\ v_o &= V + v_u + v_{bm} \cos(\omega t) + v_{b2m} \cos(2\omega t + a) \end{aligned} \quad (13)$$

in which: ω is the wave frequency,
 a is the phase shift,
 u_{bm} , u_{b2m} , v_{bm} and v_{b2m} are the velocity amplitudes given by Leont'yev (1996), Leont'yev (1997).

The above sediment transport formula has been derived directly form the Bailard primitive equations without the assumption that the only dissipation mechanism is the bed friction. This is the most important limitation of the Bailard theory and precludes the use of the original formula within the surf zone, where the dissipation of energy associated with the process of wave breaking is largely dominant.

Sediment transport in the swash zone

Adopting the procedure proposed by Leont'yev (1996), the submerged weight transport rates i_{ys} near the shoreline, in the y (shore-normal) direction, is given by:

$$i_{ys} = \frac{\varepsilon_b f_R}{2 \tan^2 \phi} \rho | < u_R^3 > (\tan \beta_{eq} - \tan \beta) \quad (14)$$

where: f_R is the run-up friction coefficient (of order 10^{-1} - 10^{-3}),
 u_R is the flow velocity in the swash zone,
 $\tan \beta$ is the actual slope gradient
 $\tan \beta_{eq}$ is the slope under equilibrium state approximated by Yamamoto et al.(1996):

$$\tan \beta_{eq} = \left(\frac{0.0864 s g d_{50} T^2}{H_b^2} \right)^{2/3} \quad (15)$$

where: s is the specific gravity of sediment in water,
 d_{50} is the median grain size,
 H_b is the breaker height
 T is the wave period.

The flow velocity in the swash zone u_R is parameterized in terms of the run-up height R according to Leont'yev (1996): $u_R = (2g(R - z_c))$, where z_c is the height of water mass above the water level which increases proportionally to the distance from the upper run-up boundary.

If the bottom gradient exceeds the equilibrium value then $i_{ys} < 0$ (erosion). In opposite case $i_{ys} > 0$ (accretion).

The longshore (x direction) total swash sediment transport i_{xs} is calculated by the global expression proposed by Briad and Kamphuis (1993).

3D bed evolution and one-line models

The submodel CIRC-L is coupled with a 3D bed evolution model or with an one-line model to provide bathymetry or shoreline changes.

The nearshore morphological changes are calculated by solving the conservation of sediment transport equation:

$$\frac{\partial d}{\partial t} = \frac{\partial q_x}{\partial x} + \frac{\partial q_y}{\partial y} \quad (16)$$

where: d is the still water depth

q_x, q_y are the volumetric longshore and cross-shore sediment transport rates, related to the immersed weight sediment transport through:

$$q_{x,y} = \frac{i_{x,y}}{(\rho_s - \rho)gN} \quad (17)$$

in which: N is the volume concentration of solids of the sediment ($N = 0.6$)
 ρ_s and ρ are the sediment and fluid densities.

Under certain assumptions eqn (16) can be transformed into a 1D equation (one-line model). The one-line models find wider engineering use as they are much less costly to run.

Let us define the total longshore sediment transport Q and the mean (cross-shore) water depth \bar{d} by the equations:

$$Q = \int_0^{y_s} q_x dy \quad \bar{d} = \frac{1}{y_s} \int_0^{y_s} d dy \quad (18)$$

where: y_s is the width of the nearshore zone.

The integration of eqn (17) over the width of the nearshore zone from its outer boundary ($y=0$) to the shoreline ($y=y_s$), using the Leibnitz relation, leads to the following equation:

$$\frac{\partial(y_s \bar{d})}{\partial t} = \frac{\partial Q}{\partial x} - q_x(y_s) \frac{\partial y_s}{\partial x} + q_y(y_s) \quad (19)$$

where: we have supposed that the following conditions are valid: $d=0$ at shoreline ($y=y_s$) and the transport rates $q_x(0)=0$, $q_y(0)=0$ at the outer boundary ($y=0$) are zero.

Eqn (19) differs from a standard one-line model in the last two terms. The second term of the right hand side of the equation is related to the longshore transport rate near the shoreline while the last term incorporates the cross-shore related seasonal shoreline variation.

The cross-shore transport rate near the shoreline $q_y(y_s)$ is given Sunamura formula, Yamamoto et al. (1996):

$$q_y(y_s) = K U_r^{0.2} \Phi (\Phi - 0.13 U_r) w d_{50} \quad (20)$$

where: U_r is the Ursell parameter $U_r = gHT^2/h^2$ (H is the wave height and h is the wave set-up at shoreline),
 $\Phi = H^2/shd_{50}$ (s is the specific gravity of sediment)
 K is a coefficient of sediment transport rate:

$$K = Ae^{-B/T} \quad (21)$$

where the coefficient A and B are given by Yamamoto et al. (1996):

$$\begin{aligned} A &= 1.61 \cdot 10^{-10} (d_{50}/H_0)^{-1.31} \\ B &= 4.2 \cdot 10^{-3} (\tan \beta)^{1.57} \end{aligned} \quad (22)$$

where H_0 is the deep water wave height.

The coefficient K of eqn (21) is a function of time since the rate of cross-shore sediment transport decreases with the lapse of time and the beach profile approaches the equilibrium state.

Also it can be expected that the mean depth \bar{d} is relatively conservative characteristic in comparison with the local shoreline position y_s , and consequently, it can be considered as a constant in eqn (19).

PART 2. Application of the numerical models in the Region of Rethimno

The above methodology is applied in the region Rethimno in North Crete in order to determine the wave climate and the current pattern. The sediment balance of the coast is significantly influenced by the harbor in the west corner of the beach. The next step in phase C will be to determine the sediment transport pattern and the shoreline evolution trend. In figure 1 a map of the area of Rethimno in North Crete is presented. In figures 2 and 3 satellite photographs of the coast of are presented where the harbor is presented in detail.



Figure 1. Map of the area of Rethimno in North Crete.

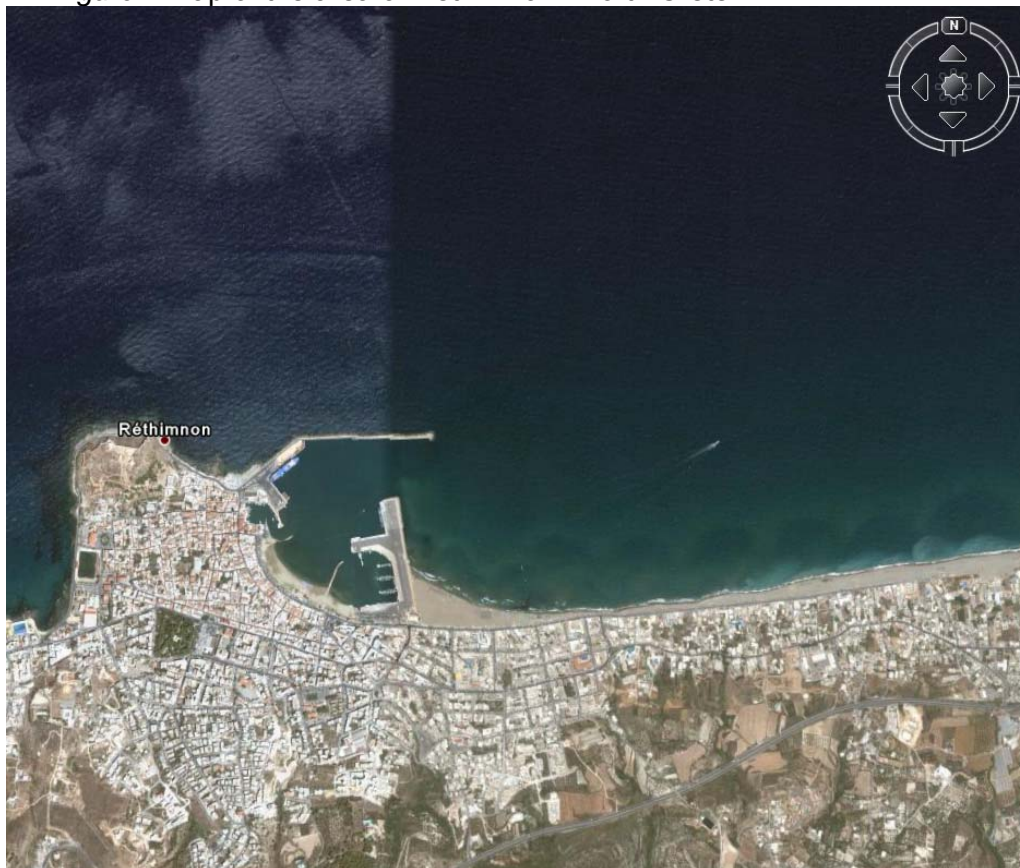


Figure 2. Satellite photograph of the area of Rethimno in North Crete.



Figure 3. Satellite photograph of the coast of Rethimno in North Crete.

WAVE CLIMATE ANALYSIS

For the calculation of the wave climate in the open sea of the specific region, the estimation of the significant wave height H_s , the peak wave period T_p , the maximum energy density and the mean period T_z are calculated using the JONSWAP approach:

$$\frac{gH_s}{U^2} = 0,0016 \left(\frac{gx}{U^2} \right)^{0.5} \quad (23)$$

$$\frac{gT_p}{U} = 0,286 \left(\frac{gx}{U^2} \right)^{0.33} \quad (24)$$

$$\frac{gT_z}{U} = 0,22 \left(\frac{gx}{U^2} \right)^{0.33} \quad (25)$$

Supposing that F is the fetch, we check the validity of the following relationship:

$$\frac{gt_D}{U} > 68,8 \left(\frac{gF}{U^2} \right)^{0.66} \quad (26)$$

where: t_D is the duration.

If eq. 26 is valid we replace x with F . If eq. 26 is not valid we set the two parts of the equation equal and solve for F in the place of x .

Numerical calculations were performed for three directions North-West, North and North-East sector. The calculation of the active fetch is performed in a sector $\pm 45^\circ$ in relation to the main direction, with radius of 10° . Mean velocities for moderate and strong/severe winds are $U=10$ and 22 m/s accordingly.

Using the wind data from Station Rethimno of the Greek Meteorological Service we get the following results:

BF	U (m/s)	Frequency of Appearance %	H_{os} (m)	T_p (s)
4	7,0	1,878	1,21	5,80
5	9,8	1,016	1,72	6,54
6	12,7	0,784	2,22	7,13
7	15,7	0,376	2,75	7,65
8	19,0	0,077	3,33	8,16
9	22,5	0,000	3,94	8,41
10	26,0	0,000	4,55	8,84
>11	31,0	0,000	5,43	9,38
Total		4,131		

Table 1. Wave parameters for North-West wind.

BF	U (m/s)	Frequency of Appearance %	H_{os} (m)	T_p (s)
4	7,0	3,535	1,21	5,80
5	9,8	1,491	1,97	7,16
6	12,7	1,248	2,63	7,98
7	15,7	0,696	3,26	8,57
8	19,0	0,221	3,94	9,13
9	22,5	0,000	4,67	9,41
10	26,0	0,000	5,40	9,88
>11	31,0	0,000	6,43	10,49
Total		7,191		

Table 2. Wave parameters for North wind.

BF	U (m/s)	Frequency of Appearance %	H_{os} (m)	T_p (s)
4	7,0	1,127	1,21	5,80
5	9,8	0,552	1,90	7,00
6	12,7	0,508	2,46	7,63
7	15,7	0,309	3,04	8,19
8	19,0	0,044	3,68	8,73
9	22,5	0,000	4,36	9,00
10	26,0	0,000	5,04	9,45
>11	31,0	0,000	6,01	10,03
Total		2,54		

Table 3. Wave parameters for North-East wind.

where: H_{os} is the significant wave height in deep waters

T_p is the peak period of the wave spectrum.

The equivalent wave height H_e on an annual basis are set according to Borah and Balloffet, (1985) as following:

$$H_e^2 T = \frac{\sum H_i^2 T_i f_i}{\sum f_i} \quad (27)$$

where; T is the equivalent wave period,

H_i , T_i , f_i are the height, the period and the frequency of the waves that correspond on the various levels of wind intensity from each incident direction.

The equivalent wave is actually the wave that appears with the frequency $\sum f_i$ and includes the same wave energy with the series of the waves of various intensity of the specific direction. Using the wind data from the specific area from the Greek Metereological Service and applying the JONSWAP wave prediction method the significant wave heights H_e , the periods T and the frequencies of the equivalent open sea waves were deduced.

Table 4. Equivalent waves characteristics:

North-West wind						
BF	U (m/s)	Frequency of appearance (f) %	H_{os} (m)	T_p (s)	H_e (m)	T_e (m)
4	7,0	1,878	1,21	5,80	1,86	6,45
5	9,8	1,016	1,72	6,54		
6	12,7	0,784	2,22	7,13		
7	15,7	0,376	2,75	7,65		
8	19,0	0,077	3,33	8,16		
9	22,5	0,000	3,94	8,41		
10	26,0	0,000	4,55	8,84		
>11	31,0	0,000	5,43	9,38		
Total		4,131				

North wind						
BF	U (m/s)	Frequency of appearance (f) %	H_{os} (m)	T_p (s)	H_e (m)	T_e (m)
4	7,0	3,535	1,21	5,80	2,19	6,83
5	9,8	1,491	1,97	7,16		
6	12,7	1,248	2,63	7,98		
7	15,7	0,696	3,26	8,57		
8	19,0	0,221	3,94	9,13		
9	22,5	0,000	4,67	9,41		
10	26,0	0,000	5,40	9,88		
>11	31,0	0,000	6,43	10,49		
Total		7,191				

North-East

BF	U (m/s)	Frequency of appearance (f) %	H _{os} (m)	T _p (s)	H _e (m)	T _e (m)
4	7,0	1,127	1,21	5,80	2,10	6,77
5	9,8	0,552	1,90	7,00		
6	12,7	0,508	2,46	7,63		
7	15,7	0,309	3,04	8,19		
8	19,0	0,044	3,68	8,73		
9	22,5	0,000	4,36	9,00		
10	26,0	0,000	5,04	9,45		
>11	31,0	0,000	6,01	10,03		
Total		2,54				

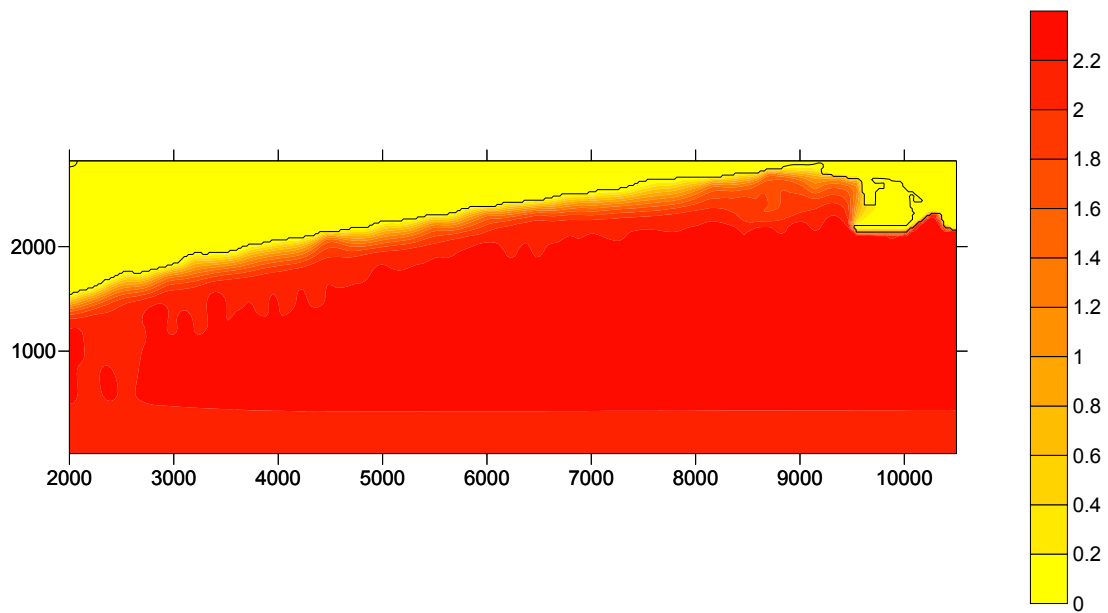


Figure 4. Current status: H_s contours for North direction winds.

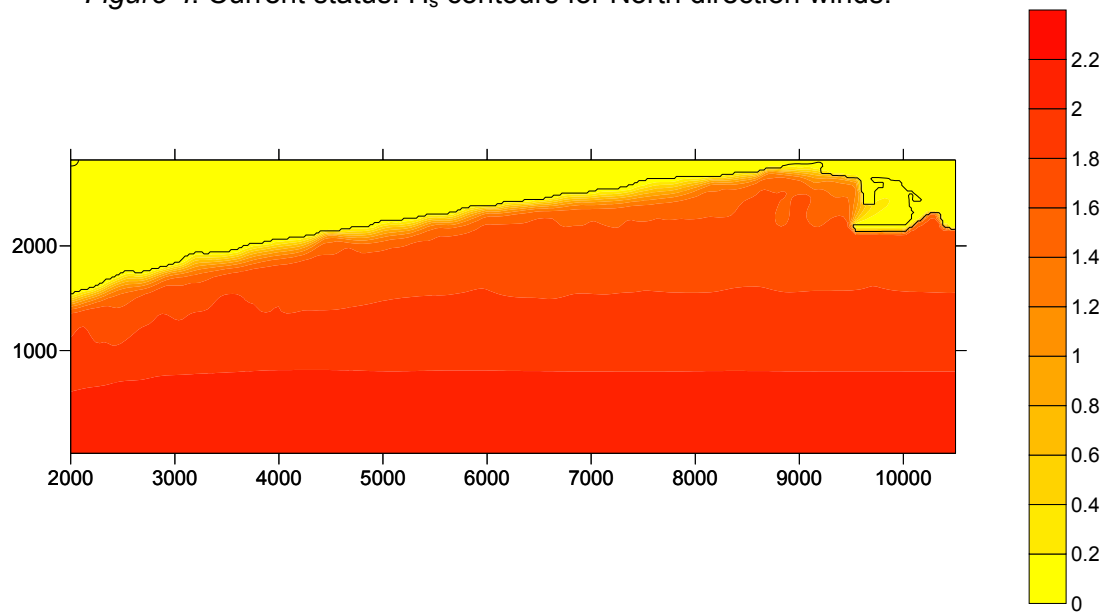


Figure 5. Current status: H_s contours for North-East direction winds.

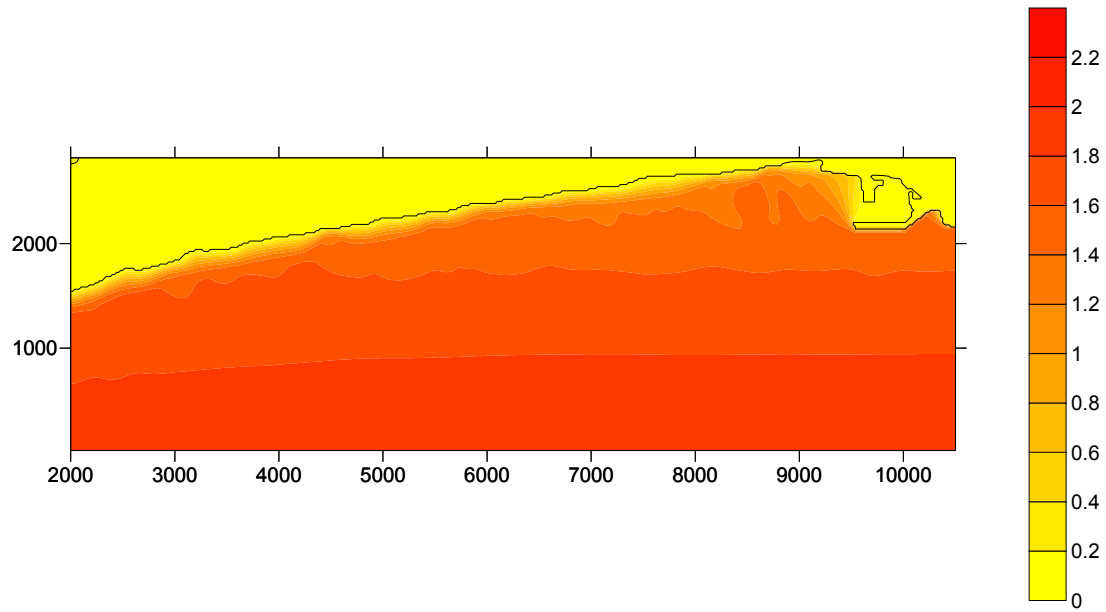


Figure 6. Current status: H_s contours for North-West direction winds.

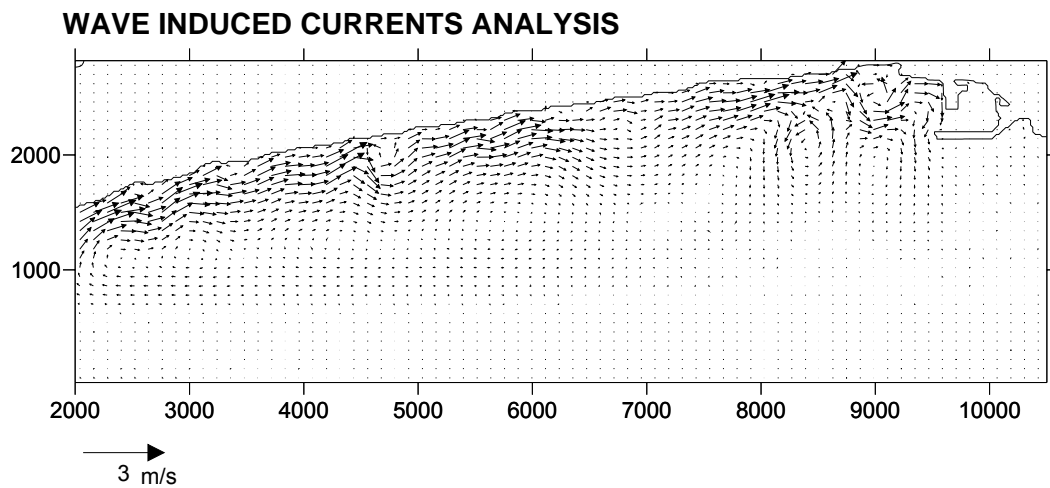


Figure 7. Current status: Wave induced current velocities for North direction winds.

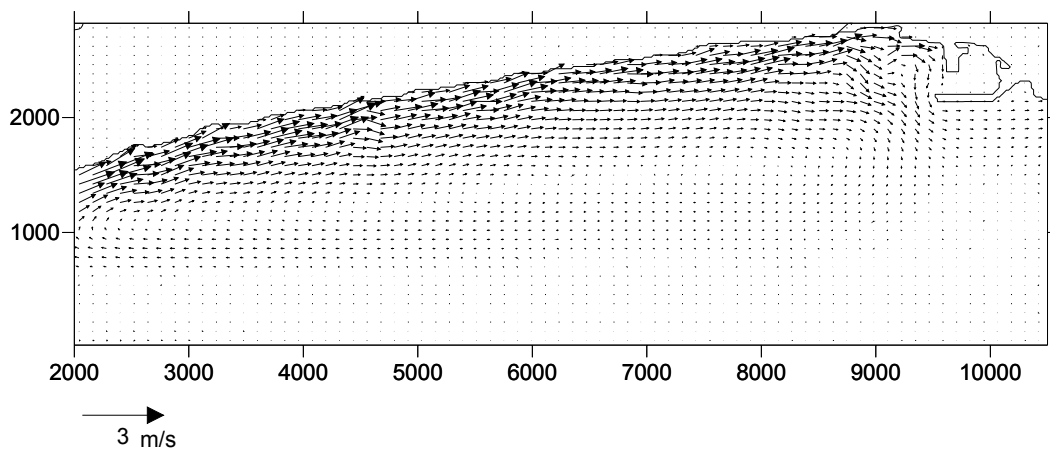


Figure 8. Current status: Wave induced current velocities for North-East direction winds.

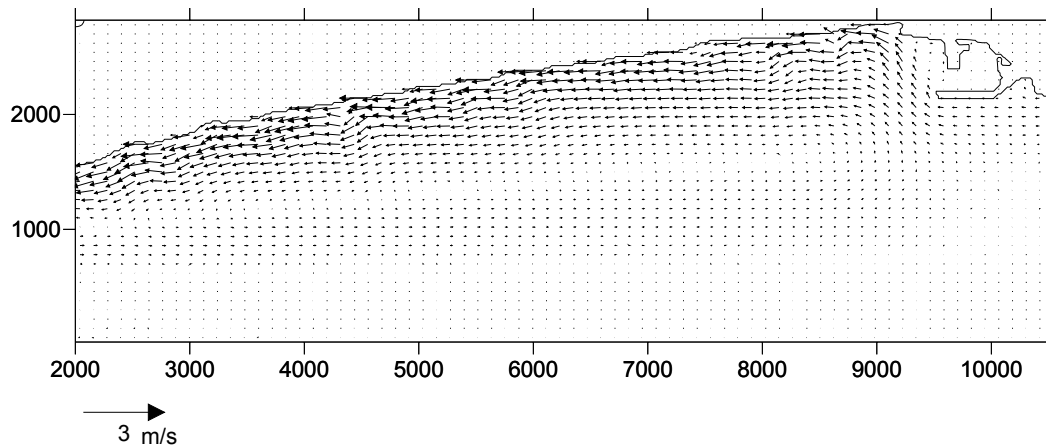


Figure 8. Current status: Wave contours current velocities for North-West direction winds.

CONCLUSIONS

In the present work the model ALS has been presented for sediment transport monitoring and the methodology followed has been analysed. The wave submodel WAVE-L, based on the hyperbolic type mild slope equation, valid for a compound wave, after the incorporation of breaking and the evaluation of the radiation stress, drives the depth-averaged circulation and sediment transport submodel CIRC-L for the description of the nearshore currents and beach deformation. A new one-line model, 1L-L, with additional terms, is proposed in order to calculate shoreline position taking into account the cross-shore related seasonal shoreline variation. The first two submodels have been applied for the region of Rethimno in North Crete in order to determine the wave climate and the current pattern due to the fact that the sediment balance of the coast is significantly influenced by the harbor in the west corner of the beach. The following conclusions have been derived:

- H_s contours reveal the wave propagation pattern for each wind direction.
- Wave refraction and breaking phenomena due to the existence of the coast and the harbour works are revealed.
- The width of the breaker zone can be estimated around 300 m.
- Wave induced currents calculations reveal the existence of a strong alongshore current in the breaker zone.
- North and North-East winds produce currents of West direction while North-West winds currents of East direction.
- On the West direction we meet the entrance of the harbor that intervenes in the alongshore current that is the main sediment transport mechanism.
- The final result is expected to be the deposition of sediments in the entrance of the harbour.

References

- BATTJES, J.A., (1995). Modelling of turbulence in the surf zone, Proc. Symp. Modelling Techniques, California, ASCE, 1050-1061.
- BATTJES, J.A., JANSSEN, J.P.F.M., (1978). Energy Loss and set-up due to breaking of random waves, Int. Conf. on Coastal Engineering '78, ASCE, 569-587.
- BORAH, D.K., BALLOFFET, A., (1985). "Beach evolution caused by littoral drift barrier", J. of Waterway, Port, Coastal and Ocean Eng., ASCE, vol 111, no4, pp. 645-660.
- BRIAD, M-H.G., KAMPHUIS, J.W., (1993). Sediment transport in the surf zone: a quasi 3-D numerical model, Coastal Engineering, 20, 135-156.

- BROKER, I., (1995). Coastal area modelling. MAST 68-M Final Workshop, Gdansk, Poland, 2-86 to 2-90.
- BROKER, I., JOHNSON, H.K., ZYSERMAN, J.A., RONBERG, J.K., PEDERSEN, C., DEIGAARD, R., FREDSOE, J., (1995). Coastal profile and coastal area morphodynamic modelling. MAST 68-M Final Workshop, Gdansk, Poland, 7-12 to 7-16.
- BRUUN, P., (1985) .Design and Construction of Mounds for Breakwaters and Coastal Protection, Elsevier, New York
- COPELAND, G.J.M., (1985) .A practical alternative to the «mild-slope» wave equation, Coastal Engineering 9, 125-149.
- COPELAND, G.J.M., (1985). Practical radiation stress calculations connected with equations of wave propagation, Coastal Engineering 9, 195-219.
- DE LA PENA J. M., (1998) .Assessment of the Malagueta beach nourishment (Malaga - Spain) period 1995-1998, SAFE report 51 8904 R5, 2nd Annual Workshop.
- DE VRIEND, H.J., ZYSERMAN, J., NICHOLSON, J., ROELVINK, J.A., PECHON, P., SOUTHGATE, H.N., (1993). Medium-term 2DH coastal area modelling. Coastal Engineering 21, 193-224.
- KARAMBAS, TH. V., KOUTITAS C., (1996) .A quasi-3D model for morphology-structures interaction in coastal environment, Protection and Restoration of the Environment III, Techn. Univ. of Crete, 65-72.
- KARAMBAS, TH. V., SOUTHGATE, H.N., KOUTITAS C., (1995).A Boussinesq model for inshore zone sediment transport using an energetics approach, Coastal Dynamics '95, Gdansk, 841-849.
- KARAMBAS, TH. V., BOWERS, E.C., (1996). Representation of partial wave reflection and transmission for rubble mound coastal structures, Hydrosoft 96, Malaysia.
- KARAMBAS, TH. V., KITOU N., (1996). A numerical model for the wave and current field estimation near coastal structures, 2nd National Congress on Computational Mechanics, Chania, Greece.
- KARAMBAS, TH. V., KRIEZI E.E., (1997). Wave Reflection and Transmission for Submerged Monolithic Breakwaters. Computational Methods and Experimental Measurements, CMEM 97, Computational Mechanics Publications, eds Anagnostopoulos P., Carlomagno G. M., Brebbia C. A., Southampton, UK and Boston USA, pp 544-550.
- KARAMBAS, TH. V. (1998). 2DH non-linear dispersive wave modelling and sediment transport in the nearshore zone, Int. Conf. on Coastal Engineering, ASCE, Copenhagen.
- KARAMBAS TH. V., (1999). A unified model for periodic non linear dispersive wave in intermediate and shallow water. to appear in Journal of Coastal Research.
- KOUTANDOS E.V., KARAMBAS TH.V., KOUTITAS C.G., PRINOS P.E., (2002). Shoreline changes in presence of a floating breakwater, International Conference 'Protection and Restoration of the Environment VI', Skiathos, Greece, vol. I, pp. 403-410.
- LARSEN, J., DANCY, H., (1983). Open Boundaries in Short Wave Simulations - A New Approach, Coastal Engineering, 7, 285-297.
- LEONT'YEV, I.O., (1996). Numerical modelling of beach erosion during storm event, Coastal Engineering, 29, 187-200.
- LEONT'YEV, I.O., (1997). Short-term changes due to cross-shore structures: a one-line numerical model, Coastal Engineering 31, 59-75.
- LEONT'YEV, I.O., (1999). Modeling of morphological changes due to coastal structures. Coastal Engineering, 38, 149-166.
- PRICE, D.M., CHESHER, T.J., SOUTHGATE, H.N., (1995). PISCES: A Morphological Coastal Area Model. Report SR 411. Wallingford, U.K. HR Wallingford.
- ROELVINK, J.A., RENIERS, A.J.H.M., WALSTRA, D.J.R., (1995) . Medium term morphodynamic modelling. MAST 68-M Final Workshop, Gdansk, Poland, 7-3 to 7-6.



- STIVE, M. J. F., WIND H. G., (1986). Cross-shore flow in the surf zone, Coastal Engineering 10, 325-340.
- YAMAMOTO, Y., HORIKAWA, K., TANIMOTO, K., (1996). Prediction of shoreline change considering cross-shore sediment transport, Int. Conf. on Coastal Engineering 1996, ASCE, 3405-3418.